ROLE OF PEPTIDE TRANSPORTER PEPT1 IN THE INTESTINAL ABSORPTION AND PHARMACOKINETICS OF THE AMINO ACID ESTER PRODRUG VALACYCLOVIR

by

Bei Yang

A dissertation submitted in partial fulfillment
of the requirements for the degree of
Doctor of Philosophy
(Pharmaceutical Sciences)
in The University of Michigan
2012

Doctoral Committee:

Professor David Eric Smith, Co-Chair
Professor Gordon L. Amidon, Co-Chair
Professor Richard F. Keep
Associate Professor Duxin Sun

DEDICATION

To my dear mother Feng, Lihua and father Yang, Bingyi

To my beloved husband Xia, Chenan and son Xia, Yunhao

ACKNOWLEDGEMENTS

First of all, I would like to thank my advisor, Professor David E. Smith, to whom I owe my deepest gratitude. In the past four years, Professor Smith has spent a tremendous amount of his time and effort mentoring me on my project on a daily basis. His scientific acumen and commitment to the highest standards has motivated me all the time. As a caring and supporting advisor, he went out of his way to get a valuable internship opportunity for me so that I could set clear career goals and be fully prepared for a post-graduation career.

I would like to thank my co-advisor, Professor Gordon L. Amidon, for inspiring me with all of his constructive advice on my work. Moreover, I feel grateful for learning the fundamental knowledge and theories about mass balance and mass transfer from his course. I benefited a lot from his wisdom and knowledge. I would like to thank my other two committee members, Professor Richard F. Keep and Professor Duxin Sun, for offering their thoughtful suggestions and gracious support to my research. I also want to thank Dr. Meihua Rose Feng, who led me into the field of pharmacometrics, and has always been willing to offer her insightful remarks on my work.

I have to thank all my current and past fellow students and coworkers: Yongjun Hu, Maria M. Posada, Shupei Wu, Ke Ma, Yeamin Huh, Yehua Xie, Xiaomei Chen, Dilara Jappar, Naoki Nishio, Arik Dahan, and Yasuhiro Tsume for their wholehearted

support and assistance in my project. I truly enjoyed working with all of these wonderful people and wish everyone good luck in their own endeavors.

I would like to thank the Department of Pharmaceutical Sciences, College of Pharmacy and the University of Michigan for the world-class facilities and generous financial support. I am indebted to the wonderful staff in the College of Pharmacy including Terri Azar, Jeanne Getty, Gail Benninghoff, Maria Herbel and Mark Nelson and others who helped me during my course of study. I must acknowledge the Fred W. Lyons Fellowship Foundation, Schering-Plough Graduate Fellowship Foundation, Elizabeth Broomfield Fellowship Foundation and our College for financial support to my studies.

Last, but not least, I would like to express my deep gratitude to my beloved family and friends. I would like to acknowledge my dearest mother Lihua Feng and father Bingyi Yang, who have always believed in me and supported me selflessly and unconditionally. I would like to acknowledge my deeply beloved husband, Dr. Chenan Xia, who has always been my pillar of strength and given me endless support and love. My special thanks go to my son, Yunhao Xia. Because of him, my life is full of joy and happiness. I would like to thank my parents-in-law Buning Xu and Yongjiang Xia, who have always been supportive of me and taken good care of my son to allow me to focus on my studies. Finally, I thank my grandparents as well as all my close relatives and good friends, who make my life full and colorful.

TABLE OF CONTENTS

LIST OF FIGURES

LIST OF TABLES

ABSTRACT

Peptide transporter 1 (PEPT1), predominantly expressed in the small intestine, is responsible for the intestinal uptake of di-/tri-peptides and other peptidomimetics. PEPT1 is a tempting delivery target for increasing the oral absorption of drugs and prodrugs which might otherwise have poor absorption. This dissertation project proposes to delineate the quantitative importance of PEPT1 in the intestinal absorption and pharmacokinetics of the model PEPT1-targeted prodrug valacyclovir.

In wildtype and *Pept1* knockout mice, the effective permeability of valacyclovir was evaluated as a function of perfusate pH, drug concentration, potential inhibitors and regional segments of the intestines using *in situ* perfusions. Results from the *in situ* studies showed that PEPT1 accounted for approximately 90% of valacyclovir permeability in mouse small intestine. Absorbed valacyclovir was rapidly and completely converted to its active drug acyclovir after passing through the enterocyte. In wildtype mice, valacyclovir permeability was pH independent, concentration dependent, saturable with a K_m of about 10 mM, and inhibited by several PEPT1 substrates. *In vivo* pharmacokinetic studies showed that PEPT1 had little impact on the pharmacokinetic profiles of acyclovir following its oral or intravenous dosing, whereas PEPT1 deletion led to approximately 78% and 58% reduction in acyclovir maximum plasma concentration (C_{max}) and area under the plasma concentration-time curve (AUC), respectively, after oral

administration of valacyclovir. Tissue distribution results suggested that PEPT1 had little if any effect on the *in vivo* distribution of acyclovir. Lastly, a mechanistic ACAT model was used to simulate the intestinal absorption and pharmacokinetic profiles of valacyclovir after its oral administration, in which the primary input parameters were obtained from previous *in situ* and *in vivo* studies. Simulation results were in good agreement with *in vivo* pharmacokinetic data for both genotypes. The duodenum (>40%) was the primary absorption site of valacyclovir in wildtype mice while the more distal jejunal (~13%) and ileal (~10%) segments played a more important role in valacyclovir absorption for *Pept1* knockout animals. Rapid luminal hydrolysis was the main cause of incomplete valacyclovir absorption in wildtype mice.

In conclusion, results from this dissertation provided convincing evidence to validate the major contribution of PEPT1 on the intestinal absorption of valacyclovir and, furthermore, the utilization of PEPT1 as an oral delivery target. *In silico* mechanistic modeling aided in the interpretation of *in situ* and *in vivo* experimental results, and could be a useful tool in facilitating our understanding of valacyclovir's complicated intestinal absorption processes.

CHAPTER 1 RESEARCH OBJECTIVE

Oligopeptide transporter 1 (PEPT1), a proton/substrate co-transporter predominantly expressed in the small intestine, plays a pivotal role in the intestinal uptake of di-/tri-peptides and diverse peptidomimetics with high capacity and low affinity. The transport properties, broad substrate specificity and apical membrane localization of PEPT1 also make it a tempting target for oral drug delivery. PEPT1 targeted prodrugs, mainly synthesized by conjugating pharmacologically active drugs to amino acid or dipeptide carriers, are being actively explored as a promising strategy for enhancing the oral absorption of poorly permeable compounds.

Valacyclovir, an L-valyl ester prodrug of the antiviral drug acyclovir, is exemplary of the success of this PEPT1 targeted prodrug strategy. Oral administration of valacyclovir delivers significantly higher concentrations of acyclovir to the systemic circulation compared with oral acyclovir. A number of cell culture studies demonstrated the uptake of valacyclovir by PEPT1 while other studies also showed the interaction of valacyclovir with various membrane transporters other than PEPT1. The current consensus is that the enhanced oral availability of acyclovir derived from oral administration of valacyclovir is mainly attributed to PEPT1-mediated intestinal absorption of valacyclovir. However, no existing research can actually substantiate this claim. In other words, the quantitative significance of intestinal PEPT1 in the oral

absorption of valacyclovir and other PEPT1 targeted prodrugs alike remain ambiguous or even controversial, as increasingly realized by different researchers. Given the ambiguity about PEPT1's contribution, the prospect of rationally designed PEPT1 prodrugs as a versatile approach for the enhancement of oral absorption is uncertain.

The availability of *Pept1* knockout mice in our laboratory offers a unique opportunity to resolve this long-standing controversy. An in-depth investigation of the *in vivo* role of PEPT1 in the oral absorption and pharmacokinetics of valacyclovir utilizing the *Pept1* knockout mouse model will help elucidate the *in vivo* quantitative significance of PEPT1 and lead to a refined rational design of PEPT1-targeted prodrugs.

The ultimate objective of this proposal is to delineate the exact contribution of PEPT1 to the intestinal absorption and pharmacokinetics of PEPT1 targeted prodrugs. Valacyclovir, as a model PEPT1 targeted prodrug, will be studied for this purpose. This research proposal consists of three specific aims:

i. To characterize the relative importance of PEPT1 in the *in situ* intestinal permeability of valacyclovir in wildtype and *Pept1* knockout mice;

ii. To determine the *in vivo* relevance of PEPT1 in the oral absorption, disposition and pharmacokinetic profiles of valacyclovir in wildtype and *Pept1* knockout mice;

iii. To evaluate the advanced compartmental absorption and transit (ACAT) model as a means to define and simulate the absorption process of valacyclovir and the significance of PEPT1 in this process.

CHAPTER 2 BACKGROUND AND LITERATURE REVIEW

PROTON-COUPLED OLIGOPEPTIDE TRANSPORTER 1 (PEPT1)

At present, membrane transporters are increasingly recognized to be key determinants in regulating drug pharmacokinetics and pharmacodynamics. Proton-coupled oligopeptide transporter 1 (PEPT1) is one of the most intensively studied transporters with physiological and pharmacological importance. PEPT1 is a member of the proton-coupled oligopeptide transporter (POT) family. POTs, also known as solute carrier 15A (SLC15A) in man, include oligopeptide transporter 2 (PEPT2, SLC15A2), peptide histidine transporter 1 (PHT1, SLC15A4) and peptide histidine transporter 2 (PHT2, SLC15A3) in addition to PEPT1 (SLC15A1). PEPT1 as well as PEPT2 are responsible for the handling of di-/tri-peptides and a broad range of peptidomimetics in organisms whereas PHT1 and PHT2 have been shown to translocate histidine in addition to some selected di-/tri-peptides (Rubio-Aliaga and Daniel, 2008). Both PEPT1 and PEPT2 have been extensively studied and reviewed with regard to their structural characteristics, transport mechanisms, substrate specificity, tissue distribution and regulation. In contrast, little is known about PHT1 and PHT2. The present review mainly focuses on PEPT1 since it is the topic of interest for my thesis project.

Structural features and genetic polymorphisms of PEPT1. PEPT1 was first cloned and characterized by Fei et al. by expressing rabbit PEPT1 cRNA in an X. laevis oocyte system (Fei et al., 1994). Later PEPT1 was also isolated from various other species such as human (Liang et al., 1995), rat (Saito et al., 1995; Miyamoto et al., 1996) and mouse (Fei et al., 2000). Mammalian PEPT1 consists of 707-710 amino acid residues depending on species. Human PEPT1 is composed of 708 amino acid residues with a molecular weight of 78 kDa, and the gene located on chromosome 13. Structurally, mammalian PEPT1 and PEPT2 are predicted to possess 12 putative transmembrane domains (TMDs), a large extracellular loop between the ninth and tenth TMDs, and two putative protein kinase C-dependent phosphorylation sites; both the N- and C-termini of PEPT1 face the cytosolic side (Figure 2.1). PEPT1 shows a high degree of sequence homology at both the nucleotide and amino acid levels across species. The genomic organization of human PEPT1 shows high similarity with its mouse orthologue (Urtti et al., 2001). PEPT1 is highly homologous between humans (Liang et al., 1995) and mice (Fei et al., 2000) with an amino acid identity of 83%. The three dimensional protein structure of PEPT1 is still unknown for the mammalian SLC transporter. However, the recently identified crystal structure of a bacterial peptide transporter, a prokaryotic homologue of mammalian PEPT1, provides a useful high-resolution structural model for understanding drug transport with PEPT1 and other POT proteins (Newstead et al., 2011). Construction of chimeric proteins revealed that TMDs 1-4 and 7-9 contribute to substrate binding and affinity. By means of site-directed mutagenesis, some amino acid residues such as Y12, Y56, Y64, Y91, Y167, H57, W294 and E595 were found to be important in modulating substrate binding and the transport activity of PEPT1 (Brandsch et al., 2008;

Rubio-Aliaga and Daniel, 2008). For instance, the mutations of Y12 in the first TMD and Y64 in the second TMD to other amino acids were found to reduce the transport capacity of PEPT1. A summary of amino acid residues that may affect the function of PEPT1 is illustrated in Figure 2.1.

Limited genetic variants of human PEPT1 have been reported. Zhang and coworkers reported nine non-synonymous single nucleotide polymorphisms (SNPs), among which only the P586L variant showed reduced transport capacity for PEPT1 substrates when expressed in HeLa cells (Zhang et al., 2004). In another study, a low-frequency PEPT1- F28Y variant was found to display significantly increased K_m toward a typical PEPT1 substrate cephalexin (Anderle et al., 2006). Taken together, a low level of genetic polymorphisms has been found for human PEPT1.

Mechanism of PEPT1-mediated transport. PEPT1 has been found to couple the transport of their substrates uphill with the movement of protons down an inwardly directed electrochemical proton gradient (Ganapathy and Leibach, 1983; Brandsch et al., 2008). The detailed mechanism of PEPT1-mediated transport of di-/tri-peptides or peptide-like drugs is graphically depicted in Figure 2.2, which illustrates that the inward proton gradient is maintained by the apical sodium/proton exchanger 3 (NHE3) on the epithelial cells. The driving force for NHE3 is the inwardly directed sodium gradient which is maintained by Na^+-K^+-ATPase located on the basolateral membrane of polarized epithelial cells. Once entering enterocytes, some peptides are further hydrolyzed to generate free amino acids, which can be pumped cross the basolateral membrane via basal amino acid transporters. Hydrolysis-resistant peptides can be shuttled into the systemic circulation in their intact form by poorly characterized basal peptide transporters

that are different from PEPT1. PEPT2 also shares the same transport mechanism with PEPT1. The transport model established PEPT1 and PEPT2 as proton-dependent transporters whose activity can be modulated directly by proton gradient, indirectly by sodium gradient, and also by membrane potential.

Substrate specificity. One of the most intriguing features of PEPT1 is its capacity to transport a wide range of substrates including naturally occurring di-/tri-peptides and diverse peptidomimetics with high capacity and low affinity. Nearly all di-/tri-peptides can be transported by PEPT1; free amino acids or tetra-oligopeptides are not recognized by PEPT1. As for foreign PEPT1 substrates, some of them are important pharmaceutical drugs including orally active β-lactam antibiotics such as ceftibuten, cephalexin and cefadroxil, angiotensin converting enzyme inhibitors such as captopril and enalapril, the anticancer drug bestatin, the photosensitizing agent 5-aminolevulinic acid, selected renin inhibitors and the antiviral prodrugs valacyclovir and valganciclovir. Our current understanding of favorable structural requirements for PEPT1 substrates were obtained mainly from pharmacophore models. The minimal requirement for PEPT1 substrates is summarized as two oppositely charged head groups separated by a spacer carbon unit with a distance > 500 pm and < 650 pm (Rubio-Aliaga and Daniel, 2008). Surprisingly, a peptide bond is not essential in the substrate structure. Other preferred features include a free N-terminal amino group, an electron-rich terminal carboxylic group and hydrophobic side chains. PEPT1 and PEPT2 share similar basic requirements for the structures of their substrates. However, unlike the low-affinity high-capacity transport feature of PEPT1, PEPT2 is usually known as a high-affinity low-capacity transporter. In addition, both PEPT1 and PEPT2 are stereoselective and prefer trans-

rather than cis-conformations. These structure-affinity models are useful in the discovery and development of new chemical entities recognized by peptide transporters PEPT1 and PEPT2. In addition, the crystal structure of a bacterial peptide transporter (Newstead et al., 2011), which shares sequence and functional similarities with mammalian PEPT1 proteins, could be another powerful tool for the design of new PEPT1 and PEPT2 substrates.

PEPT1 substrates were identified utilizing a variety of experimental methodologies. Caco-2 cells have been used to determine whether a drug is a PEPT1 substrate by some competitive inhibition studies with known PEPT1 substrates such as the synthetic non-metabolizable dipeptide glycylsarcosine. Other mammalian cell lines that were transiently or stably transfected with human PEPT1, such as HeLa, MDCK and CHO cells, were also used to examine PEPT1-mediated uptake of drugs. In addition, due to the electrogenic feature of PEPT1 activity, the uptake of PEPT1 substrates were also probed in *Xenopus laevis* oocytes injected with cRNA encoding PEPT1 using two-microelectrode voltage-clamp technique. Other *in vitro* techniques, such as brush border membrane vesicles and Ussing chamber with the small intestine, have been applied in the study of PEPT1 substrates as well. More complicated experimental methods, such as *in situ* intestinal perfusion techniques or *in vivo* pharmacokinetic studies, were also used to study PEPT1 substrates. An advantage of *in situ* and *in vivo* methods, based on whole animals, was that they can more reliably reflect the interaction of PEPT1 with substrates under physiological conditions although they require huge consumption of experimental animals and long experimental time periods. Recently, genetically modified mice deficient of PEPT1 were developed and validated in our laboratory (Hu et al., 2008),

which is deemed as a useful platform for studying the role of PEPT1 by performing different *in situ* and *in vivo* studies.

Tissue distribution. In mammalian species, PEPT1 displays a heterologous tissue distribution with predominant expression in the small intestine (Lu and Klaassen, 2006). PEPT1 is localized on the brush border membrane of epithelial cells along the small intestine (Ogihara et al., 1996; Lu and Klaassen, 2006; Jappar et al., 2010). Low-level expression of PEPT1 was found in S1 cells of the proximal convoluted tubule, where it was considered to play a minor role in the reabsorption of small peptides and peptide-like drugs (Shen et al., 1999). Moreover, expression of PEPT1 in extrahepatic biliary duct (Knutter et al., 2002), nuclei and lysosomes of the pancreas (Bockman et al., 1997), monocytes (Charrier et al., 2006) and reproductive organs (Lu and Klaassen, 2006) were also reported. However few details are available on the possible function of PEPT1 in tissues other than small intestine and kidney.

Due to the abundant expression of PEPT1 in the small intestine and its capacity of transporting various drugs and di-/tri-peptides, PEPT1 is believed to play an essential role in the intestinal absorption of its substrates. Therefore, some studies focused on the mapping of PEPT1 expression along the digestive tract in different species. Reverse-transcriptase polymerase chain reaction (RT-PCR) has been used as the main tool for studying mRNA expression of PEPT1 in various intestinal regions in man. Englund et al. (2006) reported a relatively uniform distribution of PEPT1 in the small intestine but extremely low PEPT1 mRNA levels in the colon by analyzing biopsy samples of human duodenum, jejunum, ileum and colon. Similar findings were later reported by another group of researchers independently (Meier et al., 2007). However, Herrera-Ruiz et al.

(2001) found predominant expression of PEPT1 in the duodenum and much lower expression levels in other segments of the human intestine. On the other hand, nearly uniformly high expression of PEPT1 in the small intestine and negligible expression in the colon have been reported in both rat (Hironaka et al., 2009) and mouse (Jappar et al., 2010) at the protein level. Moreover, mice and humans were found to have similar expression levels of PEPT1 in duodenum while rats exhibited three- to five-fold higher expression profiles (Kim et al., 2007). The available quantitative distribution information of PEPT1 can be potentially useful in understanding and modeling the intestinal absorption of PEPT1 substrates.

Regulation mechanism. Expression and function of PEPT1 are under the tight regulation of numerous physiological, pharmacological and pathological factors. High-protein diet and starvation (Katsura and Inui, 2003), pharmaceutical agents including pentazocine (Fujita et al., 1999), cyclosporine and tacrolimus (Motohashi et al., 2001), 5-fluorouracil (Inoue et al., 2005), various hormones (Rubio-Aliaga and Daniel, 2008) as well as inflammation (Dalmasso et al., 2008; Nguyen et al., 2009; Ingersoll et al., 2012) are some important regulators reported in literature. In particular, high protein diets and starvation were found to increase the expression of PEPT1 mRNA, protein and subsequently PEPT1 activity in rats (Naruhashi et al., 2002; Adibi et al., 2003; Katsura et al., 2003). Similarly, Ma et al. (2011) also showed fasting could up-regulate the expression of PEPT1 protein and consequently the *in vivo* oral absorption of PEPT1 substrate glycylsarcosine in mice. Regulators of PEPT1 deserve further investigation to elucidate the intra-/inter-individual variability in PEPT1 expression and activity and

consequently the absorption, distribution, elimination and pharmacokinetics of PEPT1 substrates.

PEPT1 TARGETED PRODRUGS

As discussed in the preceding section, the localization and abundant expression of PEPT1 determines its physiological and pharmacological relevance in the intestinal absorption of its substrates. Furthermore, PEPT1 shows exceptionally broad substrate specificity and low-affinity high-capacity transport characteristics, therefore making it a tempting drug delivery target for improving the oral absorption of poorly absorbable drugs. In different stages of drug discovery and development, the concept of targeting intestinal PEPT1 for improved oral absorption and availability is emerging as one of the promising means of mitigating the permeability-related absorption limitation of oral drugs (Li et al., 2008; Varma et al., 2010).

Currently, for the rational design of PEPT1 targeted prodrugs, a widely employed synthesis approach is to form dipeptide or amino acid conjugated prodrugs by linking the active parent drugs that are not recognized by PEPT1 with dipeptides or amino acid moieties (sometimes through a linker if necessary). As a result of the covalent conjugation, the entire prodrugs can be recognized as PEPT1 substrates and efficiently transported by intestinal PEPT1, leading to improved intestinal absorption. In addition to increased permeability, another key determinant of successful PEPT1 targeted prodrugs is adequate stability in the intestinal lumen but rapid and extensive enzymatic hydrolysis after absorption for exertion of its pharmacological effects. Incomplete bioconversion could impair the effectiveness of the prodrug approach and potentially lead to the formation of inactive or even toxic metabolites.

A vast number of PEPT1 targeted prodrugs, synthesized following the above-mentioned approach, have shown improved PEPT1-mediated transport and oral availability. A recent successful example is LY544344, a rationally synthesized alanyl prodrug of the potent and selective group II/cAMP-coupled metabotropic glutamate receptor agonist LY354740. LY544344 displayed PEPT1-mediated uptake in Caco-2 cells and intestinal permeability during perfusions in rats (Varma et al., 2009; Eriksson et al., 2010), and showed approximately 17-fold higher dose-normalized area under the plasma concentration-time curve (AUC) of LY354740 compared with oral dosing of the active drug (Perkins and Abraham, 2007). An L-valyl prodrug of the poorly orally absorbed chemotherapy agent cytarabine showed PEPT1-mediated uptake in Caco-2 cells that could be inhibited by an excess of PEPT1 substrate glycylsarcosine and approximately 3-fold increase in the AUC of drug following its oral administration (Sun et al., 2009).

Other examples of PEPT1 targeted prodrugs include midodrine (Tsuda et al., 2006), a series of amino acid monoester prodrugs of floxuridine (Tsume et al., 2008), prodrugs of some benzyl or benzoyl molecules conjugated with thiodipeptide carriers (Foley et al., 2009), prodrugs of polar [3-(hydroxymethyl)-phenyl]guanidine conjugated with L-valine, L-isoleucine, and L-phenylalanine (Sun et al., 2010), and L-valyl prodrug of zanamivir (Gupta et al., 2011). This PEPT1 targeted prodrug strategy has demonstrated to be suitable and feasible for improving oral absorption of highly polar and poorly permeable drugs. Recently, a shift in the discovery of new chemical entities toward more hydrophilic libraries has become noticeable, due to toxicities and metabolic liabilities frequently reported for lipophilic drugs (Varma et al., 2010). Due to the

increased importance of hydrophilic compounds, PEPT1 targeted prodrugs for enhancing permeability and absorption is likely to be continuously pursued since oral delivery is still the favorable and preferred route of drug delivery.

VALACYCLOVIR

The prototype of PEPT1 targeted prodrugs is valacyclovir, an L-valyl ester prodrug of the antiviral agent acyclovir, which shows three- to five-fold higher oral availability compared with oral acyclovir in humans. Chemical structures of acyclovir (ACV) and valacyclovir (VACV) are shown in Figure 2.3. Both acyclovir and valacyclovir are highly polar molecules with Log P values of -1.59 and -1.08, respectively. Historically, the identification of valacyclovir as a PEPT1 targeted prodrug was made retrospectively through extensive uptake and transport studies after its demonstrated improved oral availability. Although the discovery of valacyclovir's absorption mechanism was to some extent by serendipity, the knowledge and insights gained from its success lead to the concept of rationally designed PEPT1 targeted prodrugs.

In this project, valacyclovir was chosen as the model PEPT1 targeted prodrug for the assessment of the quantitative significance of intestinal PEPT1 in enhancing the oral absorption and availability of PEPT1 targeted prodrugs. We were motivated to propose such a project because, in spite of ongoing research in the area of PEPT1 targeted prodrugs, no existing studies quantitatively evaluated the importance of PEPT1 in facilitating the absorption of these targeted prodrugs. In other words, given the overlapping substrate specificity of multiple transporters and their co-expression in the small intestine, it is possible that other known or unknown transporters (or passive processes) may play an important role in the absorption of PEPT1 targeted prodrugs.

Without characterizing the quantitative relevance of PEPT1, it is risky to develop increasingly selective PEPT1 substrates with the aid of computational drug design.

In the following section, the transport mechanism, hydrolysis and pharmacokinetics of valacyclovir and/or its active drug acyclovir will be presented.

Transport mechanism of valacyclovir. The intriguing question about the mechanism responsible for the improved oral absorption of valacyclovir was raised shortly after its discovery. To investigate this question, numerous uptake and transport studies of valacyclovir were conducted. The influx of valacyclovir in cynomologus monkey intestine brush border membrane vesicles (BBMV) was found to be 6- to 10-time higher than the influx of acyclovir and was inhibited by several dipeptides, suggesting the possible involvement of intestinal PEPT1 (Smith et al., 1993). Similarly in Caco-2 cells, valacyclovir showed 7-fold higher apical-to-basolateral transport than that of acyclovir and competitively inhibited the uptake of glycyclsarcosine (de Vrueh et al., 1998; Ganapathy et al., 1998). Other cell culture systems transfected with rat PEPT1 or human PEPT1 were also used to examine the interaction of valacyclovir with PEPT1 (Balimane et al., 1998; Guo et al., 1999; Sawada et al., 1999; Balimane and Sinko, 2000; Bhardwaj et al., 2005). All in all, these studies suggested that valacyclovir was transported by PEPT1 in a saturable, concentration- and pH-dependent manner *in vitro*. Moreover, findings of two *in situ* perfusion studies in rat small intestine again confirmed the interaction of valacyclovir with intestinal PEPT1 (Han et al., 1998; Sinko and Balimane, 1998).

Although different studies collectively confirmed the ability of PEPT1 to transport the non-peptidic drug valacyclovir in cell cultures, their findings differed with respect to the transport characteristics of PEPT1-mediated uptake of valacyclovir. From these studies, the affinity of valacyclovir for PEPT1, as judged by the inhibition constant (K_i), ranged from 0.49 mM (Ganapathy et al., 1998) to 4.08 mM (Balimane et al., 1998) and, as judged by the Michaelis-Menten constant (K_m), ranged from 0.3 mM (Han et al., 1998) to about 6 mM (Balimane et al., 1998), depending on different experimental settings. Conflicting results were also reported for the pH-dependency of PEPT1-mediated uptake of valacyclovir. One study performed in Caco-2 cells reported a pH-independent PEPT1-mediated valacyclovir uptake when the medium pH was 6.0 and 7.4 (de Vrueh et al., 1998). Other cell-based studies used different optimal pH values for measuring valacyclovir uptake, such as pH 6.0 in MDCK expressing hPEPT1 cells (Bhardwaj et al., 2005), pH 6.5 in oocytes expressing hPEPT1 (Balimane et al., 1998), and pH 7.5 in CHO cells transfected with hPEPT1 (Guo et al., 1999). Balimane and Sinko (2000) conducted a systematic investigation regarding the effect of external pH values on valacyclovir uptake in CHO/hPEPT1 cells, and found that different ionic species of valacyclovir exhibited differential affinities for PEPT1. In that study, the K_m of neutral and cationic forms of valacyclovir was estimated at 1.2 and 7.4 mM, respectively.

Nevertheless, PEPT1 is not the only transporter that can recognize and transport valacyclovir. In addition to PEPT1, PEPT2 has also been shown to be able to transport valacyclovir (Ganapathy et al., 1998). In the rat intestinal perfusion study (Sinko and Balimane, 1998), the jejunal permeability of valacyclovir was significantly inhibited by a typical organic anion *p*-aminohippuric acid or a typical organic cation quinine in addition

to PEPT1 substrates, suggesting the possible interaction between valacyclovir and organic anion transporters (OATs) and cation transporters (OCTs). In S2 cells transfected with human OAT-3, valacyclovir was found to be transported in a concentration-dependent manner with K_m and maximum transport velocity (V_{max}) estimated to be 57.9 μM and 200 pmol/mg protein/min, respectively (Takeda et al., 2002). Hatanaka et al. (2004) showed that valacyclovir can be transported by a Na^+/Cl^- coupled amino acid transporter $ATB^{0,+}$. The ability of $ATB^{0,+}$ to transport valacyclovir was comparable to that of hPEPT1 using HRPE cells expressing mouse $ATB^{0,+}$ and human PEPT1 heterologously. The significance of this finding is that $ATB^{0,+}$, which is abundantly expressed on the apical membrane of colonocytes, may be a potential delivery target for amino acid based prodrugs. In addition, PHT1 was reported to significantly increase the uptake of valacyclovir into COS-7 cells expressing human PHT1 compared to mock control cells, suggesting that PHT1 may participate in the intestinal uptake of valacyclovir considering the reported expression of PHT1 protein along the human intestinal tract (Bhardwaj et al., 2006). Finally, a putative human peptide transporter (HPT1) has also been shown to actively mediate the cellular uptake of valacyclovir (Landowski et al., 2003). Overall, more than six transporters have been implicated in the intestinal transport of valacyclovir with most studies being focused on PEPT1.

Hydrolysis of valacyclovir. Chemical and enzymatic stability of valacyclovir is another prominent topic since both premature hydrolysis of valacyclovir in the intestinal lumen and incomplete bioactivation after intestinal absorption could decrease the systemic availability of acyclovir. *In vitro* stability of valacyclovir was evaluated in various aqueous solutions, biological fluids and different tissue or cell homogenates

(Burnette and de Miranda, 1994; Sinko and Balimane, 1998; Granero and Amidon, 2006). Overall, valacyclovir is chemically stable under acidic pH (pH < 4) conditions but degrades in alkaline medium by base-catalyzed pseudo-first-order kinetics. In addition, valacyclovir is stable in stomach fluid while its degradation in intestinal fluid is faster than in phosphate buffer at the same pH, suggesting its susceptibility to hydrolyzing enzymes. Valacyclovir stability, expressed in terms of its degradation half-lives under different conditions, is shown in Table 2.1. Enzymes responsible for the hydrolysis of valacyclovir have been characterized in man and rats. Burnette et al. (1995) purified and characterized a rat liver enzyme that preferentially catalyzes the hydrolysis of valacyclovir and some other amino acid esters of acyclovir. In man, a biphenyl hydrolase-like protein (BPHL), also called human valacyclovirase, was purified and enriched from the solubilized membrane of Caco-2 cells. It was later identified as a novel human serine hydrolase selectively and efficiently catalyzing the biotransformation of ester prodrugs, for example, valacyclovir (Kim et al., 2003). Other generally occurring esterases or carboxylesterases may also play a role in the *in vivo* hydrolysis of valacyclovir. These highly efficient hydrolyzing enzymes for valacyclovir ensure complete and rapid activation of valacyclovir to acyclovir in the intestine and liver of different species. For instance, valacyclovir peak plasma levels in human subjects were less than 3% of corresponding acyclovir levels (Soul-Lawton et al., 1995). Similarly, rapid and complete conversion of valacyclovir to acyclovir was also demonstrated in preclinical models (Burnette and de Miranda, 1994; de Miranda and Burnette, 1994). Because of the nearly complete presystemic hydrolysis of valacyclovir, the *in vivo*

pharmacokinetics of acyclovir is the best measure of the performance of this orally administered prodrug.

Pharmacokinetics of valacyclovir. The mean absolute availability of acyclovir after oral administration of a single dose of valacyclovir in monkeys (10 mg/kg), rats (25 mg/kg) and humans (1000 mg) were approximately 67%, 65% and 54%, respectively (Burnette and de Miranda, 1994; de Miranda and Burnette, 1994; Soul-Lawton et al., 1995). Acyclovir, derived from oral valacyclovir, exhibited dose-independent pharmacokinetics at 10 mg/kg and 25 mg/kg in both rats and monkeys (Burnette and de Miranda, 1994; de Miranda and Burnette, 1994). Linear correlations were observed between valacyclovir doses and acyclovir C_{max} and AUC. However, in human subjects, inconsistent results about dose proportionality of pharmacokinetic parameters have been found. It was reported that C_{max} and AUC values for acyclovir increased in a slightly less than dose-proportional manner in healthy volunteers receiving 100-1000 mg of valacyclovir orally (Weller et al., 1993). Acyclovir C_{max} ranged from 0.83 to 5.65 mg/L, T_{max} from 0.88 to 1.75 hr, and AUC ranged from 2.28 to 19.52 mg·hr/L. Another study also showed non-linear increases in acyclovir C_{max} and AUC following multiple dosing regimens of valacyclovir in the range of 250-2000 mg (Jacobson, 1993). In contrast, in patients with genital HSV disease, the increase of acyclovir C_{max} and AUC was linear over the dose range of 250 - 1000 mg (Ormrod et al., 2000). The *in vivo* distribution, metabolism, and elimination properties of acyclovir after its entry into the systemic circulation are identical following dosing of valacyclovir or acyclovir, and reviewed later.

Detailed pharmacokinetics of acyclovir following oral administration of valacyclovir in preclinical species and human subjects are extracted from the literature and summarized in Tables 2.2 and 2.3, respectively.

Uptake mechanism of acyclovir. The poorly permeable active drug acyclovir is not transported by PEPT1 (Han et al., 1998). The reported mechanism of acyclovir transport in the intestine is mainly passive diffusion (Meadows and Dressman, 1990; Fujioka et al., 1991). Using *in vitro* intestinal ring and *in situ* single-pass perfusion methods, Meadows and Dressman (1990) showed that the permeability of acyclovir was linear over a wide range of concentrations and was also unaffected by the addition of metabolic inhibitors. The apparent permeability of acyclovir in rat jejunum was reported to be 1.0×10^{-5} cm/sec (Zakelj et al., 2004). Because of the low jejunal permeability and high polarity of acyclovir, Kagan and Hoffman (2008) postulated that acyclovir mainly undergoes paracellularly passive diffusion in the intestine without substantiating the claim with experimental evidence. In other cell culture studies, acyclovir was found to be actively transported by OAT1 and OCT1, which may principally affect the elimination of acyclovir in the kidney (Wada et al., 2000; Takeda et al., 2002).

Pharmacokinetics of acyclovir. The kinetics and disposition of the active drug acyclovir in different species will be briefly summarized.

Plasma protein binding and distribution. Acyclovir displays minimal plasma protein binding in different species. Binding of acyclovir to plasma proteins was 15.4±4.4% by ultrafiltration of 12 plasma samples of patients receiving [^{14}C]acyclovir (de Miranda et al., 1981b). *In vitro* acyclovir plasma protein binding was about 13% in mouse plasma at

a drug concentration of 88 µM, and about 22% and 33% in human plasma at acyclovir plasma concentrations of 17.8 µM and 1.8 µM, respectively (de Miranda et al., 1981a). In a dog given intravenous acyclovir, the extent of acyclovir plasma ranged from 30% to 36% (de Miranda et al., 1981a). Acyclovir distributes well into most body tissues including the vesicular fluid and central nervous system (de Miranda et al., 1981a; Fletcher and Bean, 1985).

Renal excretion of acyclovir. The major route of acyclovir elimination is by renal excretion of unchanged drug. Renal clearance (CL_R) of acyclovir was two to three times higher than glomerular filtration over the oral dose range of 2.5-15.0 mg/kg acyclovir, suggesting the involvement of an active tubular secretion mechanism in its elimination (Laskin et al., 1982; Whitley et al., 1982).

Metabolism of acyclovir. Acyclovir metabolism exhibits significant species differences. In rats, mice, dogs and humans, acyclovir is excreted unchanged in the urine. Following intravenous dosing of [^{14}C] acyclovir, unchanged acyclovir accounted for 62-91% (de Miranda et al., 1981b), 94% (de Miranda et al., 1981a) and 95% (de Miranda et al., 1981a) of the urinary radioactivity in humans, mice and rats, respectively. In contrast, in pigs, rabbits and monkeys, acyclovir is extensively metabolized into one or two major metabolites: 9-carboxymethoxymethylguanine (9-CMMG) and 8-hydroxyacyclovir (de Miranda et al., 1981a; de Miranda and Good, 1992; de Miranda and Burnette, 1994).

Pharmacokinetics of acyclovir. Oral availability of acyclovir exhibits species differences after its oral administration. The urinary recoveries of acyclovir in dogs, mice, rats, and rhesus monkeys were estimated to be approximately 75.3%, 43.2%, 19.2%, and

3.7% respectively (de Miranda et al., 1981a). Moreover, acyclovir urinary recovery decreased with increasing doses of 100-300 mg/kg in rats and mice, suggesting a dose-limited absorption. Pharmacokinetic parameters of acyclovir following its oral or intravenous dosing in animals are shown in Table 2.4.

The availability of oral acyclovir in human subjects is low and variable, which also decreases during dose escalation (Laskin, 1983). Acyclovir was often administered as 1-hr intravenous infusions, which demonstrated dose-independent kinetics in single-dose studies over 0.5 to 5.0 mg/kg (de Miranda et al., 1979) and 2.5 to 15 mg/kg (Laskin et al., 1982), or multiple-dose studies (Whitley et al., 1982). Results from these studies showed that acyclovir usually displayed a biexponential decline, with a terminal half-life ($T_{1/2}$) of 2 to 3 hours, an apparent volume of distribution at steady state (V_{dss}) of 44 to 55 L/1.73 m^2, a total clearance (CL) of 200-300 mL/min/1.73 m^2 and a renal clearance (CL_R) similar to or slightly smaller than total CL (de Miranda and Blum, 1983). Moreover, both total and renal clearances of acyclovir were found to decrease with renal impairment while V_{dss} estimates were independent of renal function. Kinetic parameters of acyclovir after intravenous acyclovir are shown in Table 2.5.

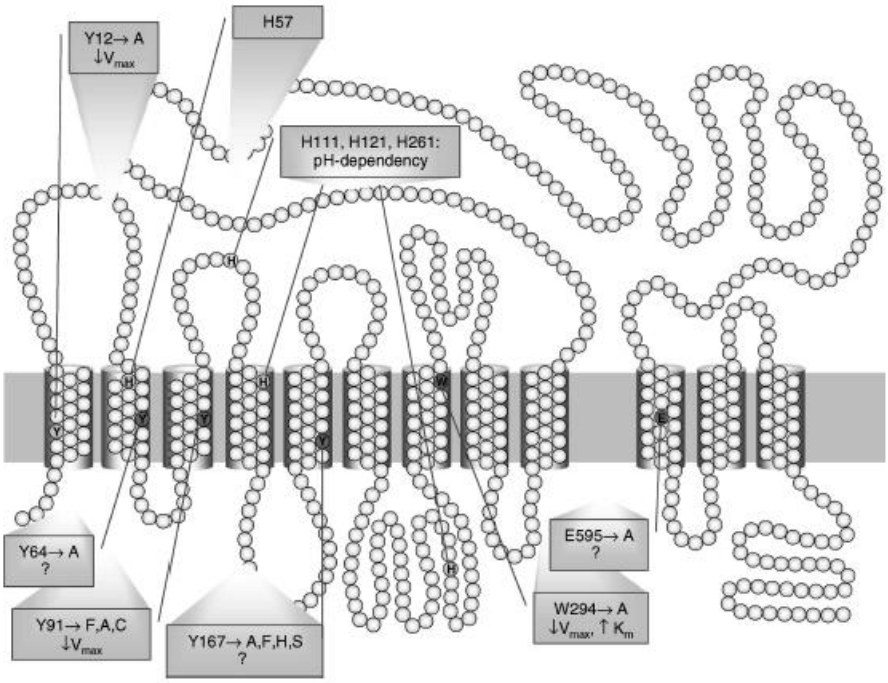

Figure 2.1 Membrane topology model of mammalian PEPT1 with key structural features and influential amino acid residues displayed (Adopted from Rubio-Aliaga and Daniel, 2008).

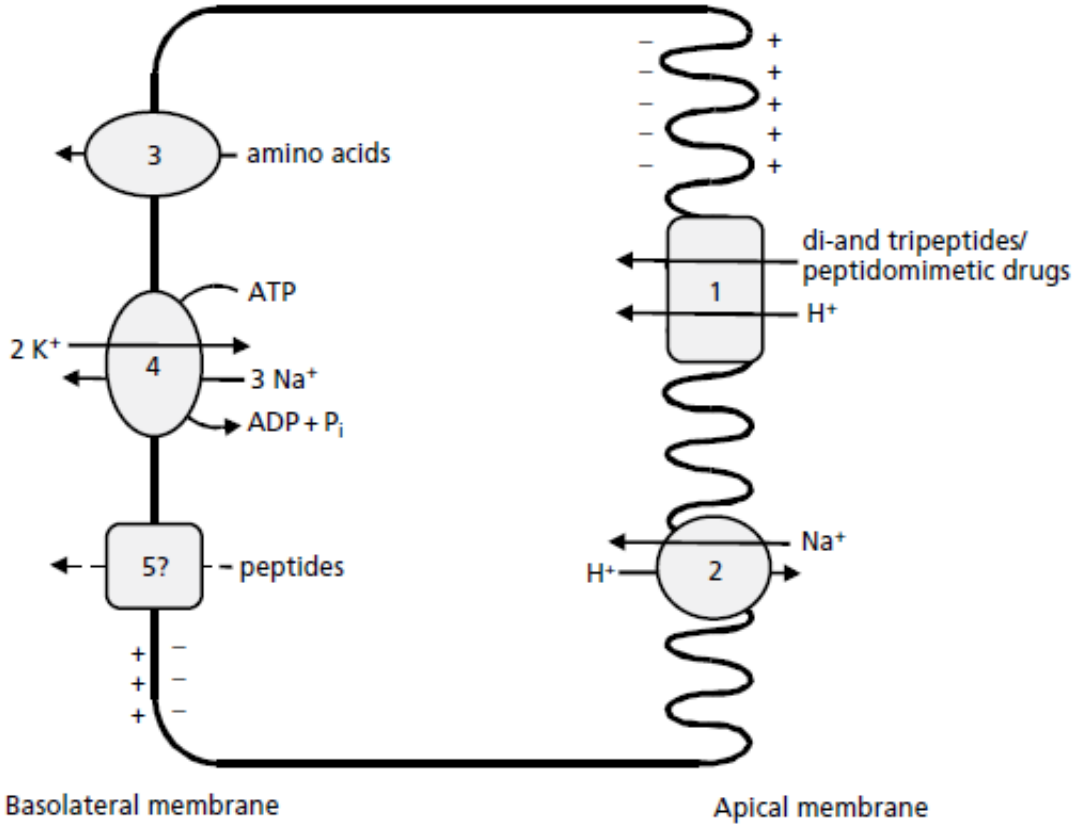

Figure 2.2 Schematic of PEPT1-mediated transport in epithelial cells: 1 represents PEPT1, 2 the sodium proton exchanger 3 (NHE3), 3 the certain amino acid transporters, 4 the Na^+-K^+-ATPase and 5 the basolateral peptide transporters. (Adopted from Brandsch et al., 2008).

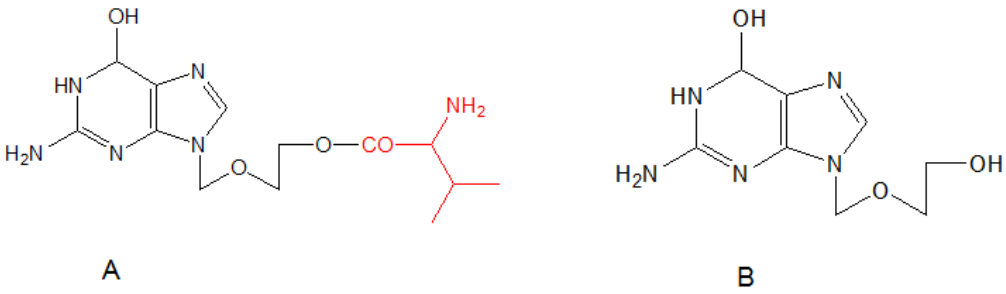

Figure 2.3 Chemical structures of (A) valacyclovir and (B) acyclovir.

Table 2.1 *In vitro* half-lives of valacyclovir

Medium	pH	37°C	25°C	References
Deionized water			2~16 days	1
TCA solution, 3%			203 days	1
Sodium phosphate buffer, 0.1 M	6.0	95 hr		3
Phosphate buffer	6.3	15.5 hr		3
Phosphate buffer	7.4	10.6 hr		3
MES buffer	5.0		577.5 hr	2
MES buffer	6.5		38.5 hr	2
MES buffer	7.5		19.3 hr	2
Gastric fluid, simulated	1.2	ND[a]		1
Intestinal fluid, simulated	7.5	6.6 hr		1
Dog gastric fluid	2.3	63 hr		3
Dog intestinal fluid	7.5	6 hr		3
Human gastric fluid	1.2	1122 hr		3
Human intestinal fluid	6.3	9.4 hr		3
Rat plasma, EDTA-treated		7.9 hr	10 hr	1
Rat intestine homogenate	7.5		1.5 hr	2
Rat intestine homogenate	7.5	0.25 hr		2
Rat intestine homogenate	7.5	4.7 hr		1
Rat liver homogenate	7.5	16 min		1

[a]No detectable hydrolysis during 1-hr incubation.
1: Burnette and de Miranda, 1994.
2: Sinko and Balimane, 1998.
3: Granero and Amidon, 2006.

Table 2.2 Pharmacokinetic parameters of acyclovir after oral dosing of valacyclovir in preclinical animals[a]

Parameter (unit)	Monkeys		Rats	
Dose (mg/kg)	10	25	10	25
Availability (%)	67±13			
Urinary Recovery (%)				65±2
T_{max} (hr)	2.2±0.8	2.2±0.8	0.4±0.2	0.6±0.2
C_{max} (µM)	8.2±2.6	22.9±6.7	4.8±1.1	12.8±2.5
$AUC_{0\text{-inf}}$ (µM·hr)	23.7±2.4	60.2±14.6	7.4±2.2	17.8±2.3
Terminal $T_{1/2}$ (hr)	1.5±0.3	1.3±0.3	1.1±0.3	0.8±0.3
References	1	1	2	2

Data are expressed as mean ±SD (n=3).
[a]Estimated using non-compartmental analysis.
1: de Miranda P and Burnette TC, 1994.
2: Burnette TC and de Miranda P, 1994.

Table 2.3 Pharmacokinetic parameters of acyclovir after oral dosing of valacyclovir in humans[a]

Parameter (unit)						
Dose (mg)	100	250	500	750	1000	1000
Availability (%)						54.2[b]
Urinary Recovery (%)	75.9±8.6	65.0±8.9	71.6±6.1	49.0±11.8	44.3±10.0	45.8±17.1
T_{max} (hr)	0.9±0.1	1.0±0.3	1.5±0.6	1.5±0.6	1.8±0.6	1.7±0.7
C_{max} (μM)	3.7±0.6	9.5±2.2	14.6±3.7	18.5±5.1	25.1±10.5	29.5 ±12.5
CL_R (mL/min)						255.3±85.8
$AUC_{0\text{-}inf}$ (μM·hr)	10.1±1.8	25.6±2.7	51.5±7.9	62.7±15.7	86.7±26.8	89.4±19.4
Terminal $T_{1/2}$ (hr)	2.8±0.6	2.8±0.4	2.9±0.2	2.9±0.5	3.0±0.1	2.6±0.4
References	1	1	1	1	1	2

Data are expressed as mean ±SD unless otherwise stated.
[a]Estimated using non-compartmental analysis.
[b]Mean availability only, with a 95% confidence interval of 49.4%-59.5%.
1: Weller et al., 1993.
2: Soul-Lawton et al., 1995.

Table 2.4 Pharmacokinetic parameters of acyclcovir after intravenous or oral dosing of acyclovir in animals

Parameter (unit)	Dog	Monkey	Rat		Mouse
Dose (mg/kg)	20 (oral)	25 (oral)	25 (oral)	25 (intravenous)	25 (oral)
Urinary Recovery (%)	75.3 ±1.3	3.7±0.5	19.2 ± 8.1 ↓[c]		43.2[a] ↓[b]
T_{max} (hr)	2.0		1.0		0.25
C_{max} (μM)	60.5 ± 3.5	<2	2.7 ± 3.5		52[a]
Terminal $T_{1/2}$ (hr)				14.4	
Vdss (L/kg)				2.22	
References			1		

Data are expressed as mean ±SD unless otherwise stated.
[a]A single value was estimated after pooling blood of five mice.
[b]Progressively decreased from 48.5% to 11.0% when dose increased from 100 mg/kg to 300 mg/kg.
[c]Progressively decreased from 12.2% to 3.2% when dose increased from 100 mg/kg to 300 mg/kg.
1: de Miranda P et al., 1981a.

Table 2.5 pharmacokinetic parameters of acyclovir after intravenous or oral dosing of acyclovir in humans

Parameter (unit)					
Dose, by 1-hr infusion	350 mg	2.5 mg/kg	5.0 mg/kg	10.0 mg/kg	15.0 mg/kg
Urinary Recovery (%)	86.7 ±19.9				
T_{max} (hr)	0.98±0.07				
C_{max} (μM)	41.0 ±8.4	20.1 ±1.4	36.8 ±11.6	64.8±10.2	100.8±46.2
CL (mL/min)[b]	322.0 ± 68.0	239.2 ±26.8 [a]	268.8 ±94.1[a]	321.1±110.2[a]	394.0±97.1[a]
CL_R (mL/min)[b]	282.9 ± 103.0	158.2 ±18.5 [a]	225.1 ±99.6 [a]	238.4±63.7 [a]	398.2±66.6 [a]
$AUC_{0\text{-inf}}$ (μM·hr)	84.0 ± 14.2	55.8 ±9.5	102.9 ±39.0	160.6±37.8	191.7±52.1
V_{dss} (L/1.73 m^2)		44.1 ±6.9	43.1 ±4.6	55.9±4.9	53.4±11.8
Terminal $T_{1/2}$ (hr)	2.4±0.3	2.9±0.2	2.8±0.9	3.3±1.1	2.4±0.4
References	1	2	2	2	2

Data are expressed as mean ±SD unless otherwise stated.
[a]Data are in mL/min/1.73m^2.
[b]Decreased with impaired renal function.
1: Soul-Lawton J et al., 1995.
2: Laskin OL et al., 1982.

REFERENCES

Anderle P, Nielsen CU, Pinsonneault J, Krog PL, Brodin B, and Sadee W (2006) Genetic variants of the human dipeptide transporter PEPT1. *Journal of Pharmacology and Experimental Therapeutics* **316:**636-646.

Balimane P and Sinko P (2000) Effect of ionization on the variable uptake of valacyclovir via the human intestinal peptide transporter (hPepT1) in CHO cells. *Biopharmaceutics & drug disposition* **21:**165-174.

Balimane PV, Tamai I, Guo A, Nakanishi T, Kitada H, Leibach FH, Tsuji A, and Sinko PJ (1998) Direct evidence for peptide transporter (PepT1)-mediated uptake of a nonpeptide prodrug, valacyclovir. *Biochem Biophys Res Commun* **250:**246-251.

Bhardwaj RK, Herrera-Ruiz D, Eltoukhy N, Saad M, and Knipp GT (2006) The functional evaluation of human peptide/histidine transporter 1 (hPHT1) in transiently transfected COS-7 cells. *European journal of pharmaceutical sciences : official journal of the European Federation for Pharmaceutical Sciences* **27:**533-542.

Bhardwaj RK, Herrera-Ruiz D, Sinko PJ, Gudmundsson OS, and Knipp G (2005) Delineation of human peptide transporter 1 (hPepT1)-mediated uptake and transport of substrates with varying transporter affinities utilizing stably transfected hPepT1/Madin-Darby canine kidney clones and Caco-2 cells. *J Pharmacol Exp Ther* **314:**1093-1100.

Bockman DE, Ganapathy V, Oblak TG, and Leibach FH (1997) Localization of peptide transporter in nuclei and lysosomes of the pancreas. *Int J Pancreatol* **22:**221-225.

Brandsch M, Knutter I, and Bosse-Doenecke E (2008) Pharmaceutical and pharmacological importance of peptide transporters. *J Pharm Pharmacol* **60:**543-585.

Burnette TC and de Miranda P (1994) Metabolic disposition of the acyclovir prodrug valaciclovir in the rat. *Drug Metab Dispos* **22:**60-64.

Burnette TC, Harrington JA, Reardon JE, Merrill BM, and de Miranda P (1995) Purification and characterization of a rat liver enzyme that hydrolyzes valaciclovir, the L-valyl ester prodrug of acyclovir. *J Biol Chem* **270:**15827-15831.

Charrier L, Driss A, Yan Y, Nduati V, Klapproth JM, Sitaraman SV, and Merlin D (2006) hPepT1 mediates bacterial tripeptide fMLP uptake in human monocytes. *Lab Invest* **86:**490-503.

Dalmasso G, Nguyen HT, Yan Y, Charrier-Hisamuddin L, Sitaraman SV, and Merlin D (2008) Butyrate transcriptionally enhances peptide transporter PepT1 expression and activity. *PLoS One* **3:**e2476.

de Miranda P and Blum MR (1983) Pharmacokinetics of acyclovir after intravenous and oral administration. *J Antimicrob Chemother* **12 Suppl B:**29-37.

de Miranda P and Burnette TC (1994) Metabolic fate and pharmacokinetics of the acyclovir prodrug valaciclovir in cynomolgus monkeys. *Drug Metab Dispos* **22:**55-59.

de Miranda P, Good SS, Laskin OL, Krasny HC, Connor JD, and Lietman PS (1981b) Disposition of intravenous radioactive acyclovir. *Clin Pharmacol Ther* **30**:662-672.

de Miranda P, Krasny HC, Page DA, and Elion GB (1981a) The disposition of acyclovir in different species. *J Pharmacol Exp Ther* **219:**309-315.

de Vrueh RL, Smith PL, and Lee CP (1998) Transport of L-valine-acyclovir via the oligopeptide transporter in the human intestinal cell line, Caco-2. *J Pharmacol Exp Ther* **286:**1166-1170.

Englund G, Rorsman F, Ronnblom A, Karlbom U, Lazorova L, Grasjo J, Kindmark A, and Artursson P (2006) Regional levels of drug transporters along the human intestinal tract: Co-expression of ABC and SLC transporters and comparison with Caco-2 cells. *European Journal of Pharmaceutical Sciences* **29:**269-277.

Eriksson AH, Varma MV, Perkins EJ, and Zimmerman CL (2010) The intestinal absorption of a prodrug of the mGlu2/3 receptor agonist LY354740 is mediated by PEPT1: in situ rat intestinal perfusion studies. *J Pharm Sci* **99:**1574-1581.

Fei YJ, Kanai Y, Nussberger S, Ganapathy V, Leibach FH, Romero MF, Singh SK, Boron WF, and Hediger MA (1994) Expression cloning of a mammalian proton-coupled oligopeptide transporter. *Nature* **368:**563-566.

Fei YJ, Sugawara M, Liu JC, Li HW, Ganapathy V, Ganapathy ME, and Leibach FH (2000) cDNA structure, genomic organization, and promoter analysis of the mouse intestinal peptide transporter PEPT1. *Biochim Biophys Acta* **1492:**145-154.

Fletcher C and Bean B (1985) Evaluation of oral acyclovir therapy. *Drug intelligence & clinical pharmacy* **19:**518-524.

Foley D, Pieri M, Pettecrew R, Price R, Miles S, Lam HK, Bailey P, and Meredith D (2009) The in vitro transport of model thiodipeptide prodrugs designed to target the intestinal oligopeptide transporter, PepT1. *Org Biomol Chem* **7:**3652-3656.

Fujioka Y, Mizuno N, Morita E, Motozono H, Takahashi K, Yamanaka Y, and Shinkuma D (1991) Effect of age on the gastrointestinal absorption of acyclovir in rats. *J Pharm Pharmacol* **43:**465-469.

Fujita T, Majikawa Y, Umehisa S, Okada N, Yamamoto A, Ganapathy V, and Leibach FH (1999) sigma Receptor ligand-induced up-regulation of the H(+)/peptide transporter PEPT1 in the human intestinal cell line Caco-2. *Biochem Biophys Res Commun* **261:**242-246.

Ganapathy ME, Huang W, Wang H, Ganapathy V, and Leibach FH (1998) Valacyclovir: a substrate for the intestinal and renal peptide transporters PEPT1 and PEPT2. *Biochem Biophys Res Commun* **246:**470-475.

Ganapathy V and Leibach FH (1983) Role of pH gradient and membrane potential in dipeptide transport in intestinal and renal brush-border membrane vesicles from the rabbit. Studies with L-carnosine and glycyl-L-proline. *J Biol Chem* **258:**14189-14192.

Granero GE and Amidon GL (2006) Stability of valacyclovir: implications for its oral bioavailability. *International journal of pharmaceutics* **317:**14-18.

Guo A, Hu P, Balimane PV, Leibach FH, and Sinko PJ (1999) Interactions of a nonpeptidic drug, valacyclovir, with the human intestinal peptide transporter (hPEPT1) expressed in a mammalian cell line. *J Pharmacol Exp Ther* **289:**448-454.

Gupta SV, Gupta D, Sun J, Dahan A, Tsume Y, Hilfinger J, Lee KD, and Amidon GL (2011) Enhancing the Intestinal Membrane Permeability of Zanamivir: A Carrier Mediated Prodrug Approach. *Molecular Pharmaceutics* **8:**2358-2367.

Han H, de Vrueh RL, Rhie JK, Covitz KM, Smith PL, Lee CP, Oh DM, Sadee W, and Amidon GL (1998) 5'-Amino acid esters of antiviral nucleosides, acyclovir, and AZT are absorbed by the intestinal PEPT1 peptide transporter. *Pharm Res* **15:**1154-1159.

Hatanaka T, Haramura M, Fei YJ, Miyauchi S, Bridges CC, Ganapathy PS, Smith SB, Ganapathy V, and Ganapathy ME (2004) Transport of amino acid-based prodrugs by the Na+- and Cl(-) -coupled amino acid transporter ATB0,+ and expression of the transporter in tissues amenable for drug delivery. *J Pharmacol Exp Ther* **308:**1138-1147.

Herrera-Ruiz D, Wang Q, Gudmundsson OS, Cook TJ, Smith RL, Faria TN, and Knipp GT (2001) Spatial expression patterns of peptide transporters in the human and rat gastrointestinal tracts, Caco-2 in vitro cell culture model, and multiple human tissues. *AAPS pharmSci* **3:**E9.

Hironaka T, Itokawa S, Ogawara KI, Higaki K, and Kimura T (2009) Quantitative Evaluation of PEPT1 Contribution to Oral Absorption of Cephalexin in Rats. *Pharmaceutical Research* **26:**40-50.

Hu Y, Smith DE, Ma K, Jappar D, Thomas W, and Hillgren KM (2008) Targeted disruption of peptide transporter Pept1 gene in mice significantly reduces dipeptide absorption in intestine. *Mol Pharm* **5:**1122-1130.

Ingersoll SA, Ayyadurai S, Charania MA, Laroui H, Yan Y, and Merlin D (2012) The role and pathophysiological relevance of membrane transporter PepT1 in intestinal inflammation and inflammatory bowel disease. *American journal of physiology Gastrointestinal and liver physiology* **302:**G484-492.

Inoue M, Terada T, Okuda M, and Inui K (2005) Regulation of human peptide transporter 1 (PEPT1) in gastric cancer cells by anticancer drugs. *Cancer Lett* **230:**72-80.

Jacobson MA (1993) Valaciclovir (BW256U87): the L-valyl ester of acyclovir. *Journal of medical virology* **Suppl 1:**150-153.

Jappar D, Wu SP, Hu Y, and Smith DE (2010) Significance and regional dependency of peptide transporter (PEPT) 1 in the intestinal permeability of glycylsarcosine: in situ single-pass perfusion studies in wild-type and Pept1 knockout mice. *Drug Metab Dispos* **38:**1740-1746.

Kagan L and Hoffman A (2008) Selection of drug candidates for gastroretentive dosage forms: pharmacokinetics following continuous intragastric mode of administration in a rat model. *Eur J Pharm Biopharm* **69:**238-246.

Katsura T and Inui K (2003) Intestinal absorption of drugs mediated by drug transporters: mechanisms and regulation. *Drug Metab Pharmacokinet* **18:**1-15.

Kim HR, Park SW, Cho HJ, Chae KA, Sung JM, Kim JS, Landowski CP, Sun D, Abd El-Aty AM, Amidon GL, and Shin HC (2007) Comparative gene expression profiles of intestinal transporters in mice, rats and humans. *Pharmacological research : the official journal of the Italian Pharmacological Society* **56:**224-236.

Kim I, Chu XY, Kim S, Provoda CJ, Lee KD, and Amidon GL (2003) Identification of a human valacyclovirase: biphenyl hydrolase-like protein as valacyclovir hydrolase. *J Biol Chem* **278:**25348-25356.

Knutter I, Rubio-Aliaga I, Boll M, Hause G, Daniel H, Neubert K, and Brandsch M (2002) H+-peptide cotransport in the human bile duct epithelium cell line SK-ChA-1. *Am J Physiol-Gastr L* **283:**G222-G229.

Landowski CP, Sun D, Foster DR, Menon SS, Barnett JL, Welage LS, Ramachandran C, and Amidon GL (2003) Gene expression in the human intestine and correlation with oral valacyclovir pharmacokinetic parameters. *J Pharmacol Exp Ther* **306:**778-786.

Laskin OL, Longstreth JA, Saral R, de Miranda P, Keeney R, and Lietman PS (1982) Pharmacokinetics and tolerance of acyclovir, a new anti-herpesvirus agent, in humans. *Antimicrob Agents Chemother* **21**:393-398.

Laskin OL (1983) Clinical pharmacokinetics of acyclovir. *Clin Pharmacokinet* **8**: 187-201.

Li FJ, Maag H, and Alfredson T (2008) Prodrugs of nucleoside analogues for improved oral absorption and tissue targeting. *Journal of Pharmaceutical Sciences* **97:**1109-1134.

Liang R, Fei YJ, Prasad PD, Ramamoorthy S, Han H, Yang-Feng TL, Hediger MA, Ganapathy V, and Leibach FH (1995) Human intestinal H+/peptide cotransporter. Cloning, functional expression, and chromosomal localization. *J Biol Chem* **270:**6456-6463.

Lu H and Klaassen C (2006) Tissue distribution and thyroid hormone regulation of Pept1 and Pept2 mRNA in rodents. *Peptides* **27:**850-857.

Ma K, Hu YJ, and Smith DE (2011) Peptide Transporter 1 Is Responsible for Intestinal Uptake of the Dipeptide Glycylsarcosine: Studies in Everted Jejunal Rings from Wild-type and Pept1 Null Mice. *Journal of Pharmaceutical Sciences* **100:**767-774.

MacDougall C and Guglielmo BJ (2004) Pharmacokinetics of valaciclovir. *J Antimicrob Chemother* **53:**899-901.

Meadows KC and Dressman JB (1990) Mechanism of acyclovir uptake in rat jejunum. *Pharm Res* **7:**299-303.

Meier Y, Eloranta JJ, Darimont J, Ismair MG, Hiller C, Fried M, Kullak-Ublick GA, and Vavricka SR (2007) Regional distribution of solute carrier mRNA expression along the human intestinal tract. *Drug Metab Dispos* **35:**590-594.

Miyamoto K, Shiraga T, Morita K, Yamamoto H, Haga H, Taketani Y, Tamai I, Sai Y, Tsuji A, and Takeda E (1996) Sequence, tissue distribution and developmental changes in rat intestinal oligopeptide transporter. *Biochim Biophys Acta* **1305:**34-38.

Motohashi H, Katsura T, Saito H, and Inui K (2001) Effects of tacrolimus and cyclosporin A on peptide transporter PEPT1 in Caco-2 cells. *Pharmaceutical Research* **18:**713-717.

Newstead S, Drew D, Cameron AD, Postis VL, Xia X, Fowler PW, Ingram JC, Carpenter EP, Sansom MS, McPherson MJ, Baldwin SA, and Iwata S (2011) Crystal structure of a prokaryotic homologue of the mammalian oligopeptide-proton symporters, PepT1 and PepT2. *EMBO J* **30**:417-426.

Nguyen HT, Dalmasso G, Powell KR, Yan Y, Bhatt S, Kalman D, Sitaraman SV, and Merlin D (2009) Pathogenic bacteria induce colonic PepT1 expression: an implication in host defense response. *Gastroenterology* **137:**1435-1447 e1431-1432.

Ogihara H, Saito H, Shin BC, Terado T, Takenoshita S, Nagamachi Y, Inui K, and Takata K (1996) Immuno-localization of H+/peptide cotransporter in rat digestive tract. *Biochem Biophys Res Commun* **220:**848-852.

Ormrod D, Scott LJ, and Perry CM (2000) Valaciclovir: a review of its long term utility in the management of genital herpes simplex virus and cytomegalovirus infections. *Drugs* **59:**839-863.

Perkins EJ and Abraham T (2007) Pharmacokinetics, metabolism, and excretion of the intestinal peptide transporter 1 (SLC15A1)-targeted prodrug (1S, 2S,5R,6S)-2-[(2 ' S)-(2-Amino)propionyl]aminobicyclo[3.1.0.]hexen-2,6-dicarboxylic acid (LY544344) in rats and dogs: Assessment of first-pass bioactivation and dose linearity. *Drug metabolism and disposition* **35:**1903-1909.

Rubio-Aliaga I and Daniel H (2008) Peptide transporters and their roles in physiological processes and drug disposition. *Xenobiotica* **38:**1022-1042.

Saito H, Okuda M, Terada T, Sasaki S, and Inui K (1995) Cloning and characterization of a rat H+/peptide cotransporter mediating absorption of beta-lactam antibiotics in the intestine and kidney. *J Pharmacol Exp Ther* **275:**1631-1637.

Sawada K, Terada T, Saito H, Hashimoto Y, and Inui KI (1999) Recognition of L-amino acid ester compounds by rat peptide transporters PEPT1 and PEPT2. *J Pharmacol Exp Ther* **291:**705-709.

Shen H, Smith DE, Yang T, Huang YG, Schnermann JB, and Brosius FC, 3rd (1999) Localization of PEPT1 and PEPT2 proton-coupled oligopeptide transporter mRNA and protein in rat kidney. *Am J Physiol* **276:**F658-665.

Sinko PJ and Balimane PV (1998) Carrier-mediated intestinal absorption of valacyclovir, the L-valyl ester prodrug of acyclovir: 1. Interactions with peptides, organic anions and organic cations in rats. *Biopharmaceutics & drug disposition* **19:**209-217.

Soul-Lawton J, Seaber E, On N, Wootton R, Rolan P, and Posner J (1995) Absolute bioavailability and metabolic disposition of valaciclovir, the L-valyl ester of acyclovir, following oral administration to humans. *Antimicrob Agents Chemother* **39:**2759-2764.

Sun J, Dahan A, and Amidon GL (2010) Enhancing the intestinal absorption of molecules containing the polar guanidino functionality: a double-targeted prodrug approach. *J Med Chem* **53:**624-632.

Sun Y, Sun J, Shi S, Jing Y, Yin S, Chen Y, Li G, Xu Y, and He Z (2009) Synthesis, transport and pharmacokinetics of 5'-amino acid ester prodrugs of 1-beta-D-arabinofuranosylcytosine. *Mol Pharm* **6:**315-325.

Takeda M, Khamdang S, Narikawa S, Kimura H, Kobayashi Y, Yamamoto T, Cha SH, Sekine T, and Endou H (2002) Human organic anion transporters and human organic cation transporters mediate renal antiviral transport. *J Pharmacol Exp Ther* **300:**918-924.

Tsuda M, Terada T, Irie M, Katsura T, Niida A, Tomita K, Fujii N, and Inui K (2006) Transport characteristics of a novel peptide transporter 1 substrate, antihypotensive drug midodrine, and its amino acid derivatives. *J Pharmacol Exp Ther* **318:**455-460.

Tsume Y, Vig BS, Sun J, Landowski CP, Hilfinger JM, Ramachandran C, and Amidon GL (2008) Enhanced absorption and growth inhibition with amino acid monoester prodrugs of floxuridine by targeting hPEPT1 transporters. *Molecules* **13:**1441-1454.

Urtti A, Johns SJ, and Sadee W (2001) Genomic structure of proton-coupled oligopeptide transporter hPEPT1 and pH-sensing regulatory splice variant. *AAPS pharmSci* **3:**E6.

Varma MV, Ambler CM, Ullah M, Rotter CJ, Sun H, Litchfield J, Fenner KS, and El-Kattan AF (2010) Targeting intestinal transporters for optimizing oral drug absorption. *Curr Drug Metab* **11:**730-742.

Varma MVS, Eriksson AH, Sawada G, Pak YA, Perkins EJ, and Zimmerman CL (2009) Transepithelial Transport of the Group II Metabotropic Glutamate 2/3 Receptor Agonist (1S,2S,5R,6S)-2-Aminobicyclo[3.1.0]hexane-2,6-dicarboxylate (LY354740) and Its Prodrug (1S,2S,5R,6S)-2[(2 ' S)-(2 '-Amino)propionyl]aminobicyclo[3.1.0]hexane-2,6-dicarboxylate (LY544344). *Drug metabolism and disposition* **37:**211-220.

Wada S, Tsuda M, Sekine T, Cha SH, Kimura M, Kanai Y, and Endou H (2000) Rat multispecific organic anion transporter 1 (rOAT1) transports zidovudine, acyclovir, and other antiviral nucleoside analogs. *J Pharmacol Exp Ther* **294:**844-849.

Weller S, Blum MR, Doucette M, Burnette T, Cederberg DM, de Miranda P, and Smiley ML (1993) Pharmacokinetics of the acyclovir pro-drug valaciclovir after escalating single- and multiple-dose administration to normal volunteers. *Clin Pharmacol Ther* **54:**595-605.

Whitley RJ, Blum MR, Barton N, de Miranda P (1982) Pharmacokinetics of acyclovir in humans following intravenous administration. A model for the development of parenteral antivirals. *Am J Med* **73**:165-171.

Zakelj S, Legen I, Veber M, and Kristl A (2004) The influence of buffer composition on tissue integrity during permeability experiments "in vitro". *International journal of pharmaceutics* **272:**173-180.

Zhang EY, Fu DJ, Pak YA, Stewart T, Mukhopadhyay N, Wrighton SA, and Hillgren KM (2004) Genetic polymorphisms in human proton-dependent dipeptide transporter PEPT1: implications for the functional role of Pro586. *J Pharmacol Exp Ther* **310:**437-445.

CHAPTER 3

SIGNIFICANCE OF PEPT1 IN THE *IN SITU* INTESTINAL PERMEABILITY OF VALACYCLOVIR IN WILDTYPE AND PEPT1 KNOCKOUT MICE

ABSTRACT

Purpose. The study evaluated the quantitative contribution of PEPT1 to the intestinal permeability of valacyclovir, an ester prodrug of the antiviral drug acyclovir.

Methods. Valacyclovir effective permeability (P_{eff}) was examined by *in situ* single-pass intestinal perfusion studies performed in wildtype and *Pept1* knockout mice. In particular, valacyclovir P_{eff} was measured as a function of perfusate pH, potential inhibitors, drug concentrations and intestinal segments under steady-state conditions. Valacyclovir effective permeability was calculated as: $P_{eff} = -Q \times \ln(C_{out}/C_{in})/(2\pi RL)$, after correcting for water flux with a gravimetric method as well as correcting for valacyclovir luminal degradation. At the end of perfusion procedures, portal vein plasma samples were collected and analyzed to determine the extent of intestinal bioconversion of valacyclovir. All perfusate and plasma samples were analyzed using a validated HPLC method coupled with fluorescence detection.

Results. Valacyclovir jejunal P_{eff} in wildtype mice was significantly inhibited by glycylsarcosine and cefadroxil, suggesting PEPT1-specific active uptake of valacyclovir. Valacyclovir uptake kinetics in wildtype jejunum was fitted by a major Michaelis–

Menten uptake term (apparent affinity constant K_m=10 mM) and a minor linear uptake term. Valacyclovir P_{eff} values were comparably high in the duodenum, jejunum and ileum and substantial lower in the colon in wildtype mice, a finding consistent with PEPT1 not being expressed in large intestine. Valacyclovir P_{eff} values in the small intestinal segments of *Pept1* knockout mice were reduced by about 90% compared to that in wildtype mice, and not significantly different from colon P_{eff}. No significant differences were observed for colon P_{eff} between the two genotypes. Jejunal P_{eff} was also insensitive to changes in perfusate pH over the range of 5.5 - 7.5. In portal vein plasma samples, only the active drug acyclovir was detected while valacyclovir levels were below the limit of detection.

Conclusions. Our findings demonstrate that PEPT1 accounted for approximately 90% of valacyclovir permeability in mouse small intestine. Other membrane transporters appeared to play a minor role, if any, in facilitating the intestinal absorption of valacyclovir. Valacyclovir was rapidly and completely converted to acyclovir, under the current study conditions, after passing the intestinal wall.

INTRODUCTION

Efficient intestinal absorption is necessary to achieve optimal clinical plasma exposure of oral pharmaceutical products. For polar and hydrophilic drugs, poor permeability across the brush border membrane of epithelial cells along the intestine poses a major barrier for their intestinal absorption and systemic availability. Recently, the permeability barriers for hydrophilic compounds seem even more relevant in light of the appreciable shift in the chemical space of new chemical entities from lipophilic to hydrophilic compounds, which is primarily driven by concerns about toxicities, metabolism liabilities and drug-drug interactions frequently reported for lipophilic drugs (Varma et al., 2010)

Currently, limited options are available to breach permeability barriers for hydrophilic drugs. Bioconvertable derivatives with increased lipophilicity have shown some success in improving the intestinal permeability and uptake of hydrophilic compounds (Jana et al., 2010). Alternatively, a novel type of prodrugs, designed to target intestinal transporters, is emerging as an attractive approach for permeability enhancement (Li et al., 2008; Varma et al., 2010). Epithelial cells in the small intestine express a variety of influx transporters including peptide transporters, amino acid transporters, organic anion transporting polypeptides, and many others, which function to actively uptake their substrates (Brandsch et al., 2008; König, 2011; Thwaites and Anderson, 2011). Targeted prodrugs of poorly permeable compounds are usually designed to hijack one or several intestinal transporter-mediated active uptake;

consequently carrier-mediated uptake of prodrugs can lead to improved absorption and oral availability of their parent molecules.

Among all the delivery target candidates for targeted oral prodrugs, peptide transporter 1 (PEPT1) is particularly promising due to some unique properties. PEPT1 is a proton-coupled oligopeptide transporter abundantly expressed on the apical membrane of both human and mouse small intestinal epithelial cells (Groneberg et al., 2001; Jappar et al., 2010). The physiological role of PEPT1 is to facilitate the uptake of dietary di-/tri-peptides after protein digestion in the intestine (Daniel, 2004). As a high-capacity low-affinity influx transporter, PEPT1 couples the active uptake of its substrates against their concentration gradients with the downhill influx of proton into enterocytes (Brandsch et al., 2008; Rubio-Aliaga and Daniel, 2008). Apical localization, abundant intestinal expression and high-capacity low-affinity transport features imply that PEPT1 can transport PEPT1-targeted prodrugs efficiently without being easily saturated even at relatively high oral doses. Moreover, PEPT1 transports structurally diverse compounds including di-/tri-peptides such as glycylsarcosine and glycyl-L-proline, β-lactam antibiotics such as cefadroxil and cephalexin, angiotensin converting enzyme (ACE) inhibitors such as captopril and enalapril, the anticancer drug bestatin and the photosensitizing agent 5-aminolevulinic acid. Broad substrate specificity suggests that intestinal PEPT1 can be a potentially versatile delivery target for prodrugs with distinct structures.

Various PEPT1 targeted prodrugs, which are commonly synthesized by linking poorly permeable active drugs with some amino acid or dipeptide carriers, are under intensive investigation (Tsume et al., 2008; Sun et al., 2010; Gupta et al., 2011; Yan et al.,

2011). Among all the PEPT1 targeted prodrugs, valacyclovir is viewed as the prototype of PEPT1 targeted prodrugs with most abundant uptake or pharmacokinetic findings available for this compound.

Valacyclovir is an L-valyl ester prodrug of the potent antiviral agent acyclovir that is orally administered for the treatment and prophylaxis of herpes simplex, varicella zoster, and cytomegalo viruse infection. In human subjects, oral valacyclovir delivered about 54% oral bioavailability of acyclovir, a value 3-5 times higher than that of oral acyclovir (Soul-Lawton et al., 1995). However, even for valacyclovir, the principal contribution of PEPT1 to the enhanced oral availability of acyclovir following orally administered valacyclovir remains controversial. Over the past two decades, numerous transport or uptake studies demonstrated the interaction of valacyclovir with multiple transporters including PEPT1. For instance, significantly increased valacyclovir cellular uptake was found in different PEPT1-expressing cells, as compared to their respective mock control cells (de Vrueh et al., 1998; Ganapathy et al., 1998; Han et al., 1998; Guo et al., 1999; Balimane and Sinko, 2000; Bhardwaj et al., 2005). In addition, valacyclovir was also found to be a substrate for another peptide transporter PEPT2 (Ganapathy et al., 1998), an amino acid transporter $ATB^{0,+}$ (Hatanaka et al., 2004), peptide histidine transporter 1 (PHT1) (Bhardwaj et al., 2006), a human peptide transporter (HPT1) (Landowski et al., 2003), as well as organic anion and cation transporters (Sinko and Balimane, 1998; Takeda et al., 2002). Since some of these valacyclovir transporters co-exist in the intestine, it is crucial to quantify the major contribution of PEPT1 in mediating the intestinal absorption of valacyclovir. Such quantitative evidence will strongly validate the effectiveness of selectively targeting PEPT1, which is the basis of

rationally designed PEPT1 targeted prodrugs. Unfortunately, studies demonstrating the quantitative importance of PEPT1 is completely lacking for the model prodrug valacyclovir and any other PEPT1 targeted prodrugs.

In our laboratory, a *Pept1* knockout mouse model has been successfully developed, validated and utilized for exploring the function of PEPT1 in nutrition absorption (Hu et al., 2008; Jappar et al., 2010; Ma et al., 2011). *Pept1* knockout mice could be a powerful tool for assessing the quantitative role of PEPT1 *in vivo*. Therefore, in the current study, we aimed to evaluate the quantitative significance of intestinal PEPT1 in the intestinal permeability of the model PEPT1 targeted prodrug valacyclovir by performing comparative *in situ* intestinal perfusions in wildtype and *Pept1* knockout mice.

MATERIALS AND METHODS

Animals. Animal studies were conducted in accordance with the Guide for the Care and Use of Laboratory Animals as adopted and promulgated by the U.S. National Institutes of Health. Gender matched wildtype and *Pept1* knockout mice, 8 to 10 weeks of age, were used for all experiments. The mice were kept in a temperature-controlled environment with 12-hr light/dark cycle and received a standard diet and water *ad libitum* (Unit for Laboratory Animal Medicine, University of Michigan, Ann Arbor, MI).

Materials. Valacyclovir hydrochloride, acyclovir, glycylsarcosine (GlySar), cefadroxil, tetraethylammonium (TEA), para-aminohippuric acid (PAH), L-histidine, L-valine and all other reagents were purchased from Sigma-Aldrich (St. Louis, MO).

***In situ* single-pass intestinal perfusion procedure.** Prior to experiment, wildtype and *Pept1* knockout mice were fasted overnight (~16 hrs) with free access to water. The perfusion procedure has been previously reported (Adachi et al., 2003; Jappar et al., 2010). Briefly, animals were anesthetized with sodium pentobarbital (40-60 mg/kg, i.p.) and placed on a warming pad to maintain body temperature. Isopropyl alcohol was used to sterilize the abdominal area and a 1.5 cm midline incision was made longitudinally to expose the small intestine. An 8-cm segment of proximal jejunum was isolated (i.e., ~2 cm distal to Treitz ligament), and incisions were then made at the proximal and distal ends. Glass cannulas (2.0 mm outer diameter) attached to flexible PVC tubings were inserted into both ends of the jejunum and secured with silk sutures. The inlet tubing was connected to a 20-mL syringe placed on a perfusion pump (Model 22, Harvard Apparatus, South Natick, MA) and the outlet tubing was placed in a collection vial. The perfusion

buffer (pH 6.5) containing 10 mM MES, 135 mM NaCl, 5 mM KCl and 100 μM valacyclovir with an osmolarity of 290 mOsm/L was incubated at 37 ℃ to maintain temperature and then pumped through the intestinal segment at a rate 0.1 mL/min for 90 min. The perfusion buffer was first perfused up to 30 min to ensure steady-state conditions. Based on our previous experience, 30 minutes was sufficient for achieving steady state. The exiting perfusates were then collected at 10-min intervals for up to 1 hr (40 min, 50 min, 60 min, 70 min, 80 min, and 90 min). All samples, including inlet and outlet perfusates as well as standard drug solutions, were assayed by a validated HPLC method coupled with fluorescence detection. Upon the completion of the experiment, the length of perfused intestinal segment was accurately measured.

For pH-dependent studies performed in the jejunum of wildtype mice, different combinations of 10 mM MES/Tris or HEPES/Tris were used in perfusate to adjust pH values between 5.5 and 7.5 with osmolarity being held constant.

For competitive inhibition studies performed in the jejunum of wildtype mice, various putative competitive inhibitors were co-perfused with 100μM valacyclovir at pH 6.5. These putative inhibitors included 25 mM GlySar, 25 mM cefadroxil, 25 mM TEA, 25 mM PAH, 25 mM L-histidine, and 25 mM L-valine, respectively.

For concentration-dependent uptake studies, drug concentrations in the perfusate were varied in a wide range of 0.01-50 mM to assess the kinetic characteristics of valacyclovir jejunal uptake in wildtype mice.

In another separate perfusion study, perfusion buffer containing 100 µM acyclovir, instead of 100 µM valacyclovir, was perfused through the jejunum of both wildtype and *Pept1* knockout mice, following the perfusion procedure described earlier.

Segment-dependent perfusion study. To characterize valacyclovir effective permeability (P_{eff}) in different intestinal regions of two genotypes, duodenum, jejunum, ileum and colon of wildtype and *Pept1* knockout mice were perfused simultaneously. The simultaneous perfusion procedure was adapted from published reports (Dahan et al., 2009; Jappar et al., 2010). A 2-cm segment of duodenum (i.e., ~0.25 cm distal to the pyloric sphincter), 8-cm segment of jejunum (i.e., ~2 cm distal to Treitz ligament), 6-cm segment of ileum (i.e., ~1 cm proximal to the cecum) and 3-cm segment of colon (i.e., ~ 0.5 cm distal to the cecum) were perfused as described previously.

Bioconversion of valacyclovir in mouse. In addition to effective permeability, the extent of valacyclovir conversion to acyclovir after passing the intestinal wall in mouse was also investigated. Experimentally, portal vein blood samples were taken upon the completion of perfusion procedures. Each blood sample was then immediately transferred to a 7.5% EDTA-containing centrifuge vial and centrifuged at 3000 g for 3 min at room temperature. A 100 µL aliquot of plasma was then collected and mixed with 200 µL of acetonitrile for deproteinization. The mixture was vigorously vortex-mixed for 1 minute and then centrifuged at 15000 g for 10 min. The clear supernatant was transferred to another clean centrifuge vial, blown dry under vacuum and reconstituted in 100 µL mobile phase prior to HPLC analysis.

Analytical methods. The HPLC system consisted of a Waters 616 pump, a Waters 717 autosampler, a Waters 2487 dual λ absorbance detector and a Waters 2475 multi λ fluorescent detector (Waters Inc., Milford, MA). A waters ODS-3 column (250×4.6 mm, 5μM), fitted with a refillable guard column, was used for the chromatographic separation. For the assay of acyclovir and valacyclovir in perfusate and plasma samples, the isocratic mobile phase consisting of 5% organic phase (0.1% v/v trifluoroacetic acid (TFA) in acetonitrile) and 95% aqueous phase (0.1% v/v TFA in water) was used at a flow rate of 1 mL/min. Excitation wavelength of 270 nm and emission wavelength of 360 nm were selected for fluorescence detection. When valacyclovir was co-perfused with various inhibitors, the mobile phase was modified accordingly if necessary. The injection volume was 50 μL. All perfusate samples were centrifuged at 15000 g for 10 min and the clear supernatants were directly taken for HPLC analysis. External standard method was used for quantifying the concentrations of valacyclovir and acyclovir in perfusates. Two separate calibration curves were constructed for the quantification of valacyclovir and acyclovir, respectively.

HPLC method validation. The HPLC method was thoroughly validated in terms of specificity, sensitivity, linearity, precision, accuracy and stability.

Specificity. The interference from endogenous compounds in perfusates was investigated by analyzing blank perfusates collected in at least six different batches.

Linearity and sensitivity. Linearity was evaluated by preparing calibration standards in the range of 200, 100, 50, 20, 10, 5 and 2 μM for valacyclovir and 50, 20, 10, 5, 2.5, 1 and 0.5 μM for acyclovir. The lower limit of quantification (LLOQ) was

calculated as the lowest concentration giving a peak with a signal to noise ratio greater than 10.

Precision and accuracy. The three concentration levels for quality control (QC) solutions of high, medium and low concentrations were 200, 50 and 5 μM for valacyclovir and 50, 10 and 1 μM for acyclovir, respectively. Intra-day precision and accuracy were assessed by the analyses of QC samples of high, medium and low concentrations in triplicate and inter-day precision and accuracy was evaluated by three replicate measurements of QC samples on three consecutive days. Method precision was expressed as relative standard deviation (RSD %) and method accuracy was expressed as the percentage of the mean observed concentration divided by the nominal spiked concentration.

Stability. Stability of QC samples was evaluated after storage at 4 ºC for 1 month and at room temperature for 4 hours. Stability was expressed as relative error (RE, (mean observed concentration-nominal concentration)/nominal concentration×100%).

Data analysis. Valacyclovir was reported to undergo luminal hydrolysis of varying degrees at different concentrations in rat intestinal perfusion studies (Sinko and Balimane, 1998). In order to accurately estimate valacyclovir P_{eff}, the loss of valacyclovir due to hydrolysis in the lumen, rather than uptake across the apical membrane, had to be accounted for. Therefore, both valacyclovir and luminally formed acyclovir concentrations in outlet perfusates were simultaneously quantified by the validated HPLC method. Furthermore, it was assumed that acyclovir intestinal permeability was

negligibly small compared to that of valacyclovir and did not affect the estimation of valacyclovir effective permeability.

Net water flux in the perfusion studies was corrected by a gravimetric method. Gravimetric correction was shown to be comparable or even superior to other water flux correction methods using nonabsorbable markers such as PEG-3350 and phenol red (Sutton et al., 2001).

Overall, drug concentration in an effluent perfusate after appropriate correction, denoted as $C_{out'}$, can be calculated as:

Eq. (1)

where $C_{out,valacyclovir}$ and $C_{out,\ acyclovir}$ are uncorrected concentrations of valacyclovir and acyclovir in an outlet perfusate, Q_{in} and Q_{out} are measured perfusate flow rates (weight/10 min, density set as 1.0 g/mL).

Valacyclovir P_{eff} was estimated from the following equation under the parallel tube assumption:

Eq. (2)

,where Q_{in} is the fixed inlet flow rate of 0.1 mL/min, C_{out}' is the corrected outlet concentration as defined in Eq. (1), C_{in} is the inlet valacyclovir concentration, R is the radius, and L is the length of the perfused segment, respectively.

The concentration-dependent flux (*V*) of valacyclovir in the jejunum of wildtype mice was best fitted by an equation consisting of a Michaelis-Menten term and a nonsaturable linear term, as shown below:

Eq. (3)

,where V_{max} is the maximal rate of carrier-mediated flux, K_m is the apparent Michaelis-Menten constant when referenced to the inlet concentration and K_d is the first-order rate constant of the linear process.

Data were reported as mean ± standard error (SE) ($n \geq 4$ per genotype) unless stated otherwise. An unpaired two-sample t-test was used to compare statistical differences between wildtype and *Pept1* knockout mice. One-way analysis of variance (ANOVA) followed by Dunnett's test or Bonfferoni's test was used in pairwise comparisons with the control group or multiple pairwise comparisons, respectively (GraphPad Prism 4.0; GraphPad Software Inc., La Jolla, CA). $p \leq 0.05$ was considered statistically significant. Nonlinear regression analyses were performed using GraphPad Prism software, where the goodness of fit was determined by the coefficient of determination (R^2), and visual inspection of the residuals.

RESULTS

HPLC method validation. The developed HPLC method was thoroughly validated with regard to specificity, linearity, sensitivity, precision, accuracy and stability.

***Specificity*.** Figure 3.1A shows a representative chromatogram for the analysis of a blank perfusate sample. Clearly no endogenous substances in intestinal perfusates interfered with the determination of acyclovir or valacyclovir.

Linearity and sensitivity. Typical calibration curves of valacyclovir and acyclovir were constructed by least squares linear regression analysis of the peak areas of analytes (y) versus their concentrations (x). A typical regression equation was y=990371x+909422 for valacyclovir, with a correlation coefficient (R^2) of 0.9999, and y=1752725x+899476 for acyclovir, with R^2 of 0.9994. Good linearity was shown in the specified concentration range for both compounds. The LLOQ was 0.2 and 0.1 μM for valacyclovir and acyclovir, respectively.

Precision and Accuracy. For valacyclovir, the intra-day and inter-day precision (RSD%) was found to be less than 8% while the accuracy varied from 94.0% to 104.0% for all the three QC levels. Similarly for acyclovir, the intra-day and inter-day precision and accuracy ranged from 5%-9% and 96%-103%, respectively.

***Stability*.** Stability results, under all experimental conditions, show that relative errors were less than 5% for both compounds.

Bioconversion of valacyclovir in mouse. Figure 3.1(B-E) suggest that valacyclovir had substantial degradation in the intestinal lumen in mice, indicating that both acyclovir and valacyclovir in outlet perfusate samples should be measured for the

accurate estimation of valacyclovir P_{eff} values. Figure 3.1F shows that the chromatographic peak corresponding to valacyclovir was completely absent in the chromatogram for a typical portal vein plasma sample, indicating that valacyclovir was rapidly and completely degraded in enterocytes under our experimental conditions.

***In situ* single-pass perfusion study.** In single-pass intestinal perfusion studies, effective jejunal permeability of 100 μM valacyclovir in wildtype mice was evaluated as a function of perfusate pH values and potential inhibitors. As depicted in Figure 3.2, although different valacyclovir P_{eff} values were obtained over the pH range of 5.5 - 7.5, none of the differences was statistically significant. Co-perfusion of valacyclovir with different putative inhibitors showed varied effects on the jejunal permeability of valacyclovir. As shown in Figure 3.3, valacyclovir jejunal P_{eff} values were significantly decreased by the presence of 25 mM cefadroxil or 25 mM dipeptide GlySar in perfusates, suggesting the involvement of PEPT1 in the jejunal permeability of valacyclovir. In contrast, co-perfusion of valacyclovir with all other inhibitors, including 25 mM TEA, 25 mM PAH, 25 mM L-histidine and 25 mM L-valine, had no significant effect on valacyclovir jejunal P_{eff}.

Valacyclovir jejunal uptake in wildtype mice was also evaluated at various drug concentrations (0.01–50 mM) to assess the uptake kinetics. Figure 3.4 show that valacyclovir uptake was concentration-dependent and best fitted by the sum of a Michaelis-Menten kinetic term and a minor linear term. When referenced to the inlet valacyclovir concentrations, the model parameters V_{max}, K_m and K_d were estimated to be 1.4 ± 0.5 nmol/cm^2/sec, 10 ± 4.6 mM and $3.0\times10^{-5} \pm 0.6\times10^{-5}$ cm/sec, respectively.

Segment-dependent study. The quantitative contribution of PEPT1 to valacyclovir regional permeability in four intestinal segments was probed by comparing segmental permeability data obtained in both wildtype and *Pept1* knockout mice. As demonstrated in Figure 3.5, in wildtype mice the effective permeability of 100 μM valacyclovir was segment-dependent, with mean P_{eff} values of 2.37×10^{-4} cm/sec in duodenum, 1.68×10^{-4} cm/sec in jejunum, 2.11×10^{-4} cm/sec in ileum, and 0.27×10^{-4} cm/sec in colon. While there were no statistical differences in valacyclovir P_{eff} estimates for different small intestinal segments, they were substantially higher than colon P_{eff} ($p<0.05$). In *Pept1* knockout mice, valacyclovir P_{eff} values for duodenal, jejunal, and ileal segments were less than 10% of that in wild-type animals. Valacyclovir P_{eff} was similarly low in the colon of both genotypes. In addition, there were no statistical differences in valacyclovir P_{eff} values between any of the intestinal regions of *Pept1* knockout mice. Figure 3.6 shows the jejunal effective permeability of acyclovir in wildtype and *Pept1* knockout mice were very low with no significant difference between them. Acyclovir intestinal permeability was indeed negligible compared to that of valacyclovir, corroborating our assumption that luminally formed acyclovir had negligible contribution to the estimation of valacyclovir permeability in perfusion studies.

DISCUSSION

In previous reports, PEPT1-mediated valacyclovir uptake was demonstrated in a number of *in vitro* studies using PEPT1-expressing cell culture systems (de Vrueh et al., 1998; Ganapathy et al., 1998; Han et al., 1998; Guo et al., 1999; Balimane and Sinko, 2000; Bhardwaj et al., 2005). However, findings from these studies are qualitative in nature and could not truthfully represent the complicated *in vivo* intestinal uptake process. In this study, we explored the quantitative contribution of PEPT1 to the intestinal permeability of valacyclovir by performing *in situ* intestinal perfusion studies in wildtype and *Pept1* knockout mice. Use of *Pept1* knockout mouse model provided us with the unique opportunity of unequivocally defining the quantitative significance of PEPT1-mediated uptake of valacyclovir relative to other uptake pathways in whole animals, which maintained intact blood supply and the complexity of transporting pathways in intestinal segments.

In wildtype mice, valacyclovir P_{eff} values were similarly high in duodenum, jejunum, and ileum while valacyclovir colon P_{eff} value was only about 11-16% of those permeability values in the three small intestinal regions. On the other hand, PEPT1 protein levels were found to be comparably abundant in the duodenum, jejunum and ileum and undetectable in the colon of wildtype mice (Jappar et al., 2010). Therefore good correlation between PEPT1 protein regional expression and valacyclovir regional P_{eff} values along the intestinal tract was observed. In sharp contrast, the residual P_{eff} of valacyclovir in the duodenal, jejunal, and ileal segments of *Pept1* knockout mice was about 10% of that in wildtype animals ($p<0.01$) and was similar to colon P_{eff}, suggesting

that PEPT1 was responsible for approximately 90% of valacyclovir uptake in mouse small intestine. Although other transporters such as human peptide transporter HPT1, peptide histidine transporter PHT1, and organic anion as well as cation transporters were suggested to be capable of transporting valacyclovir, their contributions were apparently insignificant in the absorption of valacyclovir in mouse small intestine.

Amino acid transporter $ATB^{0,+}$ was reported to be abundant on the apical membrane of colonocytes and actively shuttle valacyclovir into HRPE cells transfected with $ATB^{0,+}$ (Hatanaka et al., 2004). In our experimental setting, low colon P_{eff} of valacyclovir was observed in both genotypes, which could not support the significant contribution of colonic $ATB^{0,+}$. Moreover, following colonic administration of valacyclovir to rats, zero plasma levels of acyclovir were detected (Kagan and Hoffman, 2008), indicating the poor permeability of valacyclovir in rat colon as well. Furthermore, in light of the extensive luminal degradation of valacyclovir and a high fraction of acyclovir excreted in feces (de Miranda et al., 1981; Granero and Amidon, 2006), it is plausible that the contribution of the colonic transporter $ATB^{0,+}$ to the intestinal absorption of valacyclovir is marginal.

Inhibition studies in wildtype jejunum further supported the principal role of PEPT1 in mediating the absorption of valacyclovir. Only 25 mM GlySar or 25 mM cefadroxil, two typical PEPT1 substrates, significantly reduced valacyclovir jejunal P_{eff} values, suggesting PEPT1-specific uptake of valacyclovir. The lack of inhibition by typical organic anion PAH and typical organic cation TEA at high concentrations seemed to be contradictory to the results from rat intestinal perfusion studies (Sinko and Balimane, 1998). However it is always challenging to directly compare results obtained

in two different experimental systems. Factors such as species difference in regional transporter expression and different experimental conditions could all contribute to the discrepancy observed between the two studies.

In the current perfusion studies we also found that valacyclovir intestinal uptake was insensitive to bulk perfusate pH changes in the range of 5.5-7.5, which basically covers the physiological pH range for human intestine (Rouge et al., 1996). This finding seems to be conflicting with the common notion of PEPT1 being a proton dependent co-transporter. This apparent pH-independent uptake of valacyclovir might be associated with the fact that changes in luminal bulk pH do not necessarily translate to significant changes in pH at the membrane surface of enterocytes where a low microclimate pH is tightly maintained (Lucas et al., 1980; Hogerle and Winne, 1983; Shiau et al., 1985). Furthermore, atypical pH-dependence patterns have been frequently reported for PEPT1-mediated uptake of valacyclovir performed in various cell culture systems. For instance, de Vrueh et al. (1998) showed that varying extracellular medium pH from 6 to 7.4 almost did affect valacyclovir permeability in Caco-2 cells while Guo and his colleagues (1999) showed that maximum uptake of valacyclovir occurred at basic pH 7.5 and was almost two times higher than that at acidic pH in Chinese hamster ovary. Balimane and Sinko (2000) systematically examined the effect of ionization on the variable uptake of valacyclovir via human PEPT1 in CHO cells. Affinity constants (K_m) for the cationic and neutral forms of valacyclovir were estimated to be 7.4 mM and 1.2 mM, respectively.

Given these literature reports, our finding might also be interpreted by taking into account the dual effect of pH changes (if there is any on the enterocyte membrane surface) on proton gradient (the driving force of PEPT1) as well as on the ionization state of

valacyclovir. On one hand, PEPT1 has an optimal proton gradient under lower pH (i.e. pH 5.5) conditions while this driving force of PEPT1 is attenuated at higher pH (i.e. pH 7.5) conditions. On the other hand, the predominant ionic species of valacyclovir is cationic at lower pH (i.e. pH 5.5) and neutral at higher pH conditions (i.e. pH 7.5) (Balimane and Sinko, 2000). Consequently, the combined effect of varied driving force for PEPT1 and variable affinities of different valacyclovir species towards PEPT1, could result in little net changes in effective permeability of valacyclovir in the bulk pH range of 5.5-7.5.

Valacyclovir uptake kinetics in wildtype jejunum, estimated in the range of 0.01-50 mM of valacyclovir, was fitted by the sum of a Michaelis-Menten term and a minor linear term. Apparent Michaelis-Menten constant (K_m) was estimated at about 10 mM when referenced to inlet valacyclovir concentration, characteristic of low affinity transport activity of PEPT1. In existing literature, valacyclovir K_m estimates were remarkably variable, from approximately 0.3 mM in Caco-2 cells (Han et al., 1998) to about 6 mM in oocytes injected with PEPT1 (Balimane et al., 1998). As described earlier, cationic valacyclovir showed a K_m of 7.4 mM while neutral form of valacyclovir possessed a K_m of 1.2 mM (Balimane and Sinko, 2000). Therefore our K_m estimate is in line with literature values and consistent with the low-affinity feature of PEPT1-mediated transport. In addition, K_d was the first-order rate constant of the minor linear transport process of valacyclovir. As shown in Eq. (3), valacyclovir jejunal effective permeability could be factored as the sum of a linear component, expressed as K_d, and a PEPT1-mediated component, expressed as V_{max}/K_m, at drug concentrations far below its K_m. It is clear that approximately 83% of valacyclovir P_{eff} could be attributed to the PEPT1-

mediated pathway, again supporting the major contribution of PEPT1 in facilitating the intestinal absorption of valacyclovir.

Finally, it is also worth noting that valacyclovir P_{eff} values in the small intestine of wildtype mice were much higher than that of metoprolol, which was reported to be approximately 0.5×10^{-4} cm/sec by Jappar (2009) in her doctoral dissertation. Since metoprolol is a model compound absorbed via trans-cellular passive diffusion and a reference drug for low/high P_{eff} class border, this comparison between the permeability of the two drugs suggests that the PEPT1-targeted prodrug approach effectively overcame the permeability barrier for the poorly permeable drug acyclovir.

In conclusion, we have demonstrated the predominant contribution of PEPT1 in enhancing the intestinal permeability of the model prodrug valacyclovir by comparative *in situ* intestinal perfusion studies performed in wildtype and *Pept1* knockout mice. These findings can strongly support the application of rationally designed PEPT1-targeted prodrugs to improving the intestinal permeability and absorption of otherwise poorly absorbable drugs.

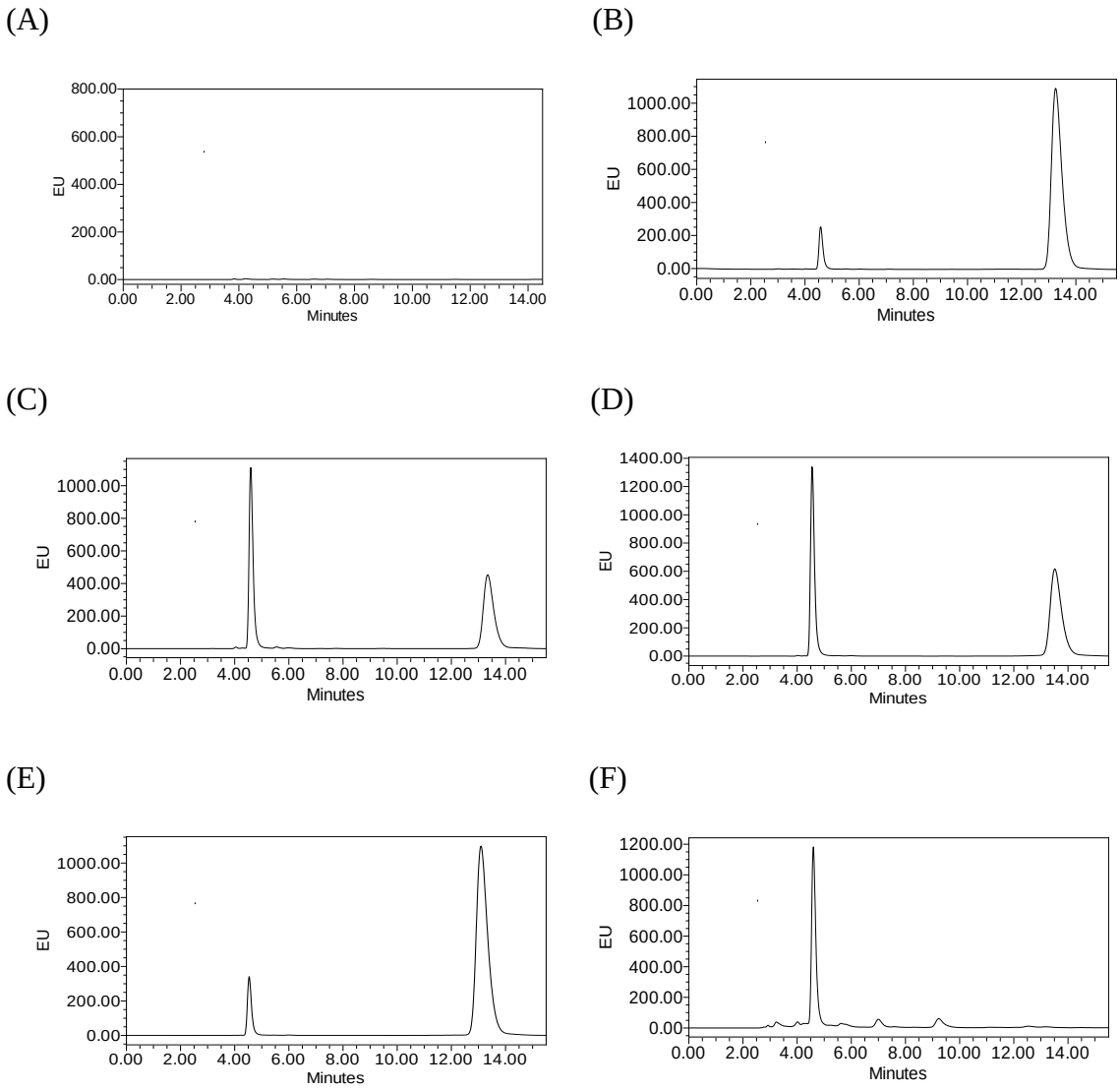

Figure 3.1 HPLC analyses of acyclovir and valacyclovir in perfusates from: (A) blank, (B) duodenum, (C) jejunum, (D) ileum, (E) colon, and (F) from portal vein plasma. The chromatographic peaks at 4.6 min and 13.4 min are corresponding to acyclovir and valacyclovir, respectively.

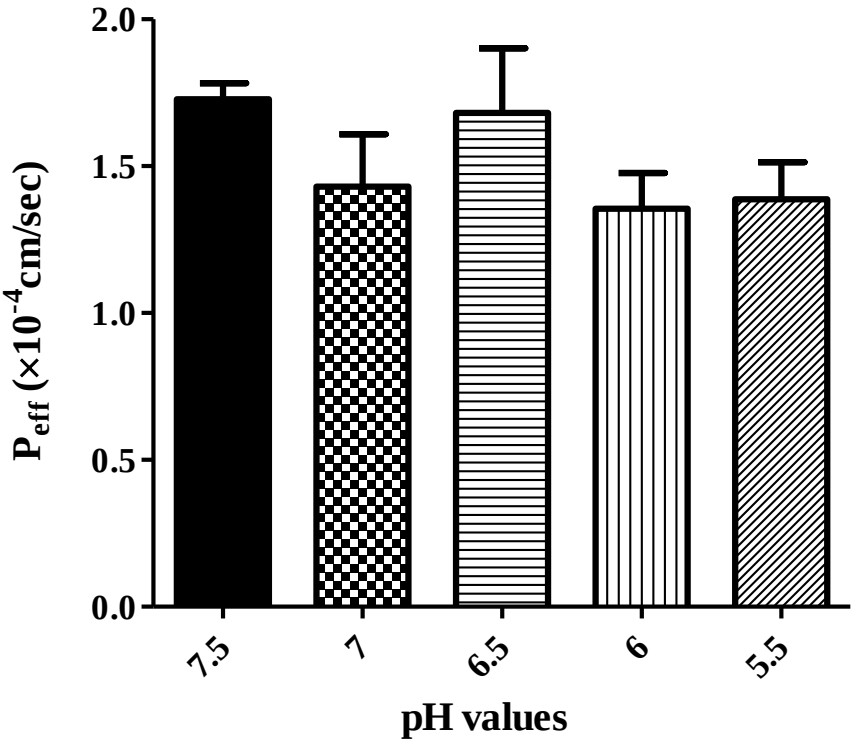

Figure 3.2 Effect of perfusate pH (5.5-7.5) on the effective permeability of 100 µM valacyclovir during jejunal perfusions of wildtype mice. Data are presented as mean ± SE (n = 4-5). No significant differences were found among different groups after one-way ANOVA followed by Bofferoni's test.

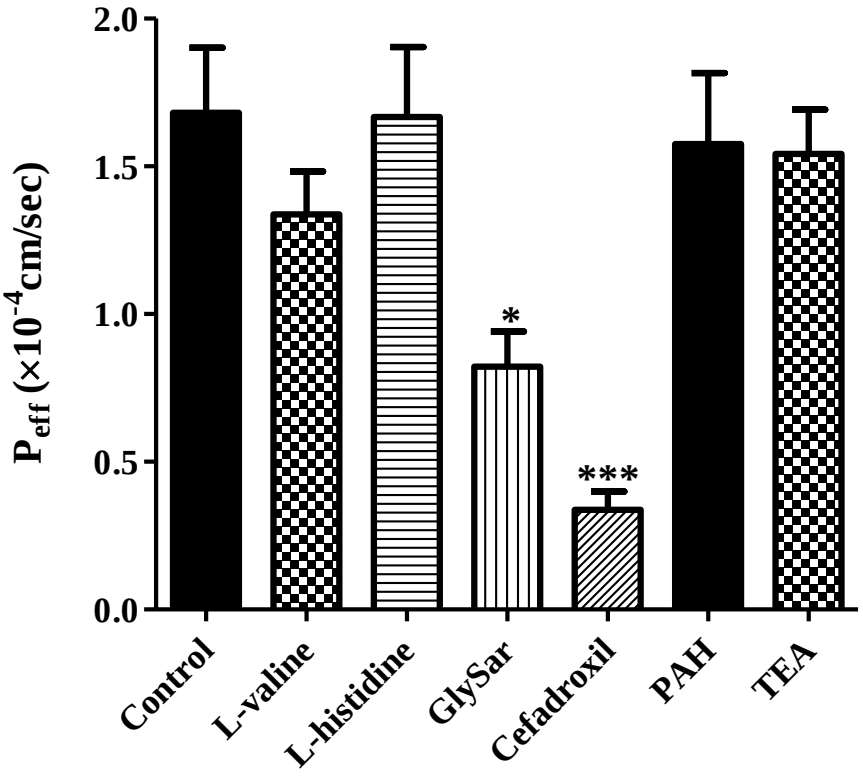

Figure 3.3 Effect of putative competitive inhibitors (25 mM) on the effective permeability of 100 µM valacyclovir during jejunal perfusions of wildtype mice. Data are presented as mean ± SE (n = 4-5). * $p<0.05$; *** $p<0.001$, compared to control values.

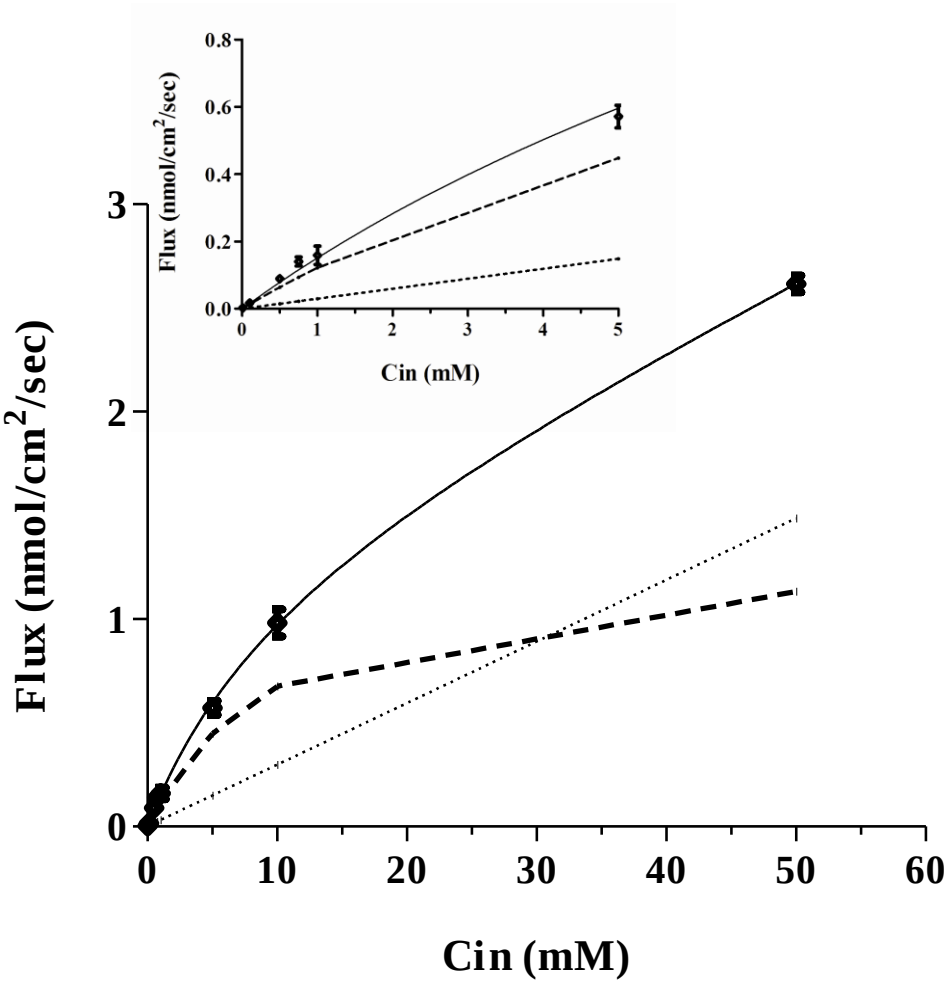

Figure 3.4 Concentration dependent flux of valacyclovir (0.01 – 50 mM) during jejunal perfusions of wildtype mice. Solid, dashed and dotted lines are simulated results using the sum of a Michaelis-Menten and a linear term, the Michaelis-Menten term, and the linear term, respectively. Inset represents the lower concentration range of 0.01–5 mM. Data are presented as mean ± SE (n = 4-5).

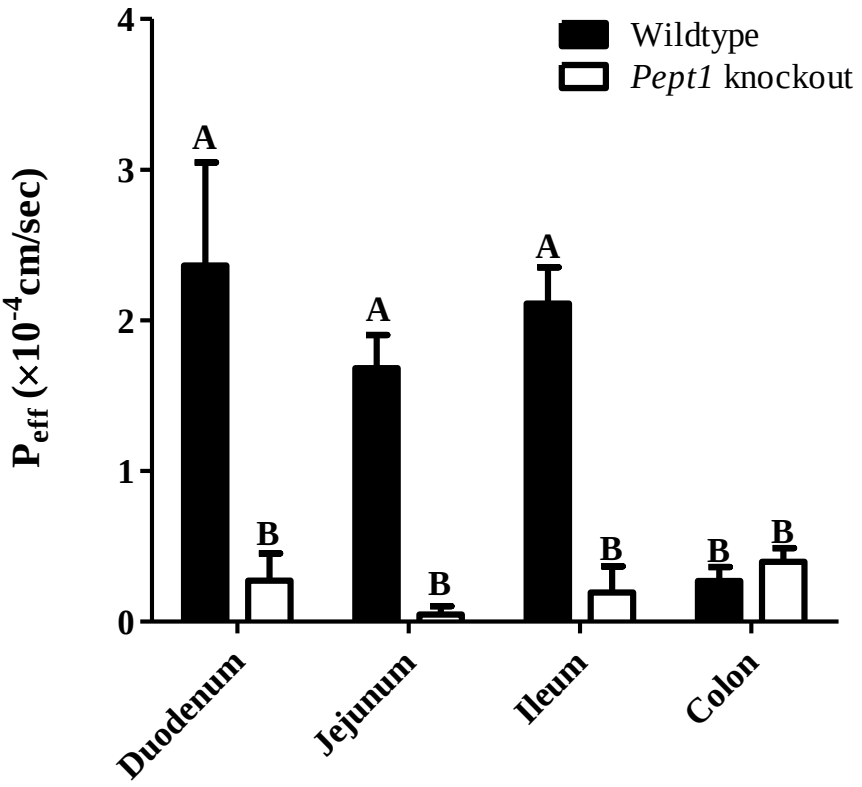

Figure 3.5 Permeability of valacyclovir in different intestinal segments of wildtype and *Pept1* knockout mice. Data are expressed as mean ± SE (n=4-5). Data with the same capital letters were not statistically different.

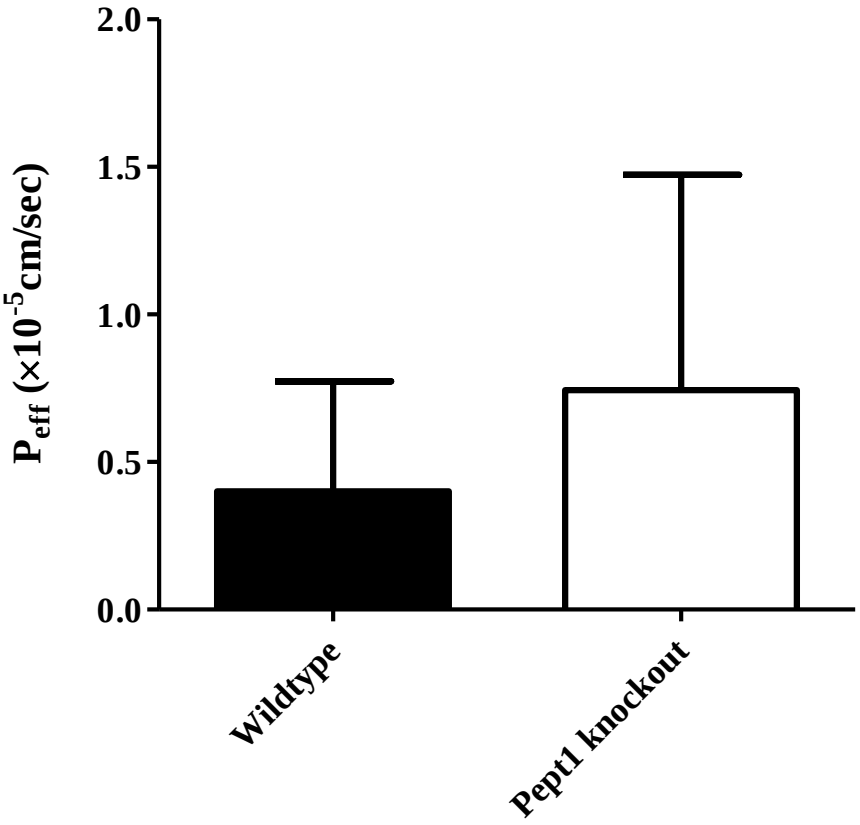

Figure 3.6 Jejunal permeability of 100 µM acyclovir during perfusions of wildtype and *Pept1* knockout mice. Data are expressed as mean ± SE (n=4). Data from the two groups were not statistically different.

REFERENCES

Adachi Y, Suzuki H, and Sugiyama Y (2003) Quantitative evaluation of the function of small intestinal P-glycoprotein: comparative studies between in situ and in vitro. *Pharm Res* **20:**1163-1169.

Balimane PV, Tamai I, Guo A, Nakanishi T, Kitada H, Leibach FH, Tsuji A, and Sinko PJ (1998) Direct evidence for peptide transporter (PepT1)-mediated uptake of a nonpeptide prodrug, valacyclovir. *Biochem Biophys Res Commun* **250:**246-251.

Balimane P and Sinko P (2000) Effect of ionization on the variable uptake of valacyclovir via the human intestinal peptide transporter (hPepT1) in CHO cells. *Biopharmaceutics & drug disposition* **21:**165-174.

Bhardwaj RK, Herrera-Ruiz D, Eltoukhy N, Saad M, and Knipp GT (2006) The functional evaluation of human peptide/histidine transporter 1 (hPHT1) in transiently transfected COS-7 cells. *European journal of pharmaceutical sciences : official journal of the European Federation for Pharmaceutical Sciences* **27:**533-542.

Bhardwaj RK, Herrera-Ruiz D, Sinko PJ, Gudmundsson OS, and Knipp G (2005) Delineation of human peptide transporter 1 (hPepT1)-mediated uptake and transport of substrates with varying transporter affinities utilizing stably transfected hPepT1/Madin-Darby canine kidney clones and Caco-2 cells. *J Pharmacol Exp Ther* **314:**1093-1100.

Brandsch M, Knutter I, and Bosse-Doenecke E (2008) Pharmaceutical and pharmacological importance of peptide transporters. *J Pharm Pharmacol* **60:**543-585.

Dahan A, West BT, and Amidon GL (2009) Segmental-dependent membrane permeability along the intestine following oral drug administration: Evaluation of a triple single-pass intestinal perfusion (TSPIP) approach in the rat. *European journal of pharmaceutical sciences : official journal of the European Federation for Pharmaceutical Sciences* **36:**320-329.

Daniel H (2004) Molecular and integrative physiology of intestinal peptide transport. *Annu Rev Physiol* **66:**361-384.

de Miranda P, Krasny HC, Page DA, and Elion GB (1981) The disposition of acyclovir in different species. *J Pharmacol Exp Ther* **219:**309-315.

de Vrueh RL, Smith PL, and Lee CP (1998) Transport of L-valine-acyclovir via the oligopeptide transporter in the human intestinal cell line, Caco-2. *J Pharmacol Exp Ther* **286:**1166-1170.

Englund G, Rorsman F, Ronnblom A, Karlbom U, Lazorova L, Grasjo J, Kindmark A, and Artursson P (2006) Regional levels of drug transporters along the human intestinal tract: Co-expression of ABC and SLC transporters and comparison with Caco-2 cells. *European Journal of Pharmaceutical Sciences* **29:**269-277.

Ganapathy ME, Huang W, Wang H, Ganapathy V, and Leibach FH (1998) Valacyclovir: a substrate for the intestinal and renal peptide transporters PEPT1 and PEPT2. *Biochem Biophys Res Commun* **246:**470-475.

Granero GE and Amidon GL (2006) Stability of valacyclovir: implications for its oral bioavailability. *International journal of pharmaceutics* **317:**14-18.

Groneberg DA, Doring F, Eynott PR, Fischer A and Daniel H (2001a) Intestinal peptide transport: ex vivo uptake studies and localization of peptide carrier PEPT1. *Am J Physiol Gastrointest Liver Physiol* **281:**G697-704.

Guo A, Hu P, Balimane PV, Leibach FH, and Sinko PJ (1999) Interactions of a nonpeptidic drug, valacyclovir, with the human intestinal peptide transporter (hPEPT1) expressed in a mammalian cell line. *J Pharmacol Exp Ther* **289:**448-454.

Gupta SV, Gupta D, Sun J, Dahan A, Tsume Y, Hilfinger J, Lee KD, and Amidon GL (2011) Enhancing the Intestinal Membrane Permeability of Zanamivir: A Carrier Mediated Prodrug Approach. *Molecular Pharmaceutics* **8:**2358-2367.

Han H, de Vrueh RL, Rhie JK, Covitz KM, Smith PL, Lee CP, Oh DM, Sadee W, and Amidon GL (1998) 5'-Amino acid esters of antiviral nucleosides, acyclovir, and AZT are absorbed by the intestinal PEPT1 peptide transporter. *Pharm Res* **15:**1154-1159.

Hatanaka T, Haramura M, Fei YJ, Miyauchi S, Bridges CC, Ganapathy PS, Smith SB, Ganapathy V, and Ganapathy ME (2004) Transport of amino acid-based prodrugs by the Na+- and Cl(-) -coupled amino acid transporter ATB0,+ and expression of the transporter in tissues amenable for drug delivery. *J Pharmacol Exp Ther* **308:**1138-1147.

Herrera-Ruiz D, Wang Q, Gudmundsson OS, Cook TJ, Smith RL, Faria TN, and Knipp GT (2001) Spatial expression patterns of peptide transporters in the human and rat gastrointestinal tracts, Caco-2 in vitro cell culture model, and multiple human tissues. *AAPS pharmSci* **3:**E9.

Hogerle ML and Winne D (1983) Drug absorption by the rat jejunum perfused in situ. Dissociation from the pH-partition theory and role of microclimate-pH and unstirred layer. *Naunyn-Schmiedeberg's archives of pharmacology* **322:**249-255.

Hu Y, Smith DE, Ma K, Jappar D, Thomas W, and Hillgren KM (2008) Targeted disruption of peptide transporter Pept1 gene in mice significantly reduces dipeptide absorption in intestine. *Mol Pharm* **5:**1122-1130.

Jana S, Mandlekar S, and Marathe P (2010) Prodrug design to improve pharmacokinetic and drug delivery properties: challenges to the discovery scientists. *Current medicinal chemistry* **17:**3874-3908.

Jappar D, Wu SP, Hu Y, and Smith DE (2010) Significance and regional dependency of peptide transporter (PEPT) 1 in the intestinal permeability of glycylsarcosine: in

situ single-pass perfusion studies in wild-type and Pept1 knockout mice. *Drug Metab Dispos* **38:**1740-1746.

Jappar D (2009) Role of proton-coupled oligopeptide transporters in small peptide absorption and disposition.

Kagan L and Hoffman A (2008) Selection of drug candidates for gastroretentive dosage forms: pharmacokinetics following continuous intragastric mode of administration in a rat model. *Eur J Pharm Biopharm* **69:**238-246.

Konig J (2011) Uptake transporters of the human OATP family: molecular characteristics, substrates, their role in drug-drug interactions, and functional consequences of polymorphisms. *Handb Exp Pharmacol* **201**:1-28.

Landowski CP, Sun D, Foster DR, Menon SS, Barnett JL, Welage LS, Ramachandran C, and Amidon GL (2003) Gene expression in the human intestine and correlation with oral valacyclovir pharmacokinetic parameters. *J Pharmacol Exp Ther* **306:**778-786.

Li FJ, Maag H, and Alfredson T (2008) Prodrugs of nucleoside analogues for improved oral absorption and tissue targeting. *Journal of Pharmaceutical Sciences* **97:**1109-1134.

Lucas ML, Lei FH, and Blair JA (1980) The influence of buffer pH, glucose and sodium ion concentration on the acid microclimate in rat proximal jejunum in vitro. *Pflugers Arch* **385:**137-142.

Ma K, Hu YJ, and Smith DE (2011) Peptide Transporter 1 Is Responsible for Intestinal Uptake of the Dipeptide Glycylsarcosine: Studies in Everted Jejunal Rings from Wild-type and Pept1 Null Mice. *Journal of Pharmaceutical Sciences* **100:**767-774.

Meier Y, Eloranta JJ, Darimont J, Ismair MG, Hiller C, Fried M, Kullak-Ublick GA, and Vavricka SR (2007) Regional distribution of solute carrier mRNA expression along the human intestinal tract. *Drug Metab Dispos* **35:**590-594.

Rouge N, Buri P, and Doelker E (1996) Drug absorption sites in the gastrointestinal tract and dosage forms for site-specific delivery. *Int J Pharm* **136**: 117-139.

Rubio-Aliaga I and Daniel H (2008) Peptide transporters and their roles in physiological processes and drug disposition. *Xenobiotica* **38:**1022-1042.

Shiau YF, Fernandez P, Jackson MJ, and McMonagle S (1985) Mechanisms maintaining a low-pH microclimate in the intestine. *Am J Physiol* **248:**G608-617.

Sinko PJ and Balimane PV (1998) Carrier-mediated intestinal absorption of valacyclovir, the L-valyl ester prodrug of acyclovir: 1. Interactions with peptides, organic anions and organic cations in rats. *Biopharmaceutics & drug disposition* **19:**209-217.

Soul-Lawton J, Seaber E, On N, Wootton R, Rolan P, and Posner J (1995) Absolute bioavailability and metabolic disposition of valaciclovir, the L-valyl ester of

acyclovir, following oral administration to humans. *Antimicrob Agents Chemother* **39:**2759-2764.

Sun J, Dahan A, and Amidon GL (2010) Enhancing the intestinal absorption of molecules containing the polar guanidino functionality: a double-targeted prodrug approach. *J Med Chem* **53:**624-632.

Sutton SC, Rinaldi MT, and Vukovinsky KE (2001) Comparison of the gravimetric, phenol red, and 14C-PEG-3350 methods to determine water absorption in the rat single-pass intestinal perfusion model. *AAPS pharmSci* **3:**E25.

Takeda M, Khamdang S, Narikawa S, Kimura H, Kobayashi Y, Yamamoto T, Cha SH, Sekine T, and Endou H (2002) Human organic anion transporters and human organic cation transporters mediate renal antiviral transport. *J Pharmacol Exp Ther* **300:**918-924.

Thwaites DT, Anderson CM (2011) The SLC36 family of proton-coupled amino acid transporters and their potential role in drug transport. *Br J Pharmacol* **164**:1802-1816.

Tsume Y, Vig BS, Sun J, Landowski CP, Hilfinger JM, Ramachandran C, and Amidon GL (2008) Enhanced absorption and growth inhibition with amino acid monoester prodrugs of floxuridine by targeting hPEPT1 transporters. *Molecules* **13:**1441-1454.

Varma MV, Ambler CM, Ullah M, Rotter CJ, Sun H, Litchfield J, Fenner KS, and El-Kattan AF (2010) Targeting intestinal transporters for optimizing oral drug absorption. *Curr Drug Metab* **11:**730-742.

Yan Z, Sun J, Chang Y, Liu Y, Fu Q, Xu Y, Sun Y, Pu X, Zhang Y, Jing Y, Yin S, Zhu M, Wang Y, and He Z (2011) Bifunctional peptidomimetic prodrugs of didanosine for improved intestinal permeability and enhanced acidic stability: synthesis, transepithelial transport, chemical stability and pharmacokinetics. *Mol Pharm* **8:**319-329.

CHAPTER 4

IMPACT OF PEPT1 ON THE INTESTINAL ABSORPTION AND PHARMACOKINETICS OF VALACYCLOVIR DURING DOSE ESCALATION IN WILDTYPE AND PEPT1 KNOCKOUT MICE

ABSTRACT

Purpose. To assess the quantitative significance of PEPT1 on the intestinal absorption and pharmacokinetics of orally administered valacyclovir during dose escalation in wildtype and *Pept1* knockout mice.

Methods. [^{3}H]Valacyclovir was administered to wildtype and *Pept1* knockout mice by oral gavage at increasing doses of 10, 25, 50 and 100 nmol/g body weight. [^{3}H]Acyclovir (25 nmol/g body weight), which is not a PEPT1 substrate, was also administered to both genotypes via intravenous or oral routes. Serial blood samples (20 μL per sample) following acyclovir or valacyclovir dosing were collected up to 180 minutes. Tissue distribution studies were performed 20 minutes and 360 minutes after oral dosing of 25 nmol/g valacyclovir in two genotypes. [^{14}C]Dextran (0.25 μCi per mouse) was administered by tail vein injection 5 min prior to harvesting tissue samples to correct for vascular space. Acyclovir concentrations in select tissue, plasma and blood samples were determined by liquid scintillation counting. Pharmacokinetic parameters

such as peak plasma concentration of acyclovir (C_{max}), time to reach C_{max} (T_{max}), and area under the acyclovir plasma concentration-time curve (AUC), as well as acyclovir tissue distribution profiles were compared between the two genotypes.

Results. Upon oral administration of [^{3}H]valacyclovir at all four doses, acyclovir C_{max} and $AUC_{0\text{-}180min}$ were on average 78% ($p<0.05$) and 58% ($p<0.01$) lower in *Pept1* knockout mice than that in wildtype mice. Acyclovir T_{max} estimates in *Pept1* knockout mice were also significantly greater than those in wildtype mice ($p<0.05$). Acyclovir C_{max} and $AUC_{0\text{-}180min}$ were linearly correlated with valacyclovir doses in the range of 10-100 nmol/g for both genotypes (i.e., dose proportionality). On the other hand, acyclovir plasma concentration-time curves obtained after intravenous or oral administration of acyclovir in both genotypes were almost superimposable. For tissue samples other than from gastrointestinal segments, acyclovir tissue concentrations were significantly higher in wildtype mice than in *Pept1* knockout mice 20 minutes after dosing but were similar 360 minutes after dosing. After acyclovir concentrations in non-gastrointestinal tissues were corrected by corresponding blood levels, no statistical differences were observed.

Conclusions. These findings suggest that PEPT1 played a crucial role in facilitating the intestinal absorption of valacyclovir; its deletion significantly reduced the rate and extent of the intestinal absorption of valacyclovir. Dose proportionality of acyclovir C_{max} and $AUC_{0\text{-}180min}$ over a wide oral dose range of valacyclovir was consistent with the high-capacity, low-affinity feature of PEPT1-mediated transport. PEPT1 ablation showed no effect on the *in vivo* absorption, distribution and disposition of acyclovir after oral and intravenous acyclovir dosing.

INTRODUCTION

Proton-coupled peptide transporter 1 (PEPT1) is one of the best characterized membrane transporters because of its physiological and pharmacological importance (Herrera-Ruiz and Knipp, 2003; Brandsch et al., 2008; Rubio-Aliaga and Daniel, 2008). PEPT1, a member of the proton-coupled oligopeptide transporter (POT) family, is a highly conserved influx transporter and commonly expressed in different mammalian species including human, rat and mouse. The mammalian PEPT1, comprised of 707-710 amino acid residues depending on species, is predicted to have 12 trans-membrane domains with both N- and C-terminal facing the cytosolic side. PEPT1 couples the influx of its substrates and proton, where the inwardly directly proton gradient and negative membrane potential are the driving force for this movement. As a high-capacity low-affinity influx transporter, PEPT1 is principally localized on the brush border membrane of epithelial cells in the small intestine and functions as the active uptake carrier of di-/tri-peptides generated by the digestion of dietary proteins. Since approximately 80% of digested proteins are absorbed in the form of di-/tri-peptides while only 20% in the form of free amino acids, PEPT1 plays an essential physiological role in protein assimilation (Daniel, 2004).

The pharmacological relevance of PEPT1 mainly lies in its ability to transport a wide spectrum of drugs from some important therapeutic classes, in addition to its physiological substrates. For example, many cephalosporins and aminopenicillins and some selected angiotensin-converting enzyme inhibitors are known substrates for PEPT1 (Bretschneider et al., 1999; Knutter et al., 2008). More interestingly, a number of amino

acid or dipeptide conjugated prodrugs such as midorine, valacyclovir, valaganciclovir and LY544344, were also found to undergo PEPT1-mediated transport (Han et al., 1998; Sinko and Balimane, 1998; Sugawara et al., 2000; Tsuda et al., 2006; Varma et al., 2009; Eriksson et al., 2010). Prodrugs of this type are commonly called PEPT1 targeted prodrugs. This targeted prodrug strategy is under intensive investigation as a promising way to improve the oral availability of polar and hydrophilic compounds (Varma et al., 2010).

Valacyclovir is widely viewed as the model of PEPT1 targeted prodrugs. Valacyclovir is an L-valyl ester prodrug of the potent antiviral agent acyclovir used for the treatment and prophylaxis of herpes, varicella zoster, and cytomegalovirus infection. In humans, the absolute oral availability of acyclovir after oral administration of valacyclovir was nearly 54.2%, as opposed to only 10-20% after oral dosing of acyclovir (Soul-Lawton et al., 1995). Among these PEPT1 targeted prodrugs, the uptake and pharmacokinetic characteristics of valacyclovir have been most extensively with some inconsistent or even controversial findings. On one hand, numerous cell culture studies showed PEPT1-mediated valacyclovir uptake into cells constitutively expressing or transfected with PEPT1 (Balimane et al., 1998; Ganapathy et al., 1998; Han et al., 1998; Guo et al., 1999; Balimane and Sinko, 2000). One the other hand, valacyclovir was also found to interact with other transporters such as organic anion transporter 3 (OAT3) (Takeda et al., 2002), peptide histidine transporter 1 (PHT1) (Bhardwaj et al., 2006), organic cation transporters (OCTs) (Sinko and Balimane, 1998), a human peptide transporter (HPT1) (Landowski et al., 2003), and an amino acid transporter $ATB^{0,+}$ (Hatanaka et al., 2004). Currently, the general consensus is that the improved oral

availability of acyclovir after oral dosing of valacyclovir is mainly attributable to PEPT1 mediated uptake; however, convincing quantitative evidence is completely lacking supporting the main contribution of PEPT1 relative to other valacyclovir transporters.

Moreover, some human pharmacokinetic studies failed to reveal the relevance of PEPT1 in the intestinal absorption of valacyclovir, making the role of PEPT1 in valacyclovir absorption even more controversial. For instance, Landowski and his coworkers (2003) showed a strong positive correlation of pharmacokinetic parameters of acyclovir, after oral dosing of valacyclovir, with human oligopeptide transporter (HPT1) levels but no significant correlation with PEPT1 expression. Another pharmacokinetic study showed that co-administration of valacyclovir and cephalexin, another PEPT1 substrate, at a single oral dose of 500 mg for both compounds had minimal impact on the pharmacokinetic parameters of oral valacyclovir, suggesting either higher doses of cephalexin or more potent PEPT1 substrates are needed for noticeable PEPT1-related drug-drug interactions or PEPT1-mediated uptake is not the only important pathway for the oral absorption of valacyclovir (Phan et al., 2003).

Given these inconsistencies, future studies that can conclusively elucidate the quantitative importance of PEPT1 in the absorption of valacyclovir and other PEPT1 targeted prodrugs are warranted. The aim of the current study was to clarify the ambiguous contribution of PEPT1 to the *in vivo* oral absorption and pharmacokinetics of valacyclovir, by performing comparative pharmacokinetic and tissue distribution studies in wildtype and *Pept1* knockout mice. With the use of *Pept1* knockout animal model, this study can provide the first quantitative evidence supporting PEPT1 targeted prodrug strategy.

MATERIALS AND METHODS

Animals. Animal studies were conducted in accordance with the Guide for the Care and Use of Laboratory Animals as adopted and promulgated by the U.S. National Institutes of Health. Gender matched wildtype and *Pept1* knockout mice, 8 to 10 weeks of age, were used for all experiments. The mice were kept in a temperature-controlled environment with a 12-hr light/dark cycle and received a standard diet and water *ad libitum* (Unit for Laboratory Animal Medicine, University of Michigan, Ann Arbor, MI).

Materials. Unlabeled valacyclovir hydrochloride, unlabeled acyclovir and hydrogen peroxide were purchased from Sigma-Aldrich (St. Louis, MO). Hyamine hydroxide was purchased from ICN Radiochemicals (Irvine, CA). [^{3}H]Valacyclovir (2.1 Ci/mmol), [^{3}H]acyclovir (12.1 Ci/mmol) and [^{14}C]dextran-carboxyl (1.1 mCi/g) were acquired from Moravek Biochemicals and Radiochemicals (Brea, CA).

Pharmacokinetic (PK) studies following oral valacyclovir. Wildtype and *Pept1* knokout mice were fasted overnight (~16 hours) prior to each experiment. Valacyclovir solutions were prepared by dissolving appropriate amounts of ^{3}H-labeled and unlabeled valacyclovir in normal saline. Valacyclovir solution (200 µL, 10 µCi per mouse) was administered by gastric gavage at single doses of 10, 25, 50 and 100 nmol/g body weight. Serial blood samples (20 µL per sample) were collected by tail nicks at 0, 5, 15, 30, 45, 60, 90, 120, and 180 after dosing. Blood samples were transferred to 0.2 mL microcentrifuge tubes containing 7.5% potassium EDTA and centrifuged at 3000 g for 3 min, ambient temperature. A 5-10 µL aliquot of plasma was then transferred to a scintillation vial and 6 mL CytoScint scintillation fluid (MP Biomedicals, Solon, OH)

was added to the sample. Radioactivity of the plasma sample was measured on a dual-channel liquid scintillation counter (Beckman LS 6000 SC; Beckman Coulter Inc., Fullerton, CA). Mice were returned to cages between blood sampling and had free access to water.

In a separate pharmacokinetic study, acyclovir plasma concentrations following oral administration of 100 nmol/g unlabeled valacyclovir in wildtype mice were also determined using a validated HPLC method. Due to the low quantification sensitivity of the HPLC method, at least 20 µL aliquot of plasma was needed for HPLC analysis. On the other hand, due to the limited blood volume that can be taken from a mouse, no more than 4 blood samples (40~60 µL per sample) could be collected from each animal. Since only 4 mice were used in this preliminary study, one single acyclovir plasma concentration-time curve was constructed by plotting a single concentration value (or an average of two concentration data if available) against time. Detailed blood sampling scheme is listed in Table 4.1.

Tissue distribution studies following oral valacyclovir. Tissue distribution studies were performed 20 minutes and 360 minutes after oral administration of 25 nmol/g [^{3}H]valacyclovir in both wildtype and *Pept1* knockout mice. 100 µL [^{14}C]dextran solution (0.25 µCi per mouse) was administered by tail vein injection to each mouse 5 minutes before harvesting tissues to determine the tissue vascular space. Following decapitation, selected organs/tissues including brain, eyes, heart, lung, liver, kidney, spleen, muscle and gastrointestinal (GI) segments including stomach, duodenum, jejunum, ileum and colon were isolated, blotted dry, weighed, and then solubilized in 330 µL of 1

M hyamine hydroxide at 37℃ overnight, as described by the manufacturer. Three 10-μL whole blood samples were also collected. The GI segments were flushed 2-3 times with ice-cold saline solution to remove contents prior to weighing. After solubilization of all organs/tissues, 40 μL H_2O_2 (30%) was slowly added to each sample for decolorization. 6 mL CytoScint scintillation fluid was added to each sample and the radioactivity of tissue samples were also measured by a dual-channel liquid scintillation counter.

Pharmacokinetic studies following oral or intravenous acyclovir. Acyclovir solutions were prepared by dissolving appropriate amounts of ^{3}H-labeled and unlabeled acyclovir in normal saline. For oral studies, 200 μL acyclovir solution (10 μCi per mouse) was administered to each animal by gastric gavage at a single acyclovir dose of 25 nmol/g body weight. Blood sample collection time points were the same as for oral valacyclovir. For intravenous studies, 100 μL acyclovir solution (5 μCi per mouse) was administered by tail vein injection at a single dose of 25 nmol/g body weight. Serial blood samples (20 μL per sample) were collected at 0, 2, 5, 15, 30, 60, 90, 120 and 180 minutes after intravenous dosing. Other experimental procedures such as plasma collection and radioactivity assay were the same as previously described.

Sample preparation and HPLC analysis. A 20-μL aliquot of plasma sample obtained in PK studies was mixed with an 80-μL blank mouse plasma sample containing internal standard (IS) ganciclovir to prepare a final plasma sample. Each final plasma sample (100 μL) was mixed with HPLC-grade acetonitrile at a ratio of 1:2 (v/v) and then vigorously vortex-mixed for 1 minute at room temperature for complete protein precipitation. The resulting mixture was then centrifuged at 15000 g at 4 °C for 10

minutes. Clean supernatant was carefully collected and transferred to a new 1.5-mL centrifuge tube and evaporated to dryness under vacuum. The residue was then reconstituted by the addition of 40 µL mobile phase prior to HPLC analysis. Each calibration standard plasma sample of acyclovir (20 µL per sample) was also mixed with 80 µL blank IS-containing mouse plasma and then prepared following the above-mentioned procedure. The linearity range of acyclovir concentration in the 20-µL plasma sample was 6.25 to 500 µM. In the HPLC analysis, The isocratic mobile phase consisted of 3% organic phase (0.1% v/v trifluoroacetic acid (TFA) in acetonitrile) and 97% aqueous phase (0.1% v/v TFA in water). Other HPLC conditions were the same as previously described in Chapter 3.

Data analysis. Acyclovir plasma concentration versus time curves following different dosing routes were fitted by non-compartmental analysis (WinNonlin, version 5.3; Pharsight Inc., Mountainview, CA). Following oral administration of valacyclovir or acyclovir, peak acyclovir plasma concentrations (C_{max}) and time to reach C_{max} (T_{max}) were observed values. Area under the acyclovir plasma concentration-time curve (AUC) was calculated by linear trapezoidal rules. For intravenous administration of acyclovir, AUC, total clearance (CL), the volume of distribution at steady state (V_{dss}) were also reported. Terminal half-life ($T_{1/2}$) was estimated as $T_{1/2}=\ln 2/\lambda_z$, where λ_z is the log-linear slope determined by using ≥ 3 data points from the terminal phase.

For tissue distribution studies, acyclovir tissue concentrations were corrected for the vascular space using the following equation: $C_{tiss,\ corr}=C_{tiss} - DS\times C_b$, where $C_{tiss,\ corr}$ and C_{tiss} stand for the corrected and uncorrected acyclovir tissue concentrations (nmol/g),

DS is the dextran space (blood vascular space) in the tissue (mL/g), and C_b is acyclovir blood concentrations (nmol/mL).

All results were expressed as mean ± standard error (SE) unless otherwise indicated. Unpaired two-tail T-test was used to compare differences between two different experimental groups of mice. A p value of less than 0.05 was considered statistically significant.

RESULTS

HPLC analysis. Figure 4.1 depicts representative HPLC chromatograms for the quantification of acyclovir in mouse plasma. The IS and acyclovir were well separated with no interference from endogenous substances in plasma. A calibration curve was constructed by least squares linear regression analysis of the peak area ratios of acyclovir to the IS (y) versus analyte concentrations (x). A typical regression equation was y=0.066x-0.063 with a correlation coefficient (R^2) of 0.9997. Good linearity was shown in the stated concentration range.

Pharmacokinetic studies following oral or intravenous acyclovir. As demonstrated in Figure 4.2 (A-D), mean acyclovir plasma concentration versus time curves were almost superimposable following either oral or intravenous administration of 25 nmol/g acyclovir in wildtype and *Pept1* knockout mice. Non-compartmental PK parameters of acyclovir derived after its oral or intravenous administration for each genotype are shown in Table 4.2. Lack of significant difference in each PK parameter between two genotypes confirms that PEPT1 ablation does not affect the absorption and *in vivo* disposition of acyclovir in mice.

Pharmacokinetic studies following oral valacyclovir. The mean acyclovir plasma concentration-time curves following oral administration of valacyclovir at increasing doses in both wildtype and *Pept1* knockout mice are depicted in both linear (Figure 4.3) and logarithmic (Figure 4.4) scales. As shown in Figures 4.3 and 4.4, acyclovir plasma concentrations displayed different time courses in the two genotypes. In wildtype mice, acyclovir plasma concentrations increased quickly to reach C_{max} within 30

minutes after oral dosing of valacyclovir. Right after reaching peak concentrations, acyclovir plasma concentrations decreased rapidly up to 60 minutes, followed by a much slower deccline up to 180 minutes. In contrast, *Pept1* knockout mice had substantially lower acyclovir peak concentrations at much delayed time points for each dose group. In addition, acyclovir concentrations nearly plateaued out with time after reaching C_{max} in *Pept1* knockout mice.

In addition to the visual inspection of acyclovir plasma concentration-time curves, the contribution of PEPT1 to the rate and extent of valacyclovir absorption was further assessed by comparing metrics including C_{max}, T_{max}, early cumulative partial AUC, and AUC, among which the first three metrics are proposed as indicators of absorption rate while AUC is a measure of the extent of oral absorption (Chen et al., 2001). As seen in Table 4.3, there was approximately a 54-65% reduction in $AUC_{0\text{-}180\ min}$ in *Pept1* knockout mice compared with wildtype animals ($p<0.01$), suggesting reduced extent of valacyclovir systemic exposure due to PEPT1 ablation. Acyclovir C_{max} was approximately 5-fold lower in *Pept1* knockout than that in wildtype mice at four doses ($p<0.05$). Meanwhile, mean T_{max} ranged from 15 to 24 minutes in wildtype mice and from 71 to 156 minutes in *Pept1* knockout mice ($p<0.05$). Furthermore, the ratio of early partial AUC of *Petp1* knockout to wildtype mice, when truncated at 60 minutes, was 22%, 14%, 21% and 17%, for the four increasing dose levels. Cumulative partial AUC vs. time curves were also used in order to investigate the potential impact of PEPT1 deletion on the absorption rate of valacyclovir at four examined doses. As illustrated in Figure 4.5 (A-D), the curve slopes for wildtype mice were much steeper than those for *Pept1* knockout mice during early time intervals (5-60 min). However, the curves from both

genotypes appear to be parallel to each other and have similar slopes from 90 to 180 min. As shown in Table 4.4, at 5-60 min, the slopes were approximately 78% lower in *Pept1* knockout mice compared with wildtype mice, whereas from 90-180 min, the slopes for both genotypes were similar with less than 21% difference. Jointly, comparison of all these metrics described above suggests significantly reduced rate and extent of valacyclovir absorption due to PEPT1 deficiency.

Following oral dosing of 100 nmol/g unlabeled valacyclovir in wildtype mice, the plasma concentration-time curve of acyclovir was also measured by HPLC coupled with fluorescence detection. As shown in Figure 4.6, the acyclovir plasma concentration-time curve determined by HPLC was similar to the previously shown mean concentration-time curve determined by radioactive assay, suggesting the total radioactivity measured in plasma was attributable to plasma acyclovir rather than prodrug valacyclovir and possible minor metabolites of acyclovir.

Dose-proportionality of acyclovir C_{max} and $AUC_{0\text{-}180min}$ following oral valacyclovir in both genotypes was evaluated over the oral dose range of 10-100 nmol/g valacyclovir. As shown in Figure 4.7 (A-B), both C_{max} and $AUC_{0\text{-}180min}$ of acyclovir were linearly correlated with oral valacyclovir doses in the two genotypes, with non-zero regression slopes ($p<0.0001$). Figure 4.7 (C-D) shows that ratios of C_{max}/dose and $AUC_{0\text{-}180min}$/dose were independent of doses, evidenced by the slopes of linear regression lines not being different from zero.

Acyclovir tissue distribution following oral valacyclovir. Tissue distribution studies were performed 20 minutes and 360 minutes after oral administration of 25

nmol/g valacyclovir to examine the impact of PEPT1 ablation on the *in vivo* distribution of acyclovir. As shown in Figure 4.8 (A), 20 minutes after oral dosing of valacyclovir, acyclovir concentrations in non-GI tissues were always significantly higher in wildtype mice than that in *Pept1* knockout mice. A 5-fold significant difference was also observed between whole blood concentrations ($p<0.001$). As demonstrated in Figure 4.8 (B), for proximal GI segments including stomach, duodenum and jejunum, no significant differences in these tissue concentrations were observed between two genotypes; however, for distal intestinal segments including ileum and colon, significantly higher tissue concentrations were found in wildtype mice, similar to the pattern observed in non-GI tissues. As shown in Figure 4.9 (A-B), 360 minutes after oral dosing of valacyclovir, no statistically significant differences were observed in acyclovir tissue and whole blood concentrations between wildtype and *Pept1* knockout mice, except for brain. Acyclovir brain concentrations were significantly higher in *Pept1* knockout mice with a p value of 0.017.

After oral administration of valacyclovir, non-GI tissues only received acyclovir from arterial blood perfusing them. Therefore acyclovir concentrations in non-GI tissues, corrected by their corresponding whole blood concentrations, were also examined to rule out the differences in tissue concentrations caused by the differences in systemic exposure. As shown in Figure 4.10, except for brain, no significant differences were observed between two genotypes for the tissue-to-blood concentration ratios of non-GI samples at both 20 min and 360 min. 20 minutes after dosing, acyclovir brain-to-blood concentration ratios were significantly higher in *Pept1* knockout mice with a p value of 0.025.

DISCUSSION

Valacyclovir was found to be actively transported by PEPT1 in various cell culture systems expressing PEPT1. Our *in situ* intestinal perfusion studies of valacyclovir in wildtype and *Pept1* knockout mice further demonstrated that intestinal PEPT1 is the predominant route of valacyclovir uptake in mouse small intestine, accounting for nearly 90% of valacyclovir permeability in various small intestinal segments of wildtype mice. The finding on PEPT1-mediated intestinal permeability of valacyclovir provides the first quantitative measure for the relative significance of PEPT1 in enhancing intestinal absorption of valacyclovir. However, the potential limitation of perfusion studies is that it does not account for other simultaneous intestinal kinetic processes of valacyclovir such as physiological gastrointestinal transit kinetics and valacyclovir luminal degradation. Furthermore, the direct influence of PEPT1 on the *in vivo* absorption and overall pharmacokinetic profiles of valacyclovir cannot be reflected by permeability studies. The current pharmacokinetic and tissue distribution studies, performed in wildtype and *Pept1* knockout mice in parallel, were designed to examine the *in vivo* contribution of PEPT1 over a wide dose range.

When parent drug acyclovir was administered to wildtype and *Pept1* knockout mice via oral or intravenous routes, no significant differences were observed in either acyclovir plasma concentration versus time curves (Figure 4.2) or its PK parameters (Table 4.1), indicating that PEPT1 does not affect the oral absorption and i*n vivo* disposition of acyclovir, consistent with the previous *in situ* perfusion finding of acyclovir not being transported by PEPT1. Furthermore, lack of significant differences in

acyclovir pharmacokinetics between two genotypes also suggests that pharmacokinetic processes that may affect the *in vivo* disposition of acyclovir, such as distribution and elimination, remain similar in two genotypes. When the ratio of AUC following oral and intravenous dosing of acyclovir was used to measure oral bioavailability, the mean oral bioavailability of acyclovir was 51% in wildtype and 46% in *Pept1* knockout mice respectively, similar to the previous report that the oral availability of acyclovir in mouse was 43.2%, a value higher than the oral availability of acyclovir in rat and human (de Miranda et al., 1981; Soul-Lawton et al., 1995).

The purpose of comparing acyclovir plasma concentration time profiles determined by HPLC and radioactivity assay was to confirm that the total radioactivity measured in mouse plasma (or tissues) is only corresponding to acyclovir. As shown Figure 4.6, the two curves are nearly superimposable with each other. Besides, in previous perfusion studies, valacyclovir was found to undergo rapid and nearly complete hydrolysis in the intestinal wall and only acyclovir was detected in portal vein blood. Previous metabolic studies of acyclovir also showed 94% of the urinary radioactivity in mice was unchanged acyclovir (de Miranda et al., 1981). Given all the literature and our own experimental evidence, we concluded that the measured radioactivity in plasma is attributable to acyclovir and the pharmacokinetics of the active drug acyclovir is a suitable measure of the prodrug's performance *in vivo*.

In the PK studies following oral administration of valacyclovir, marked differences were observed in acyclovir plasma concentration versus time profiles between two genotypes. For each dose, acyclovir plasma levels in wildtype were always significantly higher than that in *Pept1* knockout mice at the same time point up to 90

minutes after administration, indicative of different absorption profiles between two genotypes (Figure 4.3 and 4.4). Various metrics were also employed to assess the differences in the extent and rate of valacyclovir absorption in mouse. The key finding from this part of the pharmacokinetic study is that PEPT1 deletion leads to 2-fold difference in AUC (a well-accepted indicator of systemic exposure) and 5-fold difference in C_{max} (a much-criticized indicator of the absorption rate), supporting the quantitative significance of PEPT1 in the intestinal absorption of valacyclovir. Partial AUC during early time interval after drug administration was also proposed as a measure of the rate of absorption, which is more discriminating than C_{max} and/or T_{max} in the evaluation of absorption rates (Chen, 1992; Chen et al., 2001). In our study, partial AUC in *Pept1* knockout mice, when truncated at 60 minutes, was 80% less than that in wildtype mice, revealing marked differences in the rate of valacyclovir absorption. Similarly, slopes of the cumulative partial AUC-time curves (from 5 to 60 minutes) were also reduced by about 80% in *Pept1* knockout mice compared to wildtype mice, again suggesting significantly decreased absorption rate of valacyclovir due to PEPT1 deletion.

Wide dose proportionality of AUC and C_{max} of acyclovir was revealed after oral dosing of valacyclovir in two genotypes in the dose range of 10-100 nmol/g. This dose range was selected by allometric scaling of commonly prescribed clinical doses based on body weight. In perfusion studies, apparent affinity constant of valacyclovir toward intestinal PEPT1 was estimated to be approximately 10 mM at pH 6.5. Assuming a stomach volume of 0.4 mL, the maximum possible stomach concentration of valacyclovir after oral administration of 100 nmol/g body weight valacyclovir (assuming a typical body weight of 20 g) was 5 mM, which is much lower than apparent K_m for PEPT1. The

luminal concentration of valacyclovir down the intestinal tract longitudinally may further decrease due to various factors such as simultaneous transit, absorption, degradation and changes in fluid volume of each segment. Consequently, no appreciable saturation in the pharmacokinetics of orally administered valacyclovir was observed. Overall, the apparent linearity of PK parameters with doses in wildtype animals is in agreement with the low-affinity high-capacity characteristics of PEPT1-mediated transport.

Results from the current comparative pharmacokinetic study corroborate our previous *in situ* perfusion findings regarding the major role of PEPT1 in the intestinal uptake of valacyclovir; however, the magnitude of the contribution of PEPT1 was found to be less pronounced *in vivo* than *in situ*. Intuitively, one reasonable explanation for the discrepancy is the effect of the *in vivo* transit of valacyclovir from proximal small intestine to distal large intestine. The transit time was reported to be around 1 hour in mouse small intestine. Assuming identical transit kinetics for wildtype and *Pept1* knockout mice, valacyclovir can be expected to undergo rapid PEPT1-mediated absorption in the small intestine and negligible absorption in the colon due to small concentration gradient available for passive diffusion in wildtype mice. In contrast, in *Pept1* knockout mice, valacyclovir has a slow passive absorption in the small intestine with greater residual concentration of drug reaching the colon, leading to greater compensatory passive absorption in the distal segment for a sufficient time period. In addition, in the *in vivo* absorption process, valacyclovir is simultaneously degraded to generate acyclovir in the lumen all the time, resulting in less valacyclovir available for rapid PEPT1 mediated uptake in the small intestine of wildtype mice. In the following chapter, simulation and modeling will be used as a means to integrate *in situ* and *in vivo*

results and further facilitate our mechanistic understanding of variable factors that may affect valacyclovir absorption.

The rationale of characterizing tissue distribution of acyclovir at 20 minutes after oral valacyclovir was that on average acyclovir T_{max} was found to be nearly 20 minutes in wildtype animals. Conceivably, absorption process is still playing a major role in determining the systemic levels of acyclovir at this time point. To the contrary, 360 minutes after dosing was selected based on the assumption that valacyclovir intestinal absorption is completed and only the *in vivo* disposition kinetics dictates the tissue levels of acyclovir.

For non-GI tissues, when acyclovir tissue levels were examined at 20 minutes and 360 minutes post dosing, it was confirmed that the differences in acyclovir tissue concentrations was only driven by the differences in acyclovir blood levels under equilibrium conditions, as evidenced by lack of significant differences in tissue-to-blood concentration ratios between two genotypes (Figure 4.10). These results support our previous finding that PEPT1 does not play a role in affecting the *in vivo* disposition of acyclovir. The only exception was brain, which showed significantly higher brain-to-blood concentration ratios in *Pept1* knockout than in wildtype mice at 20 minutes. This erratic result might be explained by altered uptake of acyclovir in the brain of *Pept1* knockout mice. However no existing experimental results can support this postulation.

Gastrointestinal segments are the site of absorption for orally administered valacyclovir. 20 Minutes after oral administration of valacyclovir, the gastrointestinal tissues may still receiving valacyclovir from the luminal side. Therefore, we expected the

differences in valacyclovir intestinal uptake between two genotypes would translate into different tissue levels of acyclovir in GI segments. However, no significant differences in acyclovir concentrations were found for upper GI segments (stomach, duodenum and jejunum) between the two genotypes while acyclovir ileal and colonic concentrations were significantly higher in wildtype mice than those in *Pept1* knockout mice. At first, the lack of differences in acyclovir levels in upper GI segments between the two genotypes was ascribed to a flawed experimental procedure, in which the washing step might not be sufficient for the removal of high luminal levels of valacyclovir that may attach onto the membrane surface of GI tissue samples. However, increasing the number of washes did not improve the result. Future experiment is warranted for a meaningful interpretation of this result. 360 Minutes post dosing, acyclovir levels in GI tissues are presumably only in equilibration with plasma acyclovir. No significant differences were found either in acyclovir blood levels or in acyclovir tissue levels for GI segments (Figure 4.9).

In conclusion, this study demonstrates that PEPT1 deletion significantly reduced the extent and rate of the intestinal absorption of valacyclovir in *Pept1* knockout mice while PEPT1 did not affect the *in vivo* distribution and disposition of acyclovir. Future modeling studies are needed to extrapolate *in situ* findings to *in vivo* cases in a quantitative way.

(A)

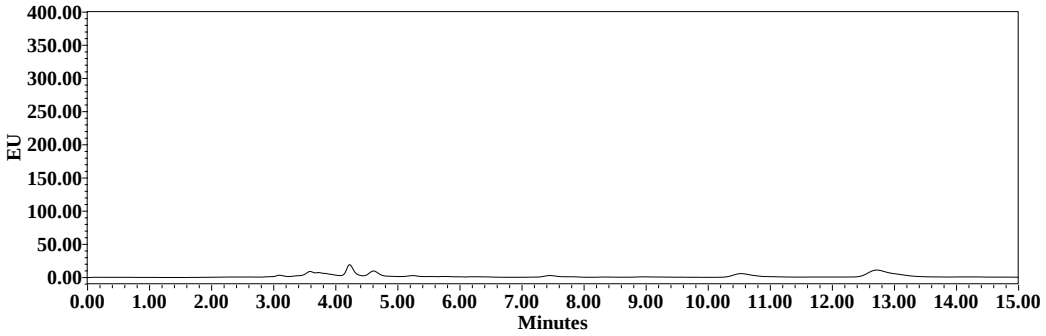

(B)

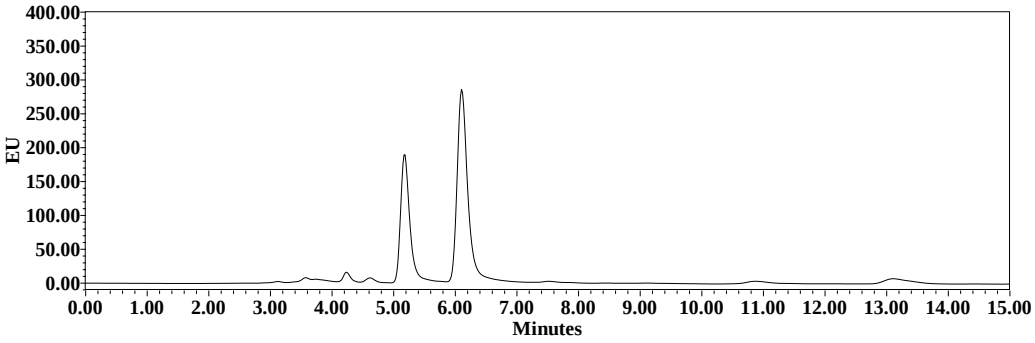

(C)

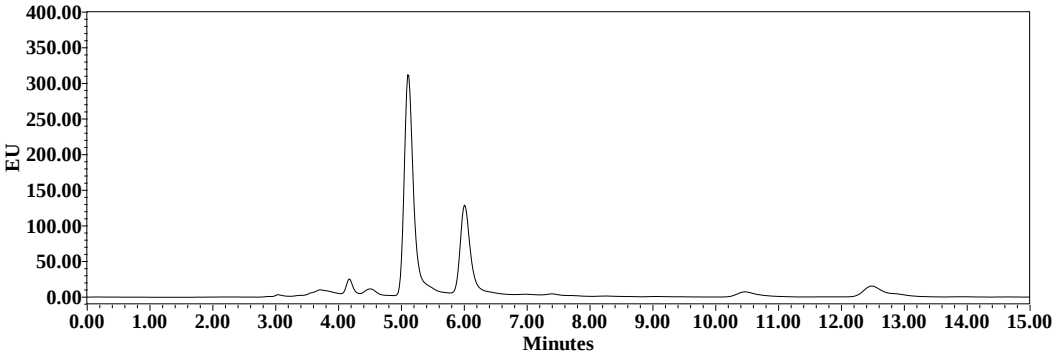

Figure 4.1 HPLC chromatograms for the analyses of acyclovir and the internal standard (IS) ganciclovir in: (A) a blank plasma sample; (B) an acyclovir calibration standard of 250 µM; (C) a real PK sample 15 minutes after oral administration of 100 nmol/g unlabeled valacyclovir in a wildtype mouse. Chromatographic peaks at 5.1 and 6.1 minutes correspond to ganciclovir and acyclovir, respectively.

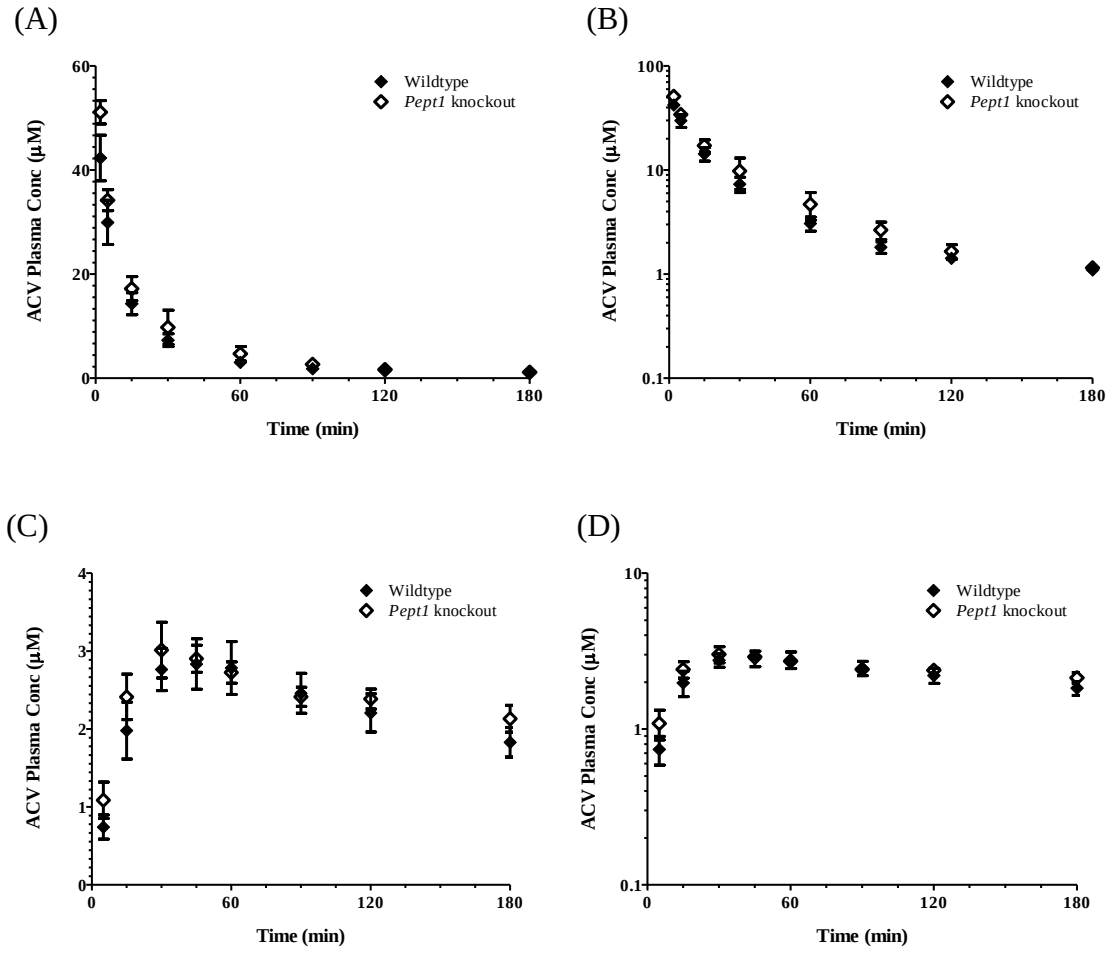

Figure 4.2 Acyclovir plasma concentration-time curves in wildtype and *Pept1* knockout mice after dosing acyclovir: (A) intravenous bolus administration of 25 nmol/g body weight (y-axis shown as a linear scale); (B) intravenous bolus administration of 25 nmol/g body weight (y-axis shown as a logarithmic scale); (C) oral administration of 25 nmol/g body weight (y-axis shown as a linear scale); (D) oral administration of 25 nmol/g body weight (y-axis shown as a logarithmic scale). Data are expressed as mean ± SE (n=3-6).

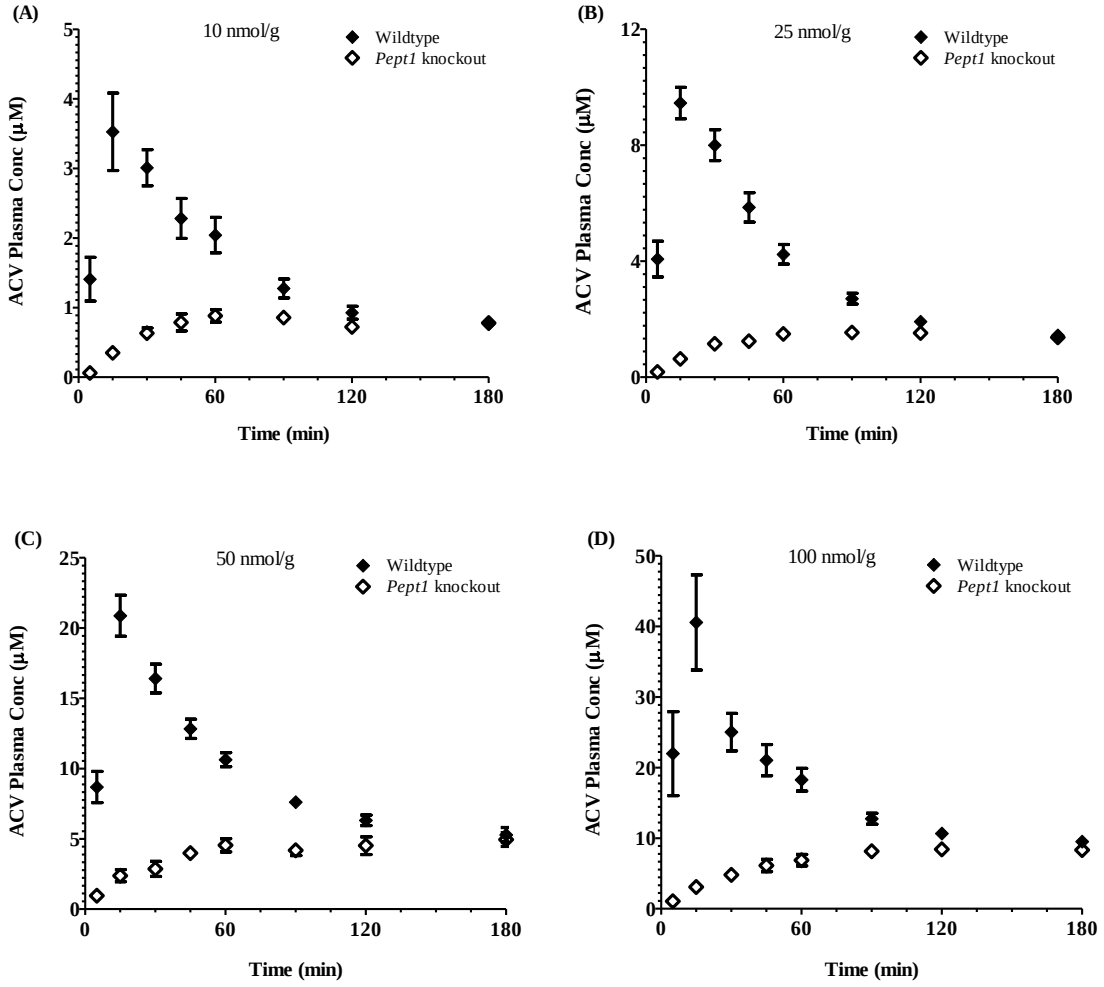

Figure 4.3 Acyclovir plasma concentration-time curves in wildtype and *Pept1* knockout mice after oral administration of [^{3}H]valacyclovir of: (A) 10 nmol/g body weight; (B) 25 nmol/g body weight; (C) 50 nmol/g body weight; (D) 100 nmol/g body weight (y-axis shown as a linear scale). Data are expressed as mean ± SE (n=4-7).

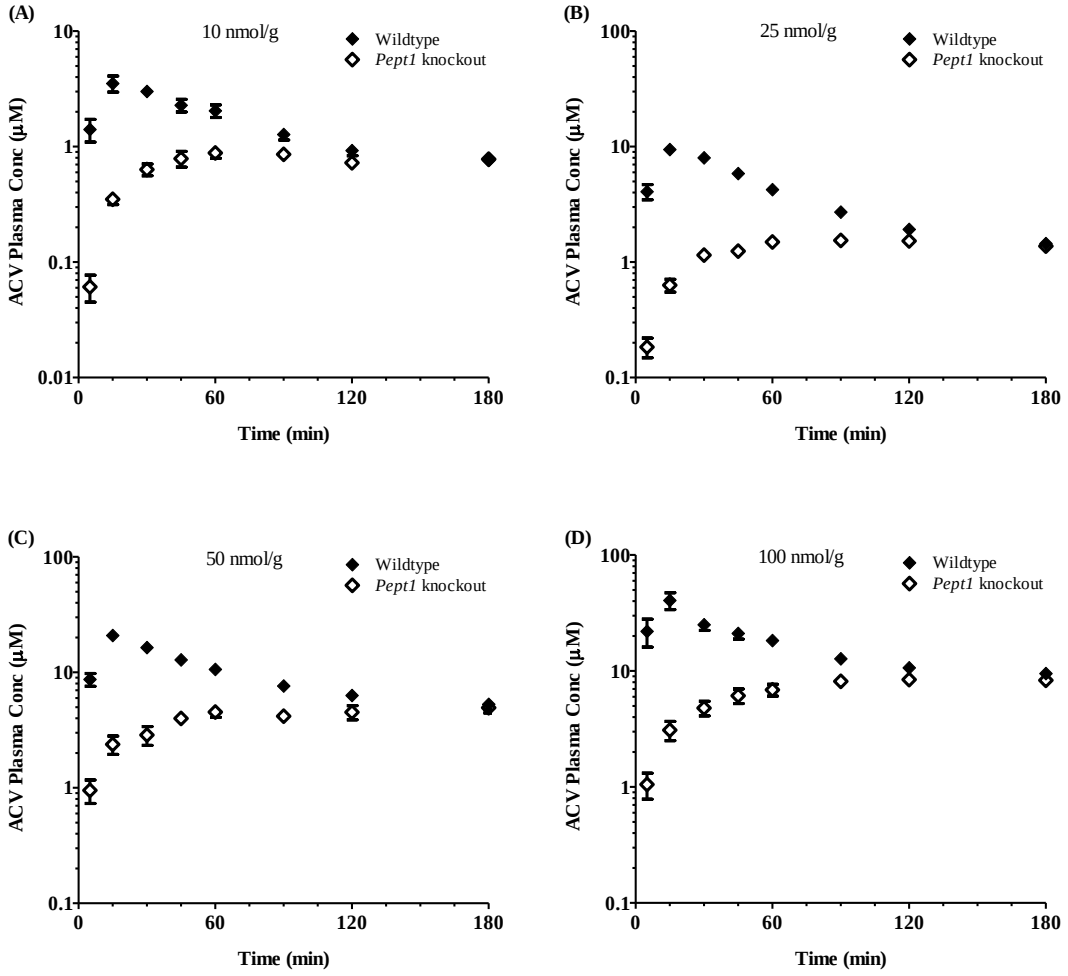

Figure 4.4 Acyclovir plasma concentration-time curves in wildtype and *Pept1* knockout mice after oral administration of [^{3}H]valacyclovir of: (A) 10 nmol/g body weight; (B) 25 nmol/g body weight; (C) 50 nmol/g body weight; (D) 100 nmol/g body weight (y-axis shown as a logarithmic scale). Data are expressed as mean ± SE (n=4-7).

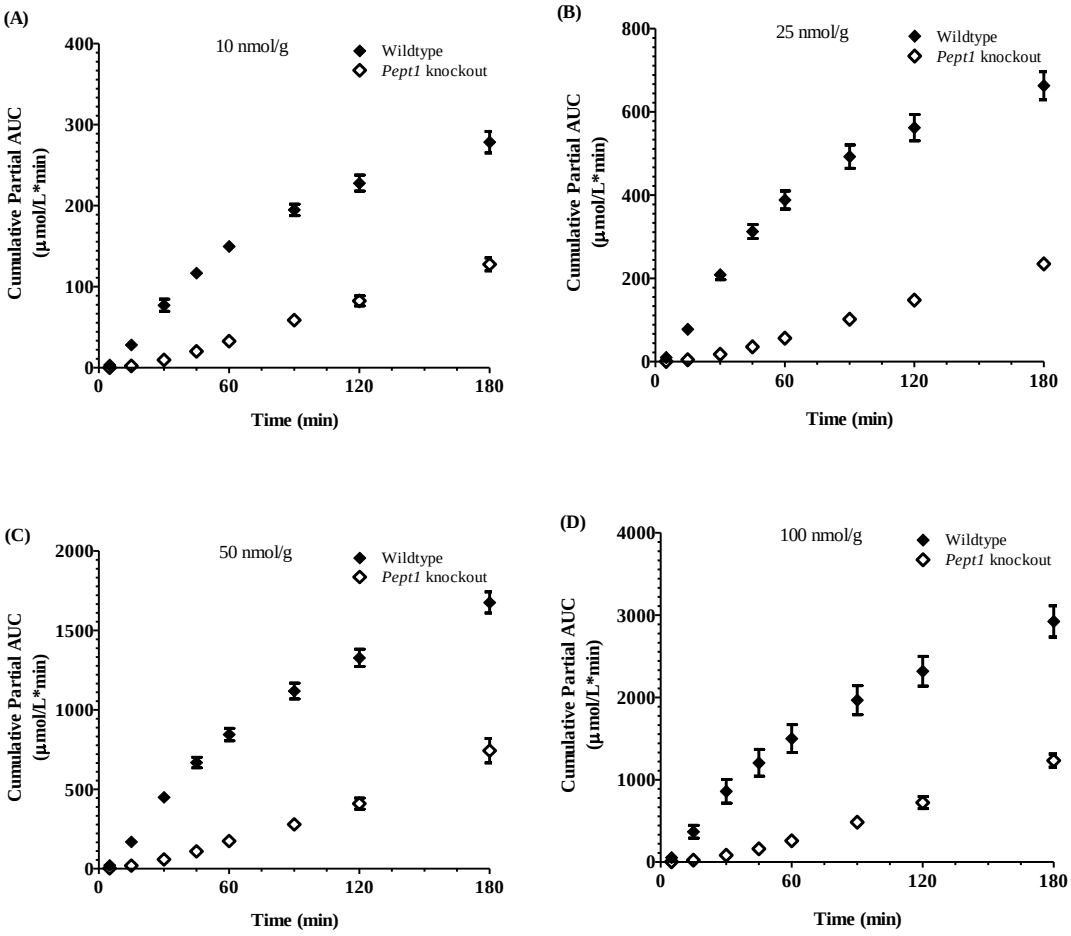

Figure 4.5 Partial AUC of acyclovir as a function of time in wildtype and *Pept1* knockout mice after oral administration of valacyclovir of: (A) 10 nmol/g body weight; (B) 25 nmol/g body weight; (C) 50 nmol/g body weight; (D) 100 nmol/g body weight. Data are expressed mean ±SE (n=4-7).

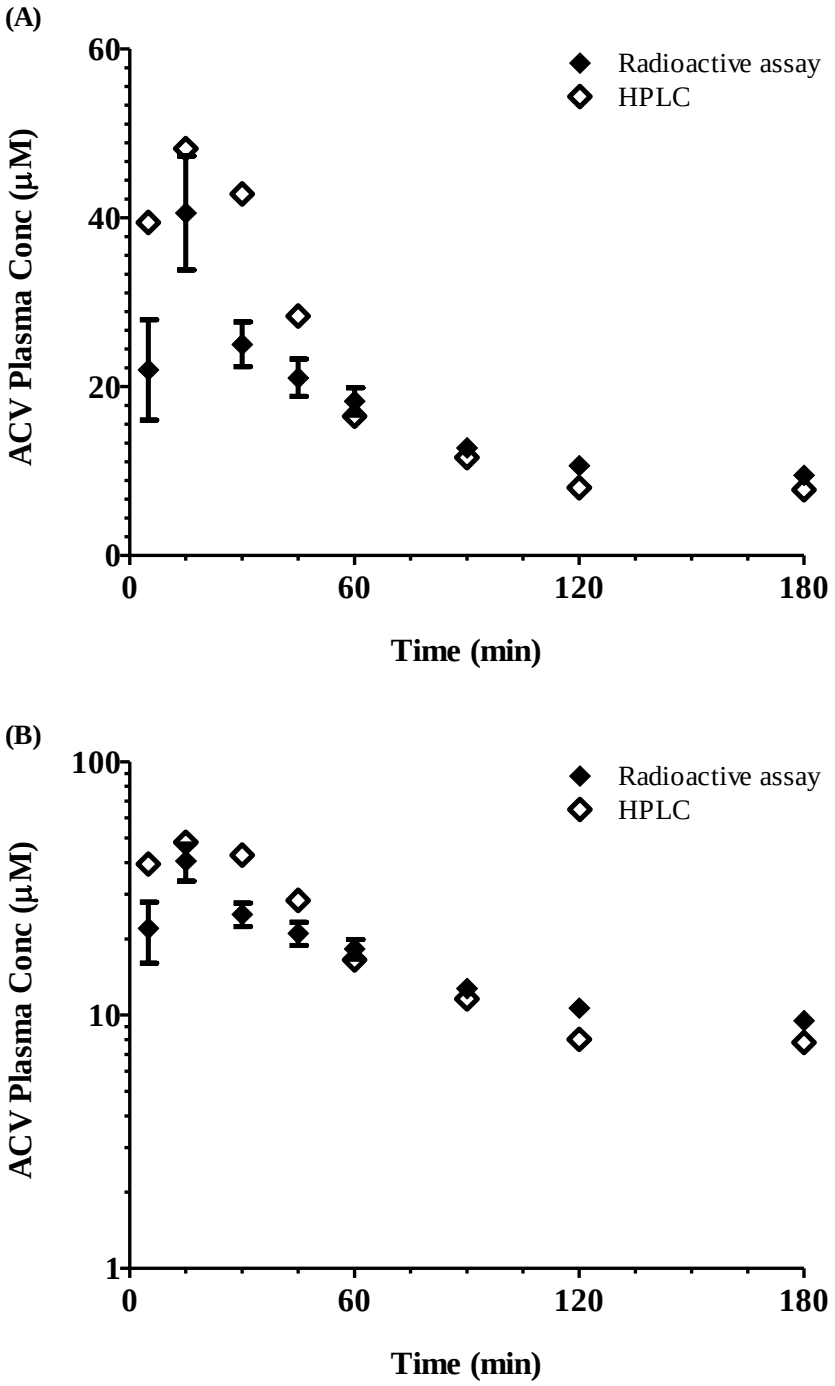

Figure 4.6 Comparison of acyclovir plasma concentration-time curves following oral administration of 100 nmol/g valacyclovir in wildtype mice measured by HPLC and radioactive assay: (A) in a linear scale; (B) in a logarithmic scale. Data are expressed as mean ± SE for radioactive assay (n=4) while a single or duplicate value is used for HPLC.

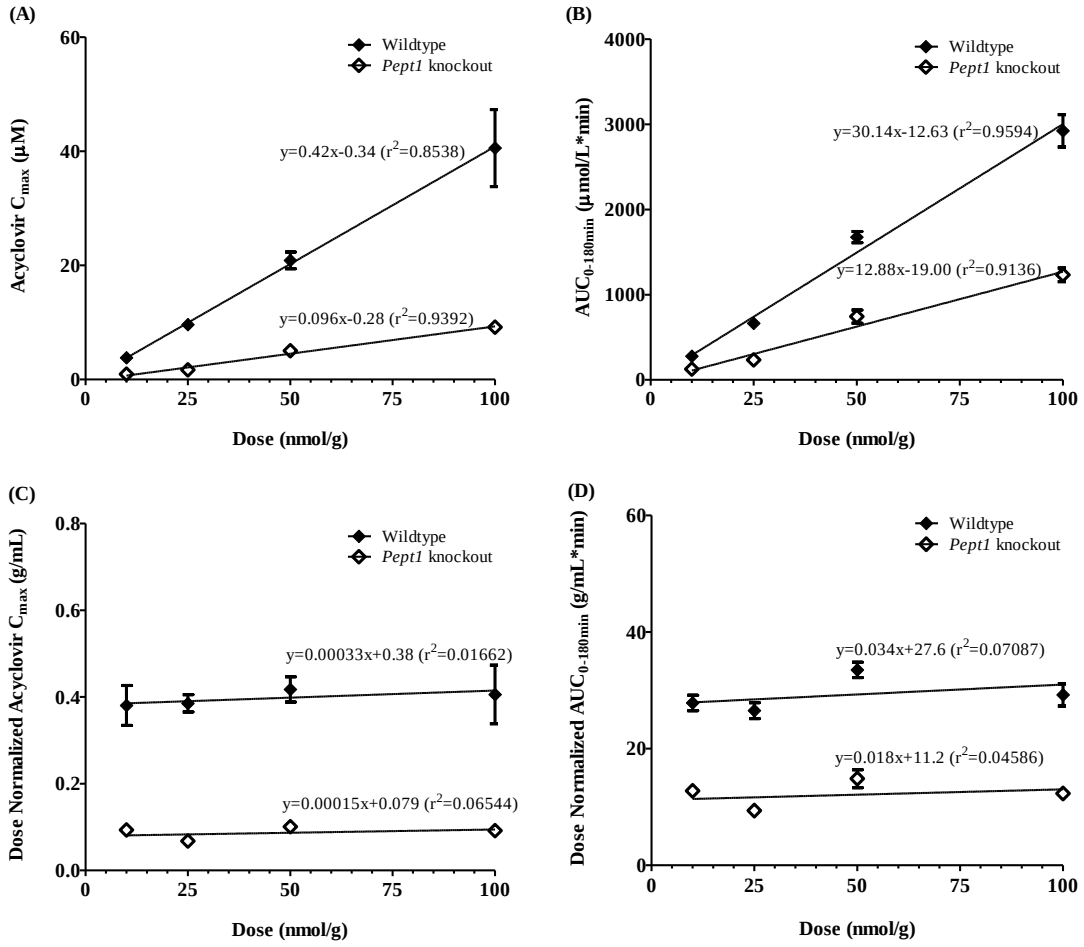

Figure 4.7 Dose proportionality of (A) acyclovir C_{max}; (B) acyclovir $AUC_{0\text{-}180min}$; (C) dose normalized acyclovir C_{max}; (D) dose normalized acyclovir $AUC_{0\text{-}180min}$ for wildtype and *Pept1* knockout mice. Linear regression lines, regression equations and associated r^2, fitted between pharmacokinetic parameters (y) and valacyclovir doses (x), are displayed for each dose group. Data are expressed as mean ± SE (n=4-7).

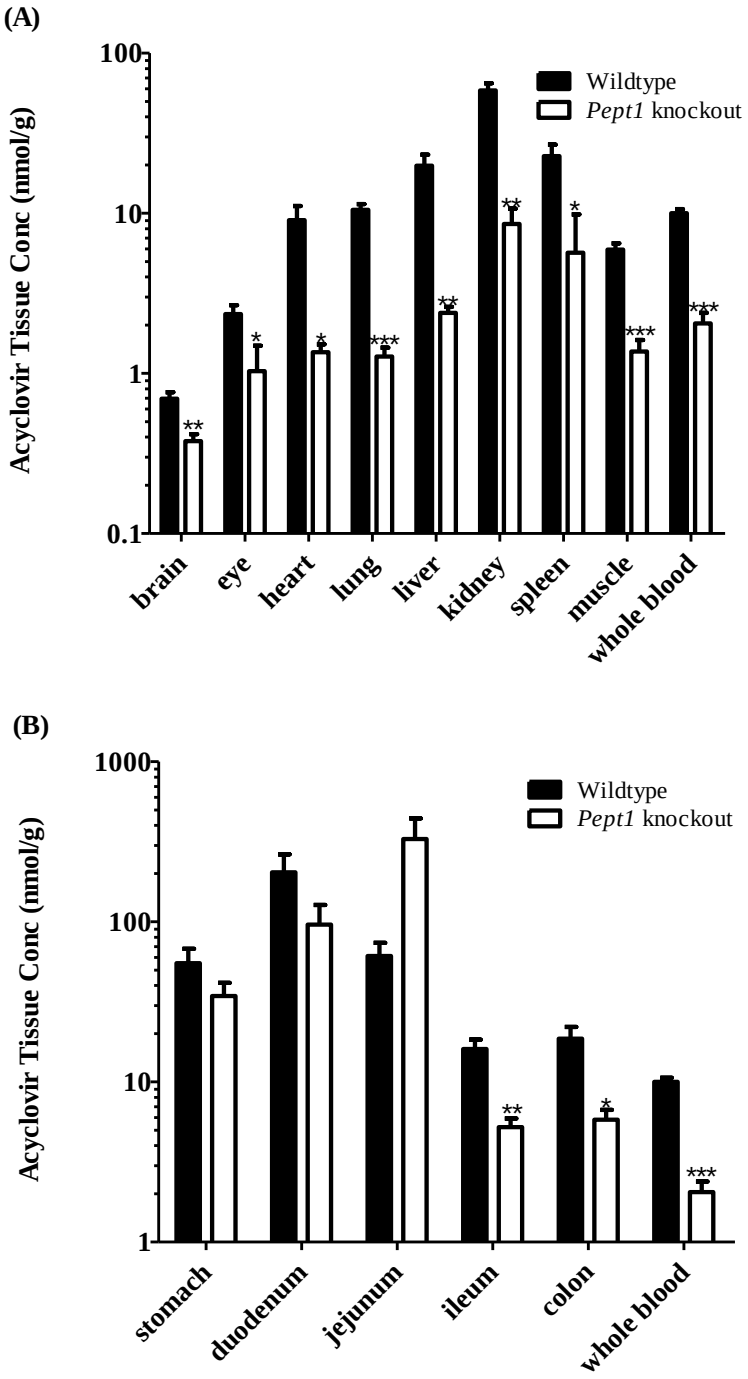

Figure 4.8 Tissue concentrations of acyclovir 20 min after oral administration of 25 nmol/g [^{3}H]valacyclovir in wildtype and *Pept1* knockout mice: (A) non-gastrointestinal tissues; (B) Gastrointestinal segments. Data are expressed as mean ± SE (n=4-6). * $p<0.05$, ** $p<0.01$, *** $p<0.001$, compared with wildtype mice.

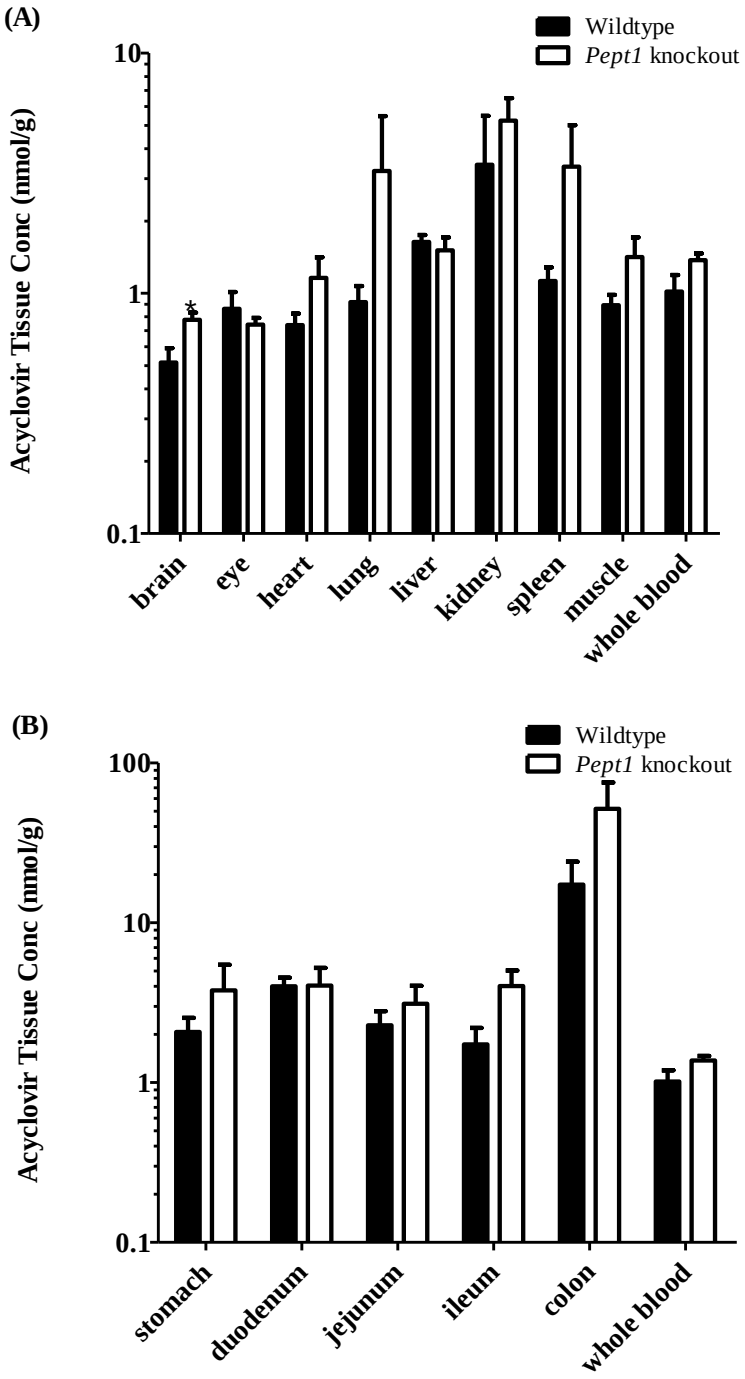

Figure 4.9 Tissue concentrations of acyclovir 360 min after oral administration of 25 nmol/g [^{3}H]valacyclovir in wildtype and *Pept1* knockout mice: (A) non-gastrointestinal tissues; (B) gastrointestinal segments. Data are expressed as mean ± SE (n=4-7). * $p<0.05$, compared with wildtype mice.

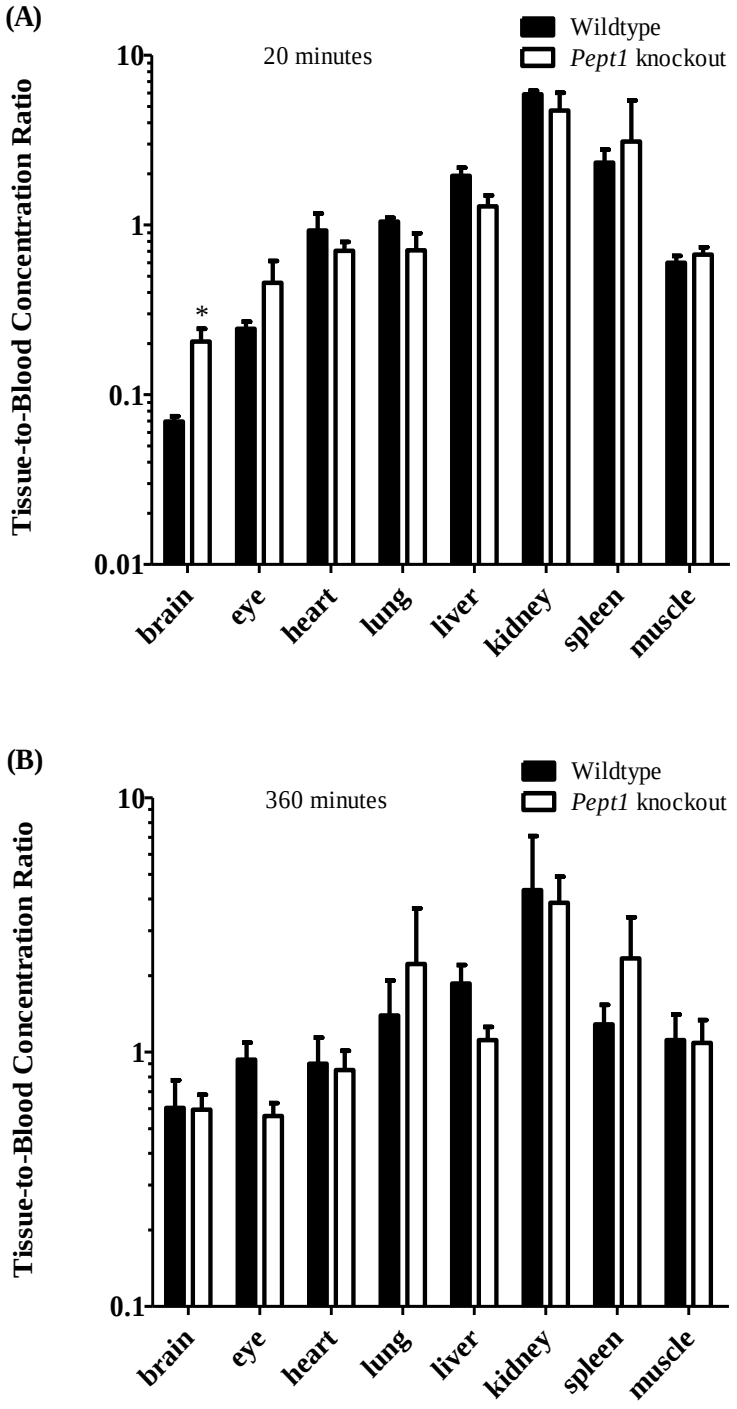

Figure 4.10 Tissue-to-blood concentration ratios of acyclovir for non-gastrointestinal tissues (A) 20 minutes and (B) 360 minutes after oral administration of 25 nmol/g [^{3}H] valacyclovir in wildtype and *Pept1* knockout mice. Data are expressed as mean ± SE (n=4-7). * $p<0.05$, compared with wildtype mice.

Table 4.1 Blood sampling scheme for HPLC analysis after oral administration of 100 nmol/g unlabeled valacyclovir in wildtype mice

Mouse ID	Time points (min)	Blood sample volume (µL)
1	5, 15, 30	40-60
2	15, 30, 45	40-60
3	45, 60, 90	40-60
4	120, 180	40-60

Table 4.2 Pharmacokinetic parameters of acyclovir after oral (p.o.) or intravenous (i.v.) administration of 25 nmol/g acyclovir in wildtype (WT) and *Pept1* knockout (KO) mice

Route	Parameter (unit)	Acyclovir (25 nmol/g)	
		WT	KO
p.o.	T_{max} (min)	43±6	45±15
	C_{max} (μM)	3.1±0.3	3.2±0.2
	$AUC_{0\text{-}180min}$ (μmol /L·min)	405±42	431±21
i.v.	CL (L/hr/kg)	1.33 ± 0.12	1.17 ± 0.15
	V_{dss} (L/kg)	2.3 ± 0.5	1.4 ± 0.3
	$T_{1/2}$ (min)	135 ± 16	88 ± 15
	$AUC_{0\text{-}180min}$ (μmol/L·min)	941 ± 126	1181 ± 192

Data are expressed as mean ±SE (n=3). No significant differences were found for all these pharmacokinetic parameters between the two genotypes.

Table 4.3 Pharmacokinetic parameters of acyclovir after oral administration of valacyclovir in wildtype (WT) and *Pept1* knockout (KO) mice

	Parameter (unit)	Dose (nmol/g body weight)			
		10	25	50	100
WT	T_{max} (min)	24±4	19±3	15±0	15±0
	C_{max} (μM)	3.8±0.5	9.6±0.5	20.9±1.5	40.6±6.8
	$AUC_{0\text{-}180min}$ (μmol/L·min)	278±13	663±34	1675±66	2923±190
KO	T_{max} (min)	71±11*	96±16**	156±24**	150±19**
	C_{max} (μM)	0.9±0.1**	1.7±0.1***	5.0±0.5***	8.8±0.5*
	$AUC_{0\text{-}180min}$ (μmol/L·min)	128±8***	235±11***	743±78***	1233±79**
Ratios of $AUC_{0\text{-}180min}$ (KO/WT)		46%	35%	44%	42%

Data are expressed as mean ±SE (n=4-7). * $p<0.05$, ** $p<0.01$, *** $p<0.001$, compared with wildtype mice given the same doses.

Table 4.4 Dose-corrected slopes of cumulative partial AUC vs. time in wildtype (WT) and *Pept1* knockout (KO) mice (Corresponds to Figure 4.5)

Dose (nmol/g)	Slope for 5-60 min			Slope for 90-180 min		
	WT	KO	Ratio (KO/WT)	WT	KO	Ratio (KO/WT)
10	0.27	0.060	0.22	0.092	0.076	0.83
25	0.28	0.041	0.15	0.075	0.059	0.79
50	0.31	0.062	0.20	0.12	0.10	0.83
100	0.27	0.046	0.17	0.11	0.084	0.76

REFERENCES

Balimane PV, Tamai I, Guo A, Nakanishi T, Kitada H, Leibach FH, Tsuji A, and Sinko PJ (1998) Direct evidence for peptide transporter (PepT1)-mediated uptake of a nonpeptide prodrug, valacyclovir. *Biochem Biophys Res Commun* **250:**246-251.

Balimane P and Sinko P (2000) Effect of ionization on the variable uptake of valacyclovir via the human intestinal peptide transporter (hPepT1) in CHO cells. *Biopharmaceutics & drug disposition* **21:**165-174.

Bhardwaj RK, Herrera-Ruiz D, Eltoukhy N, Saad M, and Knipp GT (2006) The functional evaluation of human peptide/histidine transporter 1 (hPHT1) in transiently transfected COS-7 cells. *European journal of pharmaceutical sciences : official journal of the European Federation for Pharmaceutical Sciences* **27:**533-542.

Brandsch M, Knutter I, and Bosse-Doenecke E (2008) Pharmaceutical and pharmacological importance of peptide transporters. *J Pharm Pharmacol* **60:**543-585.

Bretschneider B, Brandsch M, and Neubert R (1999) Intestinal transport of beta-lactam antibiotics: analysis of the affinity at the H+/peptide symporter (PEPT1), the uptake into Caco-2 cell monolayers and the transepithelial flux. *Pharm Res* **16:**55-61.

Chen ML (1992) An alternative approach for assessment of rate of absorption in bioequivalence studies. *Pharm Res* **9:**1380-1385.

Chen ML, Lesko L, and Williams RL (2001) Measures of exposure versus measures of rate and extent of absorption. *Clinical pharmacokinetics* **40:**565-572.

Daniel H (2004) Molecular and integrative physiology of intestinal peptide transport. *Annu Rev Physiol* **66:**361-384.

de Miranda P, Krasny HC, Page DA, and Elion GB (1981) The disposition of acyclovir in different species. *J Pharmacol Exp Ther* **219:**309-315.

Eriksson AH, Varma MV, Perkins EJ, and Zimmerman CL (2010) The intestinal absorption of a prodrug of the mGlu2/3 receptor agonist LY354740 is mediated by PEPT1: in situ rat intestinal perfusion studies. *J Pharm Sci* **99:**1574-1581.

Ganapathy ME, Huang W, Wang H, Ganapathy V, and Leibach FH (1998) Valacyclovir: a substrate for the intestinal and renal peptide transporters PEPT1 and PEPT2. *Biochem Biophys Res Commun* **246:**470-475.

Guo A, Hu P, Balimane PV, Leibach FH, and Sinko PJ (1999) Interactions of a nonpeptidic drug, valacyclovir, with the human intestinal peptide transporter (hPEPT1) expressed in a mammalian cell line. *J Pharmacol Exp Ther* **289:**448-454.

Han H, de Vrueh RL, Rhie JK, Covitz KM, Smith PL, Lee CP, Oh DM, Sadee W, and Amidon GL (1998) 5'-Amino acid esters of antiviral nucleosides, acyclovir, and AZT are absorbed by the intestinal PEPT1 peptide transporter. *Pharm Res* **15:**1154-1159.

Hatanaka T, Haramura M, Fei YJ, Miyauchi S, Bridges CC, Ganapathy PS, Smith SB, Ganapathy V, and Ganapathy ME (2004) Transport of amino acid-based prodrugs by the Na+- and Cl(-) -coupled amino acid transporter ATB0,+ and expression of the transporter in tissues amenable for drug delivery. *J Pharmacol Exp Ther* **308:**1138-1147.

Herrera-Ruiz D and Knipp GT (2003) Current perspectives on established and putative mammalian oligopeptide transporters. *J Pharm Sci* **92:**691-714.

Knutter I, Wollesky C, Kottra G, Hahn MG, Fischer W, Zebisch K, Neubert RH, Daniel H, and Brandsch M (2008) Transport of angiotensin-converting enzyme inhibitors by H+/peptide transporters revisited. *J Pharmacol Exp Ther* **327:**432-441.

Landowski CP, Sun D, Foster DR, Menon SS, Barnett JL, Welage LS, Ramachandran C, and Amidon GL (2003) Gene expression in the human intestine and correlation with oral valacyclovir pharmacokinetic parameters. *J Pharmacol Exp Ther* **306:**778-786.

Phan DD, Chin-Hong P, Lin ET, Anderle P, Sadee W, and Guglielmo BJ (2003) Intra- and interindividual variabilities of valacyclovir oral bioavailability and effect of coadministration of an hPEPT1 inhibitor. *Antimicrob Agents Chemother* **47:**2351-2353.

Rubio-Aliaga I and Daniel H (2008) Peptide transporters and their roles in physiological processes and drug disposition. *Xenobiotica* **38:**1022-1042.

Sinko PJ and Balimane PV (1998) Carrier-mediated intestinal absorption of valacyclovir, the L-valyl ester prodrug of acyclovir: 1. Interactions with peptides, organic anions and organic cations in rats. *Biopharmaceutics & drug disposition* **19:**209-217.

Soul-Lawton J, Seaber E, On N, Wootton R, Rolan P, and Posner J (1995) Absolute bioavailability and metabolic disposition of valaciclovir, the L-valyl ester of acyclovir, following oral administration to humans. *Antimicrob Agents Chemother* **39:**2759-2764.

Sugawara M, Huang W, Fei YJ, Leibach FH, Ganapathy V, and Ganapathy ME (2000) Transport of valganciclovir, a ganciclovir prodrug, via peptide transporters PEPT1 and PEPT2. *J Pharm Sci* **89:**781-789.

Takeda M, Khamdang S, Narikawa S, Kimura H, Kobayashi Y, Yamamoto T, Cha SH, Sekine T, and Endou H (2002) Human organic anion transporters and human organic cation transporters mediate renal antiviral transport. *J Pharmacol Exp Ther* **300:**918-924.

Tsuda M, Terada T, Irie M, Katsura T, Niida A, Tomita K, Fujii N, and Inui K (2006) Transport characteristics of a novel peptide transporter 1 substrate, antihypotensive drug midodrine, and its amino acid derivatives. *J Pharmacol Exp Ther* **318:**455-460.

Varma MV, Ambler CM, Ullah M, Rotter CJ, Sun H, Litchfield J, Fenner KS, and El-Kattan AF (2010) Targeting intestinal transporters for optimizing oral drug absorption. *Curr Drug Metab* **11:**730-742.

Varma MV, Eriksson AH, Sawada G, Pak YA, Perkins EJ, and Zimmerman CL (2009) Transepithelial transport of the group II metabotropic glutamate 2/3 receptor agonist (1S,2S,5R,6S)-2-aminobicyclo[3.1.0]hexane-2,6-dicarboxylate (LY354740) and its prodrug (1S,2S,5R,6S)-2-[(2'S)-(2'-amino)propionyl]aminobicyclo[3.1.0]hexane-2,6-dicarbox ylate (LY544344). *Drug Metab Dispos* **37:**211-220.

CHAPTER 5

IN SILICO SIMULATION OF THE INTESTINAL ABSORPTION AND PHARMACOKINETICS OF VALACYCLOVIR IN WILDTYPE AND PEPT1 KNOCKOUT MICE

ABSTRACT

Purpose. To delineate the contribution of PEPT1 on the intestinal absorption of valacyclovir and to predict acyclovir plasma concentration-time profiles in wildtype and *Pept1* knockout mice after oral administration of valacyclovir.

Methods. The mechanism-based "advanced compartmental absorption and transit" (ACAT) model implemented in GastroPlus was used in these simulations. The ACAT model needed all parameters to be solved prior to predictions. Mouse gastrointestinal physiology values were extracted from the literature and PEPT1 protein expression, passive and/or PEPT1-mediated permeability of valacyclovir, and luminal degradation of prodrug were estimated in previously described *in situ* perfusions. The *in vivo* disposition kinetics of acyclovir was determined by a 3-compartment model after intravenous dosing of acyclovir. After optimizing the model parameters, the *in vivo* absorption of valacyclovir and acyclovir plasma concentration-time profiles were predicted in both genotypes after oral administration of 10, 25, 50 and 100 nmol/g valacyclovir. Predictions were compared with our own experimental data.

Results. For wildtype mice, the predicted acyclovir plasma concentration-time profiles at four escalating doses of oral valacyclovir agreed well with experimental data *in vivo*. Predicted maximum acyclovir plasma concentrations (C_{max}) and area under the acyclovir plasma concentration-time curve (AUC) values were also comparable with observed values. For *Pept1* knockout mice, permeability values were optimized separately for each dose group, which were all within the 90% confidence intervals of mean estimated P_{eff} values and provided a reasonable model fit. In wildtype mice, the duodenum (42%) was the primary site of valacyclovir absorption, with less absorption occurring in the jejunum (24%), ileum (4%) and colon (<1%) for a total of 70%. In the absence of luminal degradation, the intestinal absorption of valacyclovir was nearly complete. In *Pept1* null mice, intestinal absorption by the duodenum (4%), jejunum (13%), ileum (10%) and colon (12%) accounted for a total of only 40%.

Conclusions. The ACAT model, developed herein, proved to be a useful tool in bridging the gap between *in situ* and *in vivo* experimental findings, and in facilitating our understanding of the complicated intestinal absorption process of valacyclovir. Under normal circumstances, the enhanced permeability of valacyclovir by PEPT1 resulted in almost all the prodrug being absorbed in duodenal and jejunal regions. In the absence of PEPT1, the absorption of valacyclovir was favored in jejunal, ileal and colonic regions. The ACAT model is potentially useful for predicting the intestinal absorption and *in vivo* pharmacokinetics of valacyclovir in man based on animal data.

INTRODUCTION

Modeling and simulation are becoming increasingly powerful tools in several stages of drug development. In preclinical and clinical studies, one area with intense application of model-based approaches is the predictive mechanistic modeling of the intestinal absorption of oral drugs, where a multitude of mechanism or physiology-based models have been published and well documented (Huang et al., 2009). Among these mechanistic models, ADAM, Grass, GITA and the advanced compartmental absorption and transit (ACAT) models are all compartmental models that take into consideration fluid movement along the digestive tract and absorption over time from each gastrointestinal compartment. These mechanistic absorption models have been successfully applied to describe the intestinal absorption of a number of oral drugs and greatly facilitated our understanding of the impact of various formulation-related, physicochemical and physiological factors on oral absorption (Yu and Amidon, 1998; Yokoe et al., 2003; Tubic et al., 2006; Haddish-Berhane et al., 2009; Hironaka et al., 2009; Thelen et al., 2011).

The ACAT^{TM} model, modified from the original CAT model (Yu et al., 1996; Yu and Amidon, 1999) to include first-pass metabolism and colonic absorption, is a flexible comprehensive compartmental model accounting for almost all intestinal processes such as drug release, dissolution, precipitation, luminal degradation, active and passive uptake as well as gastrointestinal transit. Details about the ACAT model were thoroughly reviewed (Agoram et al., 2001). The commercial software GastroPlus is based on the

ACAT model and suitable for the purpose of predictive simulation of the complex intestinal absorption of our model prodrug valacyclovir.

Valacyclovir is an L-valyl ester prodrug of the potent antiviral agent acyclovir and is commonly viewed as a model PEPT1 targeted prodrug. Intensive research efforts have been focused on delineating the quantitative importance of PEPT1 in the intestinal absorption of valacyclovir, which understandably lays a solid basis for promoting the rational design of prodrugs selectively targeting intestinal PEPT1 to improve the oral absorption and availability of poorly permeable molecules. Using *Pept1* knockout mice, we have thoroughly evaluated the quantitative contribution of intestinal PEPT1 in facilitating the intestinal absorption of valacyclovir in whole animals by *in situ* (see Chapter 3) and *in vivo* (see Chapter 4) experimental methods. Our previous *in situ* intestinal perfusion studies demonstrated that valacyclovir is actively transported by intestinal PEPT1, which contributes approximately 90% of the intestinal permeability of valacyclovir in mouse small intestine. In the *in vivo* pharmacokinetic studies, 5-fold and 2-fold differences were observed, respectively, for peak acyclovir plasma concentrations (C_{max}) and area under the acyclovir plasma concentration-time curve (AUC) values between the two genotypes.

Based on the *in situ* and *in vivo* findings, we concluded that PEPT1 had a major role in mediating the intestinal absorption of valacyclovir. However, there methods were more descriptive and lacked a systematic means to interpret the marked difference in plasma concentration-time profiles between wildtype and *Pept1* knockout mice. Conceivably, the intestinal absorption of valacyclovir, under either *in situ* or *in vivo* conditions, is governed by a unified absorption mechanism in mouse. Therefore, it is

feasible to utilize a mechanism-based absorption model such as ACAT to integrate these experimental findings and, more importantly, to predict a priori the involvement of PEPT1 in the intestinal absorption and pharmacokinetics of valacyclovir. In addition, the intestinal absorption of valacyclovir is influenced by numerous physicochemical, physiological and biochemical variables such as pH, absorption surface area, gastric emptying and intestinal transit among others. Therefore modeling approaches also offer the unique opportunity to assess the impact of changes of these variables on the rate and extent of valacyclovir intestinal absorption.

The main objective of the current work is to retrospectively predict and simulate the *in vivo* pharmacokinetic profiles of acyclovir, derived from oral administration of valacyclovir, in wildtype and *Pept1* knockout mice by integrating *in situ* findings about valacyclovir permeability and degradation into the ACAT model. This work was completed using GastroPlus since this software allowed us to simulate active and passive transport process and other simultaneous kinetic processes in the intestine.

MATERIALS AND METHODS

Software. Simulations were run on a standard Dell desktop computer using GastroPlus (version 7, Simulations Plus, Lancaster, California, USA).

The ACAT theoretical model. The flexible mechanism-based ACAT model was tailored to represent the intestinal process of dissolved valacyclovir in mouse. Briefly, the ACAT model describes the gastrointestinal (GI) tract as a series of nine consecutive compartments in which one compartment represents the stomach and eight compartments represent the different intestinal regions. Valacyclovir in the stomach is only governed by gastric emptying while luminal concentrations of valacyclovir within a given intestinal compartment are subjected to several simultaneous kinetic processes including intestinal transit in and out of that compartment, luminal degradation and absorption across the apical membrane of intestinal epithelial cells. Inside epithelial cells, intra-cellular valacyclovir is further governed by instantaneous biotransformation into acyclovir, which is further controlled by bi-directional passive efflux into the luminal or blood side, depending on its concentration gradient. Thus, it is possible acyclovir can be passively secreted back into the lumen.

All the GI kinetic processes describe above, combined with the *in vivo* disposition kinetics of acyclovir in mouse, can be mathematically represented by a system of coupled first-order and Michaelis-Menten rate equations. Therefore, accurate parameters of the equation systems are needed in order to obtain accurate predictions using this ACAT model in GastroPlus.

Key model assumptions. For predicting acyclovir plasma concentration-time profiles, the following six key assumptions were common for wildtype and *Pept1* knockout mice: 1) the stomach is not an absorption site; 2) GI transit is a first-order process; 3) valacyclovir luminal degradation is a first-order process; 4) valacyclovir undergoes instantaneous, complete and non-saturated metabolic biotransformation to acyclovir in intestinal epithelial cells; 5) only the active drug acyclovir is pumped bi-directionally into the intestinal lumen or portal blood by a passive (first-order) diffusion; and 6) acyclovir has linear disposition kinetics *in vivo* across the dose range studied.

In wildtype mice, one additional key assumption was that only the absorption of valacyclovir across the apical membrane of intestinal epithelial cells, via PEPT1-mediated and passive pathways, was considered. However, in *Pept1* knockout mice, two critical assumptions about the luminal absorption process that were different from the assumption for wildtype mice were needed: 1) the absorption of both valacyclovir and luminally formed acyclovir were considered; and 2) the two compounds were assumed to have identical intestinal passive permeability along the entire intestinal tract.

Schematic representations of the ACAT model with underlying assumptions for wildtype mice and *Pept1* knockout mice were adapted from the literature (Agoram et al., 2001) and illustrated in Figure 5.1 (A and B).

Model parameters. Information regarding physicochemical properties of valacyclovir and acyclovir, mouse GI physiology, acyclovir and valacyclovir permeability, valacyclovir degradation as well as acyclovir *in vivo* disposition was necessary for adequate model predictions.

Physicochemical properties. Physicochemical properties of valacyclovir and acyclovir are summarized in Table 5.1. Default values in Gastroplus® were used when no other information was available.

GI physiology. Physiological information regarding mouse GI transit time, segmental volumes, length (L) and radius (R), used for the estimation of GI transit kinetics, were all default values in GastroPlus® as shown in Table 5.2. pH profiles in the GI tract of fasted mice were also included in this table. Intestinal pH may influence various physicochemical and biochemical parameters such as drug luminal solubility, luminal degradation, ionization state and subsequently passive diffusion as well as the driving force of PEPT1. Absorption scale factors (ASF) were used to scale regional intestinal permeability (P_{eff}) to regional absorption rate constant (k_a), based on the theoretical relationship between P_{eff} and k_a:

——— Eq. (1)

Intestinal permeability of valacyclovir in wildtype mice. Valacyclovir jejunal permeability coupled with PEPT1 protein expression data were used as input parameters characterizing the uptake kinetics in wildtype mice. Based on our previous analysis of *in situ* permeability, jejunal P_{eff} of valacyclovir in wildtype mice was factored as the sum of a minor passive component and a major PEPT1-mediated component. The passive permeability was assumed to be equal in both small and large intestine. In the simulation, the passive permeability of valacyclovir ($P_{eff,passive}$) was set at 0.27×10^{-4} cm/sec. PEPT1-mediated permeability of valacyclovir ($P_{eff,PEPT1}$) was described by a Michaelis-Menten function as follows:

$$\frac{V_{max} \times C_{luminal}}{K_m + C_{luminal}}$$ Eq. (2)

,where maximum transport velocity V_{max} was estimated to be 1.4 nmol/cm^2/sec and apparent Michaelis-Menten affinity constant K_m 10 mM from previous perfusion studies. $C_{luminal}$ was the time-varying luminal concentration of valacyclovir automatically generated in GastroPlus®. In the simulation, PEPT1-mediated valacyclovir permeability was assumed to be pH-independent in the physiological pH range of 4.63 to 5.24 in mice (McConnell et al., 2008). The ACAT model further assumed PEPT1 has similar intrinsic activity in different segments of small intestine.

Immunoblot analyses showed that PEPT1 expression was highest in the jejunum, closely followed by duodenum and ileum while PEPT1 was not detected in the colon in wildtype mice (Jappar et al., 2010). Given this result, a uniform distribution of PEPT1 in the small intestine and zero expression in the large intestine of wildtype mice were employed as input parameters in the prediction. Overall, by coupling jejunal permeability of valacyclovir with PEPT1 regional distribution in the small intestine of wildtype mice, the uptake kinetics of valacyclovir could be adequately characterized.

Intestinal permeability of valacyclovir and acyclovir in Pept1 knockout mice. As stated previously, an identical passive P_{eff} was assumed for valacyclovir and acyclovir along the intestine in *Pept1* knockout mice. Four mean P_{eff} values, corresponding to the mean valacyclovir P_{eff} for the small intestine (method #1), the mean valacyclovir P_{eff} for the entire intestine (method #2), the mean valacyclovir P_{eff} for the duodenum (method #3), and the mean acyclovir jejunal P_{eff} (method #4) in *Pept1* knockout mice, were all estimated from *in situ* perfusion studies and separately used as input P_{eff} values in the

simulation. The four mean P_{eff} values, combined with their 90% confidence intervals, are summarized in Table 5.3. As seen in this table, P_{eff} values of valacyclovir and acyclovir in intestinal segments of *Pept1* knockout mice had substantial inter-subject variability in spite of the lack of statistical differences between them.

***Valacyclovir luminal degradation*.** Luminal degradation of valacyclovir is another key kinetic process that can significantly influence the absorption of valacyclovir along the GI tract. Parameters characterizing valacyclovir degradation kinetics were also evaluated from the *in situ* intestinal perfusion studies under steady state conditions as shown below.

Assuming first-order degradation of valacyclovir at a given pH and negligible acyclovir absorption, valacyclovir first-order degradation rate constant, denoted by k_{de}, was estimated from the following mass balance equation system:

Eq. (3)

Eq. (4)

Eq. (5)

Eq. (6)

,where Q is the flow rate in the perfusion studies (0.1 mL/min), V is the volume of the given intestinal compartment, and C_{ave} is the logarithmic mean of valacyclovir luminal concentration and can be calculated as a function of inlet ($C_{in,valacyclovir}$) and outlet ($C_{out,valacyclovir}$) valacyclovir concentrations as follows:

Eq. (7)

Using the above equation system, k_{de} values were estimated in the pH range of 5.5-7.5, using experimental data collected from the jejunal perfusions of wildtype mice. The relationship between k_{de} and pH was then fitted with monotonic functions such as linear and exponential functions, and goodness of fit was assessed by the coefficient of determination R^2. k_{de} at physiological pH was estimated by extrapolation with the best fitting equation. k_{de} was also estimated for different intestinal segments of wildtype mice at pH 6.5 to assess if regional differences may exist.

***In vivo disposition of acyclovir*.** Acyclovir plasma concentration-time curves after its intravenous administration in wildtype and *Pept1* knockout mice were fitted to one-, two- and three-compartment pharmacokinetic models in WinNonlin. AIC and SBC were the main criteria for selection of the specific compartmental model. After the selection of the compartmental model, mean pharmacokinetic parameters of acyclovir were calculated by averaging fitted pharmacokinetic parameters from individual animals and then applied in the simulation.

In addition, unbound fraction of acyclovir was set at 0.87, which was obtained from the literature (de Miranda et al., 1981).

Parameter sensitivity analyses. Parameter sensitivity analyses (PSA) were performed to assess the sensitivity of predicted acyclovir C_{max} and AUC values to input model parameter values. Population variability of input parameters could potentially impair the predictability of the ACAT model. Input parameters associated with PEPT1-

mediated and passive permeability of valacyclovir, and *in vivo* disposition of acyclovir, were examined in the PSA step for oral administration of 25 nmol/g valacyclovir in wildtype mice. These input parameter values were changed by multiplying initial values with 10 scaling factors in the range of 0.1-10 to allow an order of magnitude increase or decrease.

Optimization. Optimization can be used to fine-tune input parameters for better model predictions when one or several experimental pharmacokinetic profiles were available as "training" datasets. The training dataset used in the current optimization step were acyclovir plasma concentration-time profiles in wildtype mice receiving oral administration of 25 nmol/g valacyclovir. Input parameters that were found to be highly influential on the predictions were selected for optimization. In addition, i*n vivo* values for PEPT1 V_{max} were obtained by optimization since the *in situ* V_{max} value cannot be directly scaled to the *in vivo* value needed in GastroPlus®.

Simulation of acyclovir pharmacokinetic profiles. The same fixed set of input parameter values, after proper optimization (if performed), were used for predicting acyclovir concentration-time profiles after oral administration of 10, 25, 50 and 100 nmol/g valacyclovir in wildtype mice. Only input permeability values were modified for the simulation of acyclovir pharmacokinetic profiles in *Pept1* knockout mice as described earlier. The quality of the simulation was evaluated by: 1) visual evaluation of the predicted and observed acyclovir plasma concentration-time curves; 2) comparison of the predicted and observed C_{max} and AUC; 3) the coefficient of determination R^2.

Model application. The final ACAT model was used to address two important aspects of drug absorption. Firstly, the ACAT model was used to quantify the contribution of each intestinal segment to the oral absorption of valacyclovir in wildtype and *Pept1* knockout mice. The fraction of oral dose absorbed in each segment was calculated as the ratio of the amount of drug disappearing from the segment as a function of time to the administered dose. Secondly, the influence of luminal degradation on the oral availability of valacyclovir was examined.

RESULTS

Valacyclovir luminal degradation. Figure 5.2 shows that there were no significant differences in k_{de} for different intestinal segments of wildtype mice at pH 6.5. Valacyclovir k_{de} values in the pH range of 5.5-7.5 are summarized in Table 5.4. As demonstrated in Figure 5.3, when linear function was used to describe the relationship of mean degradation rate constant or log-transformed mean k_{de} (log-k_{de}) and pH, the R^2 values were 0.823 and 0.910 respectively. Therefore, a linear function between log-k_{de} and pH was favored for its better quality of fit as well as for its natural non-negative constraint on k_{de}. The function, after exponentiation, for the relationship of k_{de} (y) and pH (x) was: $y=0.0008 \cdot e^{0.771x}$. By using this equation, k_{de} values for valacyclovir were estimated for the physiological pH range of the intestinal lumen of fasted mice and are listed in Table 5.5. Degradation half-lives, calculated as $0.693/k_{de}$, are also included in this table.

Acyclovir *in vivo* disposition. A three compartmental model achieved the smallest AIC and SBC values when fitted to acyclovir plasma concentration-time profiles following intravenous administration of 25 nmol/g acyclovir in both genotypes and therefore was chosen for the estimation of acyclovir pharmacokinetic parameters.

Pharmacokinetic parameters needed to fully describe a three compartmental model included the volume of central compartment (V_1), clearance from central compartment (CL), micro-rate constants k_{12} and k_{21} for the transfer of acyclovir between central and the first peripheral compartment, and micro-rate constants k_{13} and k_{31} for the transfer of acyclovir between central and the second peripheral compartment. As shown

in Table 5.6, mean pharmacokinetic parameters were estimated by averaging model derived pharmacokinetic parameters for individual animals.

Parameter sensitivity analyses. As shown in Figure 5.4, when each parameter was changed within two orders of magnitude, predicted acyclovir C_{max} was most sensitive to changes in V_1, followed by changes in V_{max} and K_m. C_{max} was relatively less sensitive to the other parameters examined. Similarly, predicted acyclovir AUC was most sensitive to changes in CL and less sensitive to changes in V_1, k_{13}, $k_{31,}$ V_{max} and $K_{m.}$ Both acyclovir AUC and C_{max} were insensitive to changes in passive permeability of valacyclovir ($P_{eff,\ passive}$), showing less than 30% and 60% changes, respectively, when $P_{eff,\ passive}$ was varied over a 100-fold range. Since prediction was similarly sensitive to changes in V_{max} and K_m and *in situ* V_{max} was not directly applicable in the simulation, only V_{max} was selected for subsequent optimization. Pharmacokinetic parameters including V_1, CL, k_{13} and k_{31} were also optimized based on the PSA result.

Optimization. Maximum PEPT1-mediated transport velocity V_{max} was optimized to be 0.00726 mg/sec. In addition, V_1, CL, k_{13} and k_{31} were also fine-tuned using the selected training dataset. Optimized pharmacokinetic parameters are also included in Table 5.6, most of which showed a fold change of less than 1.5 compared with the original input values with the exception of k_{31}. But even for k_{31}, optimized k_{31} had an acceptable 2.1-fold change relative to the original mean value fitted in a three compartment analysis.

Simulation of acyclovir pharmacokinetic profiles following oral valacyclovir. Figure 5.5 depicts the simulated and experimental acyclovir plasma concentration-time

profiles in wildtype mice receiving oral valacyclovir at 10, 25, 50, and 100 nmol/g body weight. Figure 5.5A suggests that the simulated curves are within the range of individually observed data while Figure 5.5B shows good agreement between the simulation and mean observations with slight under-prediction at two terminal time points of two higher dose groups (50 nmol/g and 100 nmol/g). As shown in Table 5.7, adequate model prediction was further confirmed by 1) high R^2 values (on average R^2>0.9) and 2) similar simulated and observed acyclovir C_{max} and AUC.

For *Pept1* knockout mice, the simulation results over-predicted the mean observed acyclovir pharmacokinetic data for all dose groups when the simulation was run using a uniform P_{eff} value of 0.18×10^{-4} cm/sec (method #1), the mean P_{eff} value of valacyclovir estimated for the small intestine of *Pept1* knockout mice (Figure 5.6). Similarly, the other two higher mean P_{eff} input values (method #2 and #3) led to even more severe over-prediction of acyclovir plasma concentration-time profiles (figures not shown).

In contrast, when input P_{eff} was set at 0.074×10^{-4} cm/sec (method #4), the mean jejunal P_{eff} value of acyclovir in *Pept1* knockout mice, goodness of fit was improved for all four dose groups. However, as shown in Figure 5.7, under-prediction was still pronounced for early time points (time $\leq$ 45 minutes) in all dose groups. Overall, the average R^2 value was smaller than 0.8.

The lack of fit in *Pept1* knockout mice using four different P_{eff} methods suggests the high sensitivity of the simulation to P_{eff} input values for poorly permeable compounds. In order to improve model prediction, P_{eff} was optimized separately for each dose in

Pept1 knockout mice (method #5). The resultant optimal P_{eff} values were 0.09627×10^{-4} cm/sec, 0.07047×10^{-4} cm/sec, 0.10129×10^{-4} cm/sec and 0.08627×10^{-4} cm/sec for 10, 25, 50 and 100 nmol/g dose groups, respectively. These optimal P_{eff} values were similar to the jejunal P_{eff} value of acyclovir in *Pept1* knockout mice and they fell within the 90% confidence intervals of mean P_{eff} estimates listed in Table 5.3.

Figure 5.8 (A and B) suggests that model predictions agreed with experimental data reasonably well for each dose when the optimal P_{eff} values for each dose level were used. As shown in Table 5.8, there was good agreement between predicted and observed acyclovir C_{max} and AUC; R^2 on average was found to be greater than 0.85.

In addition to the optimization of permeability, we also attempted to generate simulations using the upper and lower limits corresponding to the 90% CI of the mean P_{eff} value of valacyclovir estimated for the small intestine of *Pept1* knockout mice (method #6). As shown in Figure 5.10, at a typical dose of 25 nmol/g oral valacyclovir, the observations fell between the interval enclosed by the two simulations. This suggested that even without the optimization step, a prediction interval can be generated although it is challenging to match the exact observations. Similar results were observed for the other dose groups (figures not shown).

Model application. Figure 5.10 (A-D) shows the segmental contribution to the intestinal absorption of oral valacyclovir in wildtype mice. Similar results were observed for all four dose groups in wildtype mice. For a typical dose of 25 nmol/g valacyclovir, duodenum was the most important absorption site, contributing to more than 40% of the dose absorbed. The two jejunal segments combined accounted for approximately 24% of

dose absorbed. Total fraction absorbed was predicted to be about 70%. In contrast, as shown in Figure 5.11, jejunum was the primary absorption site of valacyclovir (~13%), followed closely by combined colonic (~12%) and ileal (~10%) segments in *Pept1* knockout mice receiving 25 nmol/g oral valacyclovir. The contribution of duodenum was significantly reduced to about 4%. Total fraction absorbed from the entire intestinal tract was predicted to be about 40%. Similar results were also reported for other dose groups in *Pept1* knockout mice.

Lastly, we examined the effect of luminal degradation on the oral availability of valacyclovir in wildtype mice. As shown in Figure 5.12, in the absence of luminal degradation, valacyclovir was nearly 100% absorbed within 3 hours after oral dosing of 25 nmol/g valacyclovir, suggesting that incomplete absorption of valacyclovir observed in wildtype mice was due to the competing luminal degradation rather than insufficient permeability or intestinal residence times. Duodenum and jejunum accounted for about 90% of the dose absorbed in this hypothetical scenario.

DISCUSSION

Model assumptions. Wildtype and *Pept1* knockout mice had common model assumptions regarding GI physiology, luminal and intracellular biotransformation of valacyclovir and *in vivo* disposition of acyclovir, based on our understanding that these kinetic processes theoretically remained unchanged in our validated *Pept1* knockout mice compared to their wildtype counterparts. The main difference between model assumptions made for the two genotypes is associated with the intestinal permeability of valacyclovir and/or acyclovir. Based on the analysis of *in situ* perfusions (see Chapter 3), valacyclovir has much higher intestinal permeability than acyclovir in the small intestine of wildtype mice. For example, *in situ* jejunal permeability of valacyclovir was about 40 times higher than that of acyclovir, suggesting that the absorption of luminally formed acyclovir might be negligible. Considering that Gastroplus® can only simulate the absorption of one compound, we made the assumption that only valacyclovir was absorbed, via active and passive pathways, in wildtype mice. However, this assumption may be invalid in *Pept1* knockout mice. In the absence of PEPT1, valacyclovir and acyclovir showed similarly low jejunal permeability *in situ*. In addition, valacyclovir permeability was not statistically different between the different intestinal segments of *Pept1* knockout mice. Results from *in situ* studies showed that, during valacyclovir ablation, valacyclovir underwent rapid and extensive degradation to form acyclovir in the lumen. Consequently, the intestinal absorption of acyclovir and valacyclovir, in *Pept1* knockout mice should be accounted for in the simulation. Excluding the absorption of luminally formed acyclovir in *Pept1* knockout mice may lead to severe under-prediction. Based on these considerations and previous experimental results, the two "low-

permeability" compounds were assumed to be passively absorbed, with identical intestinal permeability along the entire intestinal tract of *Pept1* knockout mice. In other words, the two compounds were no longer differentiable in terms of absorption kinetics. Overall, these underlying model assumptions for both genotypes are reasonable. However, they are still flawed since a number of realistic aspects have to be ignored. For instance, the permeability of valacyclovir and acyclovir may vary for different intestinal regions of *Pept1* knockout mice. However, these potential flaws are unavoidable when constructing a physiologically sound and practical model under our simulation settings.

Model parameters. The accuracy of the ACAT model predictions mainly depends upon the accuracy of model parameters, the model structure and the underlying assumptions. Prior to the execution of simulation, the parameters pertaining to intestinal uptake, luminal degradation and *in vivo* disposition were reliably estimated and, when necessary, optimized.

In the current simulation work, luminal degradation of valacyclovir was first characterized by re-analyzing our previous *in situ* intestinal perfusion data in mice. Valacyclovir degradation increased with increasing pH values, a finding consistent with the literature showing that valacyclovir was stable under acidic conditions but metabolically liable under basic conditions in rats and humans (Sinko and Balimane, 1998; Granero and Amidon, 2006). In addition, valacyclovir degradation rate constants in the lumen of mice were much higher than that in buffer solutions of the same pH, suggesting that membrane-bound enzymes accelerated the hydrolysis of valacyclovir in the intestinal lumen. Only monotonic functions were used to describe the relationship of pH and degradation rate. In a preliminary analysis, a quadratic function achieved a R^2

value of 0.95 when used to characterize valacyclovir degradation as a function of pH. Even though it provided a better apparent model fit, a severe drawback of the quadratic function is that it predicted minimal degradation at about pH 5.5 and dramatically increased degradation at even more acidic conditions, which is not physiologically plausible. Therefore, non-monotonic functions were not suitable for the determination of degradation rate constants at physiological pH values (less than 5.5).

Using the best-fitting function, the degradation half-life of valacyclovir was estimated to range from 15 to 22 minutes in mouse intestinal lumen under physiological pH conditions, and was less than 5 minutes at pH 7.5. Sinko and Balimane (1998) reported that the degradation half-life of valacyclovir was about 15 minutes in rat intestine homogenates at pH 7.4 while Sun et al. (2010) reported a valacyclovir degradation half-life of about 31 minutes in Caco-2 cell homogenates at pH 7.4. Our results suggest a faster degradation of valacyclovir *in vivo* compared with these other values estimated using cell/tissue homogenates. Possible explanations may be due to species differences or experimental design.

In addition to the estimation of luminal degradation, accurate parameter estimates were needed for active and passive intestinal permeability of valacyclovir, and *in vivo* disposition of acyclovir. Substantial inter-subject variability was observed for some of these parameters. Population variability in any pharmacokinetic parameter is commonly observed and well-accepted. For this reason, parameter sensitivity analysis was first performed to evaluate the influence of parameter imprecision on the prediction results. Given the dominance of PEPT1-mediated uptake of valacyclovir, it is understandable that predictions are sensitive to changes in parameters characterizing this process (i.e. V_{max}

and K_m). Conversely, predicted acyclovir AUC and C_{max} were almost invariant to the 100-fold changes in passive permeability of valacyclovir in the context of sufficient PEPT1-mediated uptake of valacyclovir. Furthermore, acyclovir AUC and C_{max} also showed high sensitivity to *in vivo* disposition parameters of acyclovir such as clearance and volume of central compartment, suggesting imprecision in these parameters could significantly bias the model predictions.

Following the sensitivity analysis, optimization was performed for selected model parameters. Small differences were observed between optimized and initially fitted disposition parameters. For example, the optimized clearance value is less than 10% greater than the mean fitted clearance value. Overall, for all optimized pharmacokinetic parameters, less than 2.1-fold changes were observed. In addition to pharmacokinetic parameters of acyclovir, the V_{max} characterizing the maximum transport rate of valacyclovir by PEPT1 was optimized for two reasons. Firstly, predicted acyclovir C_{max} and AUC values were sensitive to changes in V_{max}. Secondly, *in situ* V_{max} values could not be directly scaled to *in vivo* V_{max} values by GastroPlus®. Considering the independence of prediction on passive permeability of valacyclovir, $P_{eff,\ passive}$ was set at the estimated value of duodenal permeability of valacyclovir in *Pept1* knockout mice with no further optimization.

The default physiological parameters in the ACAT model were not optimized since we assumed these values represent the best estimates of mouse GI physiology in the absence of our own experimental findings. Degradation kinetics was not optimized because GastroPlus® does not allow for this process. Furthermore, it should be noted that it is only feasible to perform parameter optimization in the current retrospective

prediction where experimental pharmacokinetic data are available. In the absence of observed pharmacokinetic data, population approaches accounting for the variation in input parameters might be more suitable to generate prediction intervals.

Simulation and validation. Using the mechanism-dependent ACAT model, we simulated the *in vivo* plasma concentration versus time profiles of acyclovir following oral administration of valacyclovir to mice at four different doses. For wildtype mice, reasonably good predictions were made by incorporating previously described parameters into the ACAT model. Slight under-prediction of acyclovir plasma concentrations were observed for the last two or three time points during the 50 and 100 nmol/g dose groups. One possible explanation is the inaccuracy (i.e. population variances) of a set of input model parameters for the two cohorts of mice. In addition, we assumed linear disposition of acyclovir in mice for the examined dose range. In human subjects, dose-independent pharmacokinetics of acyclovir was demonstrated following intravenous infusion of 2.5-15 mg/kg acyclovir (Laskin et al., 1982). However, dose proportionality of acyclovir pharmacokinetics was not examined at the two highest doses used in our study. Considering that acyclovir is a substrate for organic anion and cation transporters (Wada et al., 2000; Takeda et al., 2002), dose-dependent pharmacokinetics of acyclovir is possible, resulting in the currently observed under-prediction.

For *Pept1* knockout mice, the success of simulating acyclovir plasma concentration-time profiles was critically determined by the selection of passive permeability values of valacyclovir and acyclovir along the intestinal tract. As shown in Figures 5.6 and 5.7, simulation using the estimated passive permeability values could not completely match the experimental pharmacokinetic profiles of acyclovir. The use of

acyclovir jejunal permeability provided a "somewhat" better model fit compared with other values. However, we believe the improved prediction was more by chance than indicative of the suitableness of using jejunal permeability data. Overall, the quality of model prediction is worse for *Pept1* knockout mice (mean R^2 value of 0.85) than for wildtype mice (mean R^2 value of 0.9) even in the case of using the optimized permeability values. A number of factors may have contributed to the suboptimal prediction in *Pept1* knockout mice. Firstly, the assumption of equal permeability for valacyclovir and acyclovir in the intestine of *Pept1* knockout mice is flawed. As shown in Chapter 4, the acyclovir plasma concentration-time curves following oral dosing of valacyclovir or acyclovir in *Pept1* knockout mice are similar in shape but not exactly superimposable; mean acyclovir C_{max} in *Pept1* knockout mice is 1.7 μM following oral valacyclovir (Figure 4.3B) and 3.2 μM following oral acyclovir (Figure 4.2B), respectively. This comparison suggests that acyclovir and valacyclovir should have similarly low but different intestinal permeability in *Pept1* knockout mice. However, GastroPlus® can only simulate the absorption process of a single compound. Therefore, we had to treat acyclovir and valacyclovir interchangeably with respect to their permeability. Another potentially flawed assumption is equal permeability of valacyclovir (and acyclovir) in all intestinal regions of *Pept1* knockout mice, which may also contribute to the differences between model simulation and observations. Besides, as for wildtype mice, population variability of input parameters might be an additional contributor to the lack of fit observed in *Pept1* knockout mice at certain time points.

In their study, Bolger et al. (2009) showed adequate predictions of acyclovir plasma concentration-time profiles in human subjects using the ACAT model in

combination with parameter values extracted from previously published *in vitro* or animal findings. Our study can be differentiated from their work in several key aspects. Firstly, our simulation is part of an integrated effort in studying the quantitative significance of PEPT1 in the intestinal absorption of valacyclovir. Therefore, some pivotal parameter values were estimated in our experimental studies with minimal modification in the simulation. In particular, we used luminal degradation kinetic parameters that were more physiologically relevant and accurate and, therefore, eliminated the need of imposing an arbitrary first-pass extraction value of acyclovir in addition to specified luminal degradation. Without reliable PEPT1 protein expression data, they had to use multiple PEPT1 mRNA distribution data and selected the uniform distribution after comparing the prediction with experimental pharmacokinetic profiles. In our case, since PEPT1 protein expression is a more reliable indicator of PEPT1 activity than mRNA expression, we could build a predictive model by directly applying the regional PEPT1 protein distribution values as input values. In addition, we directly estimated the intestinal permeability of valacyclovir and acyclovir in *Pept1* knockout mice. In contrast, the passive permeability of valacyclovir in their work was obtained by simply scaling up valacyclovir permeability in Caco-2 cells using the ratio of propranolol human permeability to propranolol Caco-2 permeability as the scaling factor. Moreover, the absorption of luminally formed acyclovir from valacyclovir was completed ignored in their work. As a result, the availability of acyclovir was predicted to be merely 1.5% due to PEPT1 deficiency, which substantially underpredicts the *in vivo* situation.

The final ACAT model was used to examine segmental contribution to the absorption of valacyclovir. Our results indicated that the duodenum played a major role

in the absorption of valacyclovir in wildtype mice while more distal intestinal segments were more important for valacyclovir absorption in *Pept1* knockout mice. This conclusion supports our intuitive interpretation of experimental results for *in vivo* pharmacokinetic studies (Jappar et al., 2011), where a larger compensatory uptake in lower segments was assumed to occur. Similar findings were also reported by others in another simulation work. The quantitative role of PEPT1 in the intestinal absorption of cephalexin (another PEPT1 substrate) in rats has been examined using the GITA model (Hironaka et al., 2009). In their work, they found that PEPT1 accounted for about 50% of the drug absorbed. However, only a 17% reduction in bioavailability of cephalexin was predicted due to PEPT1 deficiency, which they attributed to greater absorption of drug in the lower intestinal segments. Their and our findings collectively point to the quantitative importance of PEPT1 in the small intestinal absorption of its substrates. The two studies also revealed a compensatory effect of passive diffusion in lower intestinal segments where long residence times may occur in the absence of PEPT1.

Through simulation, we also concluded that luminal hydrolysis caused the incomplete systemic availability of oral valacyclovir. This type of simulation might be potentially useful for the rational design of prodrugs, for which effective permeability, sufficient luminal stability, and conversion to active drug need to be carefully balanced. By virtually modulating these parameters for different prodrugs and examining the varied effect on the prediction of oral absorption in the ACAT model, researchers can be equipped with a roadmap for the selection of proper prodrug candidates a priori.

In conclusion, we used an ACAT model to integrate our experimental findings from *in situ* perfusions and *in vivo* pharmacokinetic studies, as well as to deepen our

knowledge about the intestinal absorption processes of valacyclovir. More importantly, this simulation tool allowed us to examine the quantitative contribution of PEPT1 to the absorption of valacyclovir and provided a successful example of a modeling strategy that might be generally useful for the design of other PEPT1 targeted prodrugs.

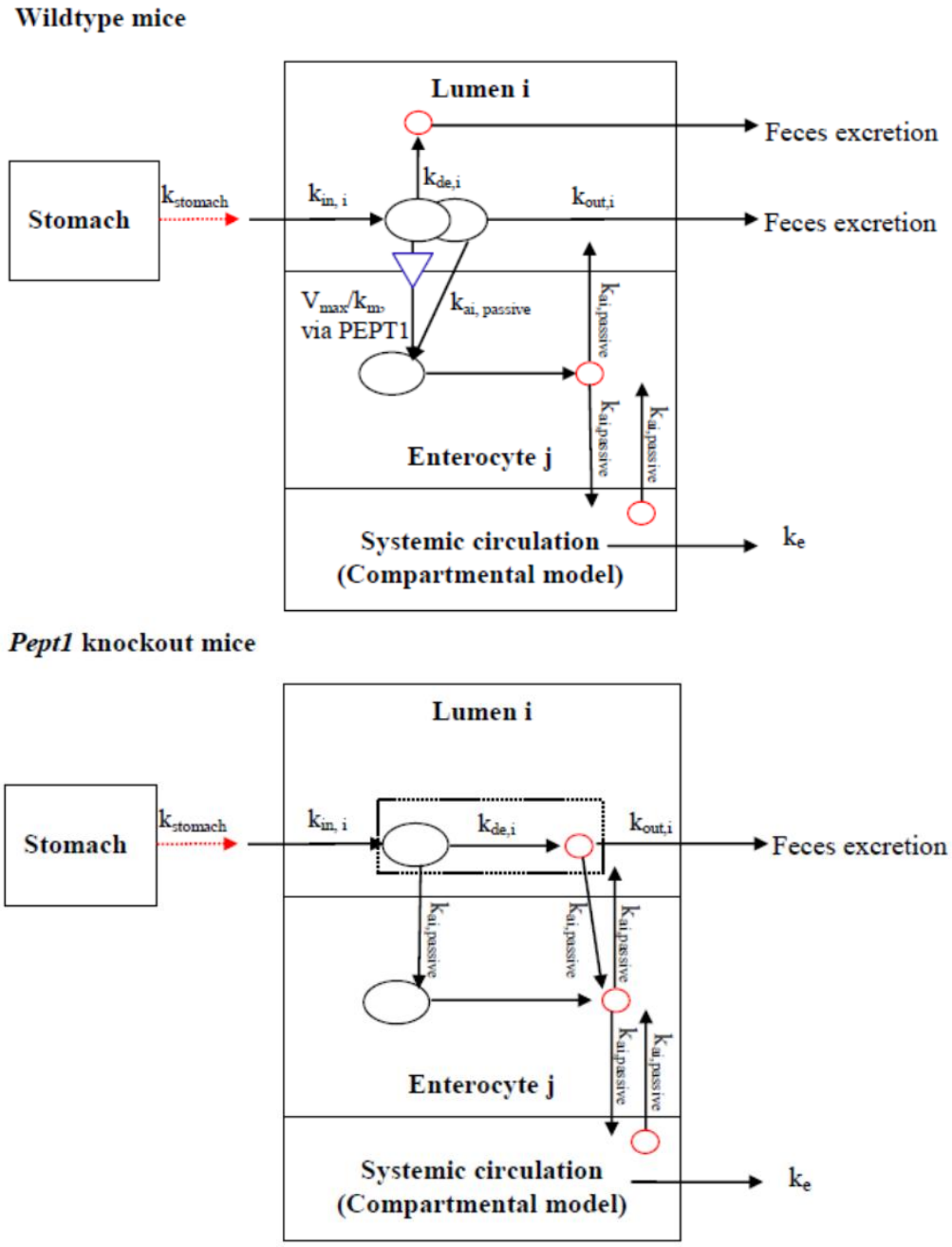

Figure 5.1 Schematic representation of the ACAT model for valacyclovir and/or acyclovir absorption. For simplicity, only the stomach, and one intestinal lumen and enterocyte compartment are shown. Black and red circles represent valacyclovir and acyclovir, respectively. The blue triangle (upper panel) represents the PEPT1-mediated pathway. *i*: intestinal lumen index that can represent any of the eight intestinal compartments; *j*: enterocyte compartment index; $k_{stomach}$: the gastric emptying rate constant; $k_{in,i}$ and $k_{out,i}$: first-order rate constants for drug transfer in and out of the lumen *i*; $k_{de,i}$: first-order degradation rate constant of valacyclovir in the lumen *i*; $k_{ai,passive}$: first-order rate constant for the passive pathway of valacyclovir and/or acyclovir; V_{max} and K_m: PEPT1-mediated pathway.

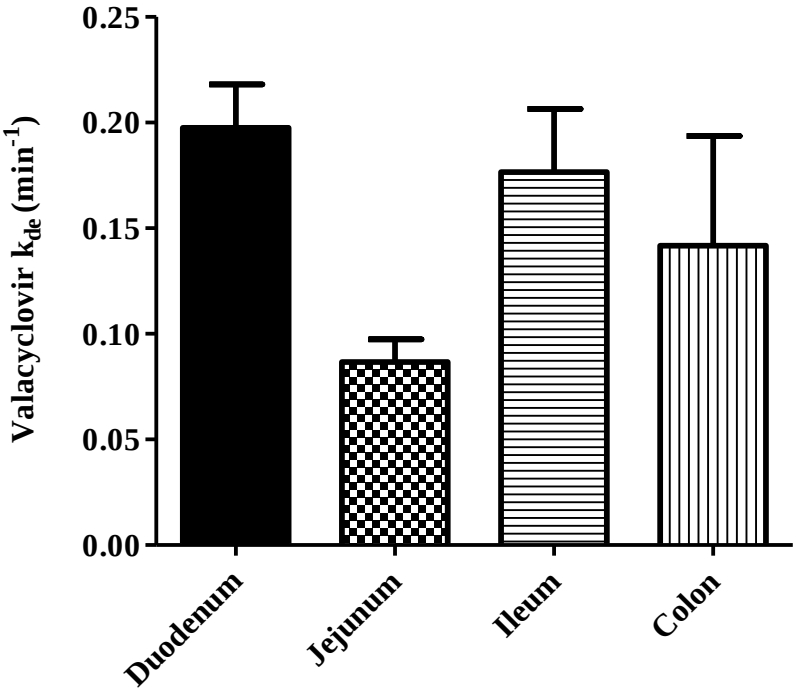

Figure 5.2 Degradation rate constant (k_{de}) of 100 µM valacyclovir in intestinal segments of wildtype mice at pH 6.5. Data are expressed as mean ± SE (n=4-5). No significant differences were found between different segments, as determined by one-way ANOVA followed by Bonferroni's test.

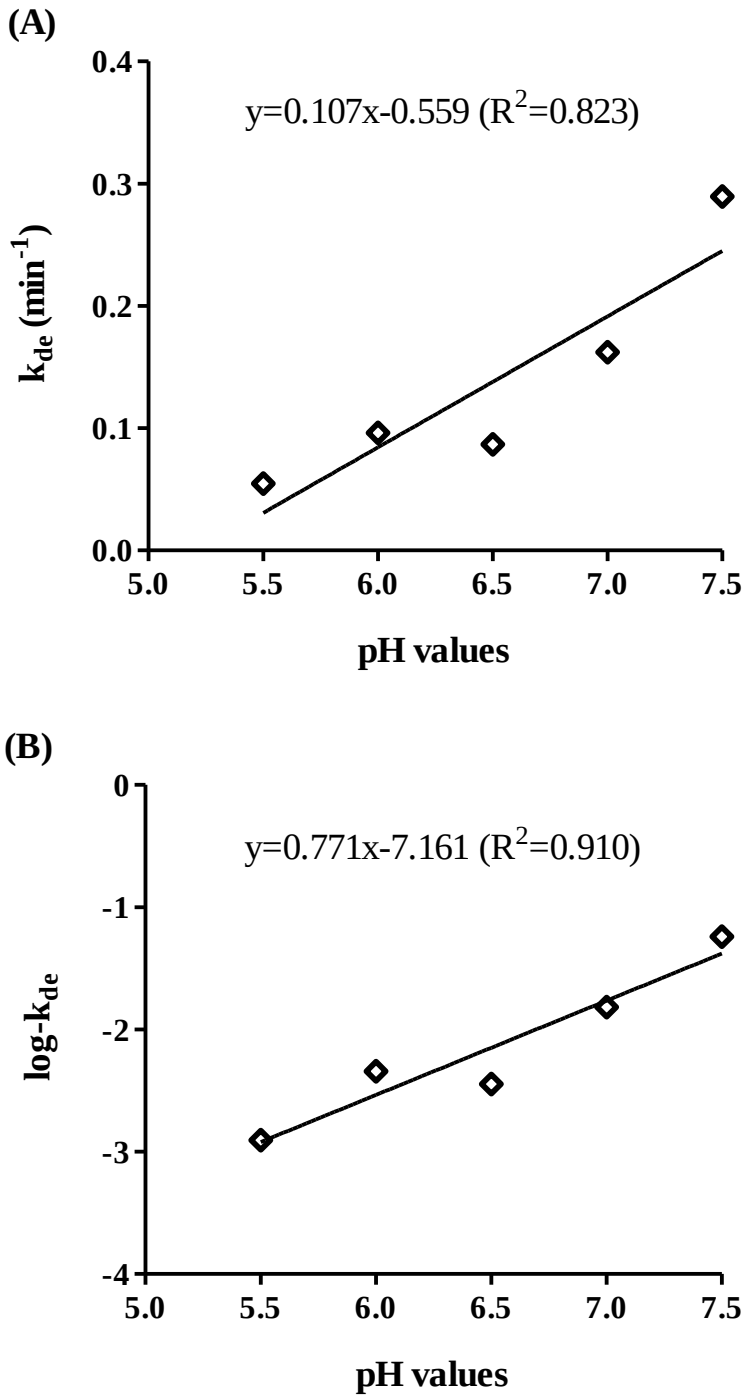

Figure 5.3 Relationship between (A) k_{de} and pH and (B) log-transformed k_{de} and pH when fitted by linear functions. Regressed lines, regression equations and R^2 are displayed.

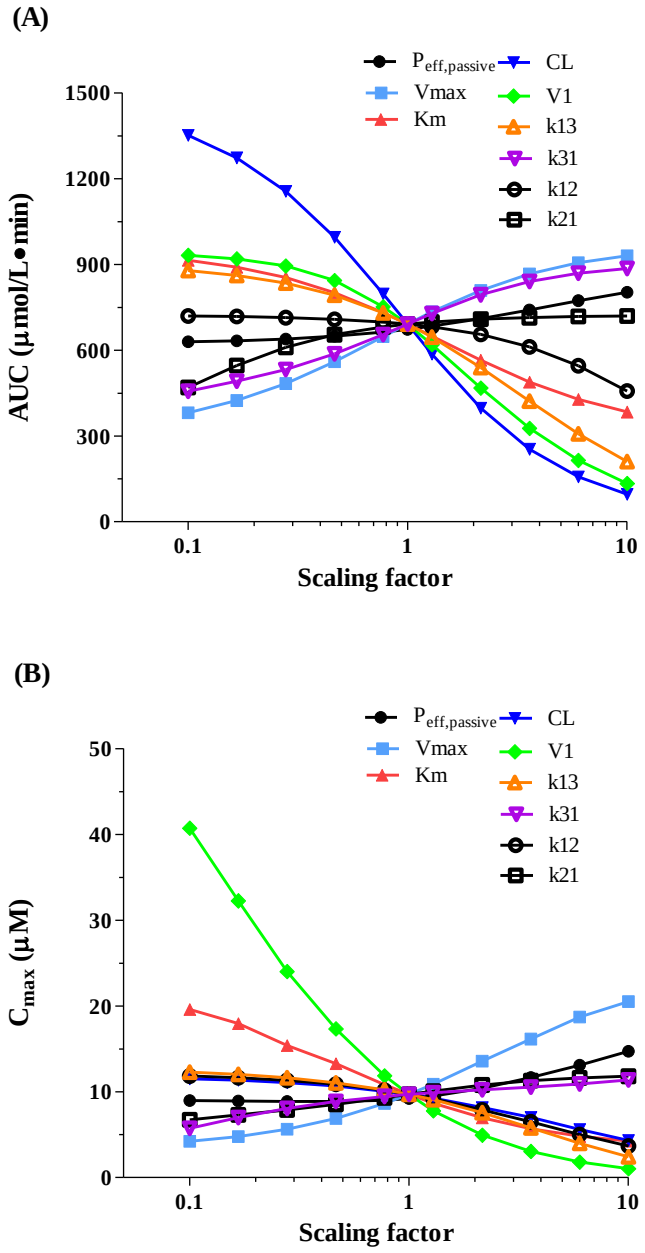

Figure 5.4 Sensitivity of predicted values for acyclovir (A) AUC and (B) C_{max} to input parameters after oral administration of 25 nmol/g valacyclovir in wildtype mice. Parameters were changed by multiplying the initial input value with scaling factors in the range of 0.1-10.

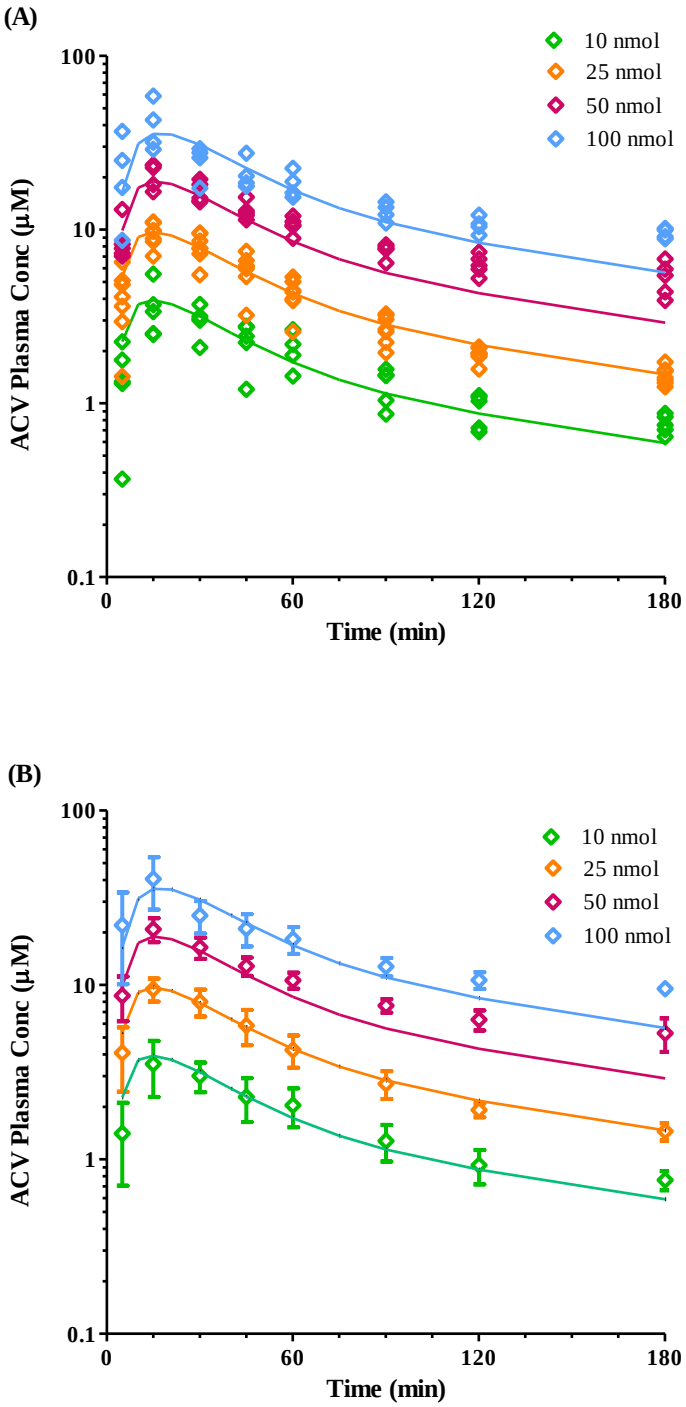

Figure 5.5 Model predicted (solid lines) and observed acyclovir plasma concentration-time profiles (open diamonds) in wildtype mice using (A) individual levels and (B) mean levels. Observed data are expressed as mean ± standard deviation in (B) (n=4-7).

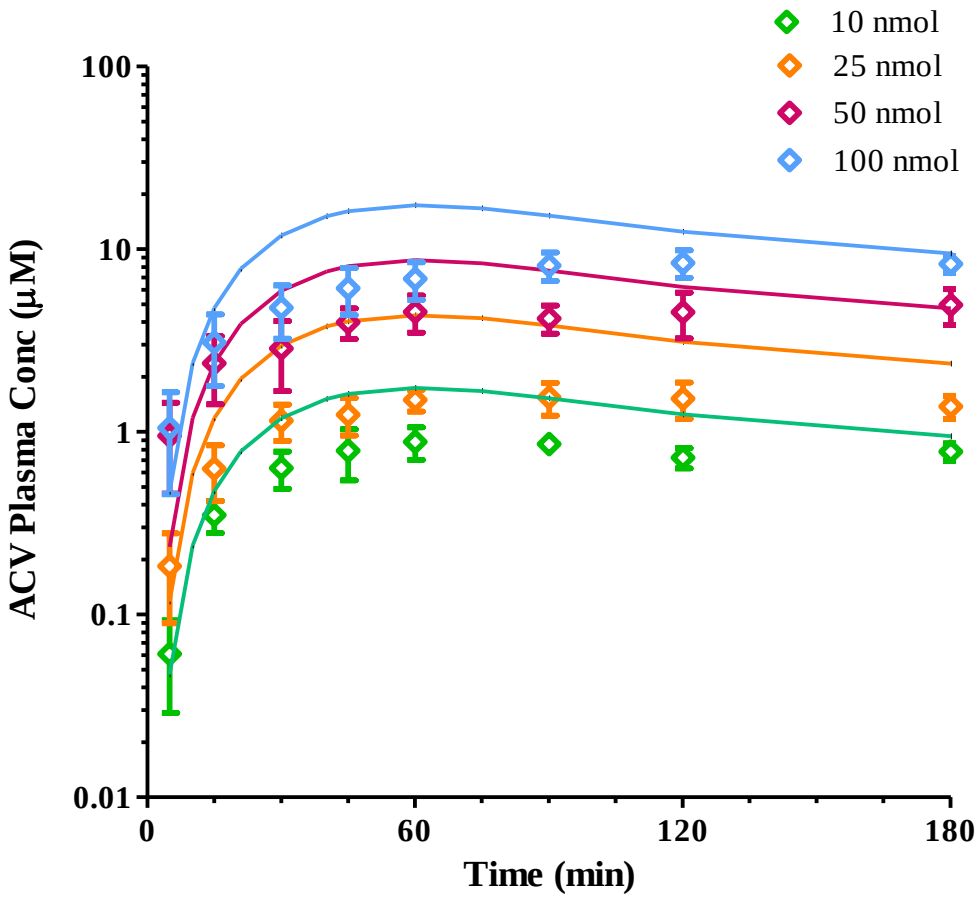

Figure 5.6 Model predicted (solid lines) and mean observed acyclovir plasma concentration-time profiles (open diamonds) in *Pept1* knockout mice. Model simulations were obtained using a P_{eff} input value of 0.18×10^{-4} cm/sec (method #1). Observed data are expressed as mean ± standard deviation (n=4-7).

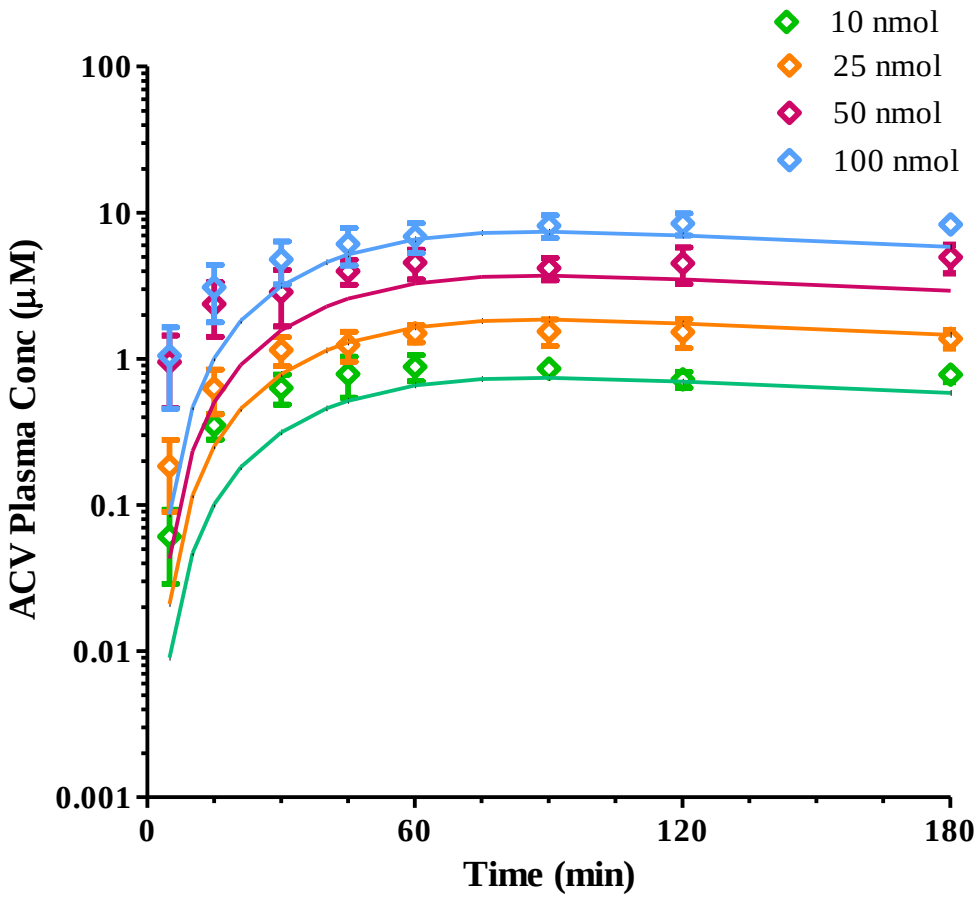

Figure 5.7 Model predicted (solid lines) and mean observed acyclovir plasma concentration-time profiles (open diamonds) in *Pept1* knockout mice. Model simulations were obtained using a P_{eff} input value of 0.074×10^{-4} cm/sec (method #4). Observed data are expressed as mean ± standard deviation (n=4-7).

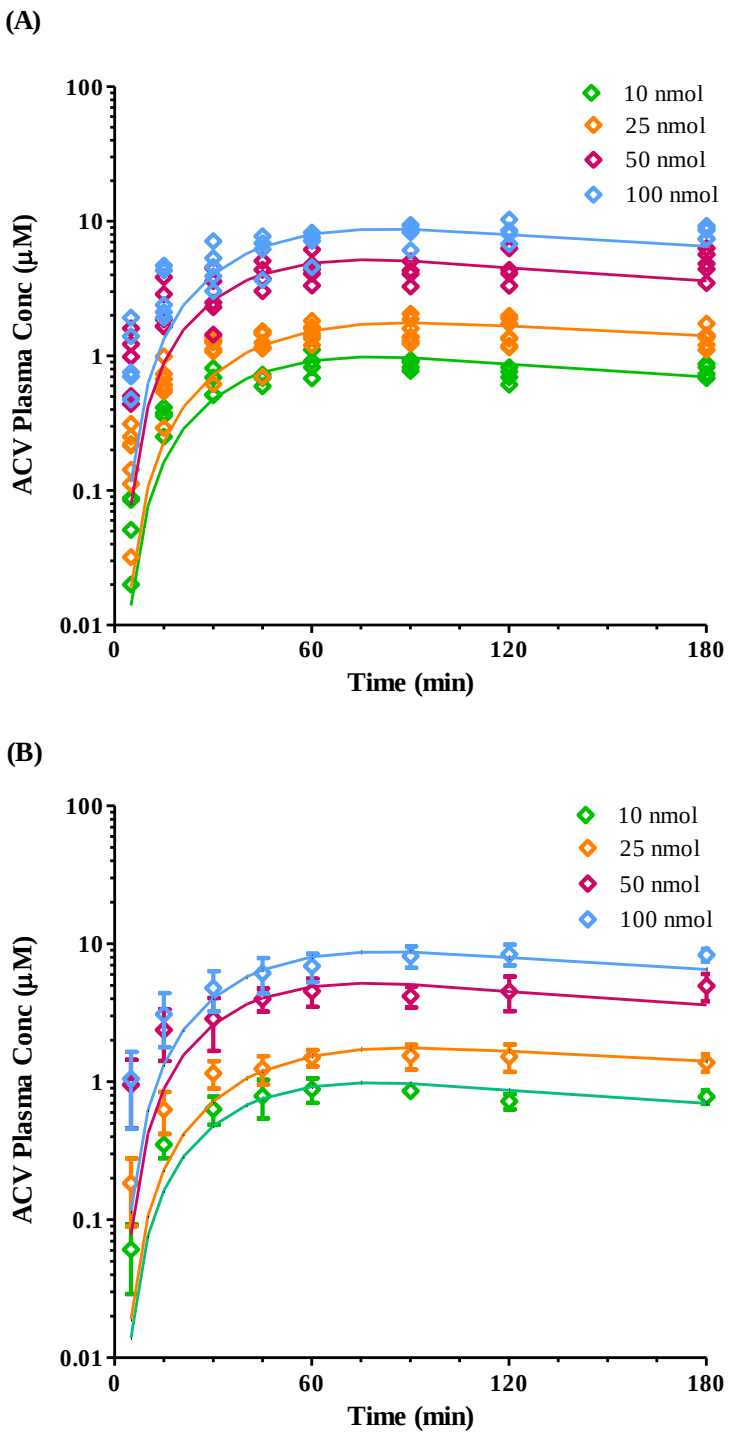

Figure 5.8 Model predicted (solid lines) and observed acyclovir plasma concentration-time profiles (open diamonds) in *Pept1* knockout mice using (A) individual levels and (B) mean levels. Model simulations were obtained using separately optimized P_{eff} values (method #5). Observed data are expressed as mean ± standard deviation in (B) (n=4-7).

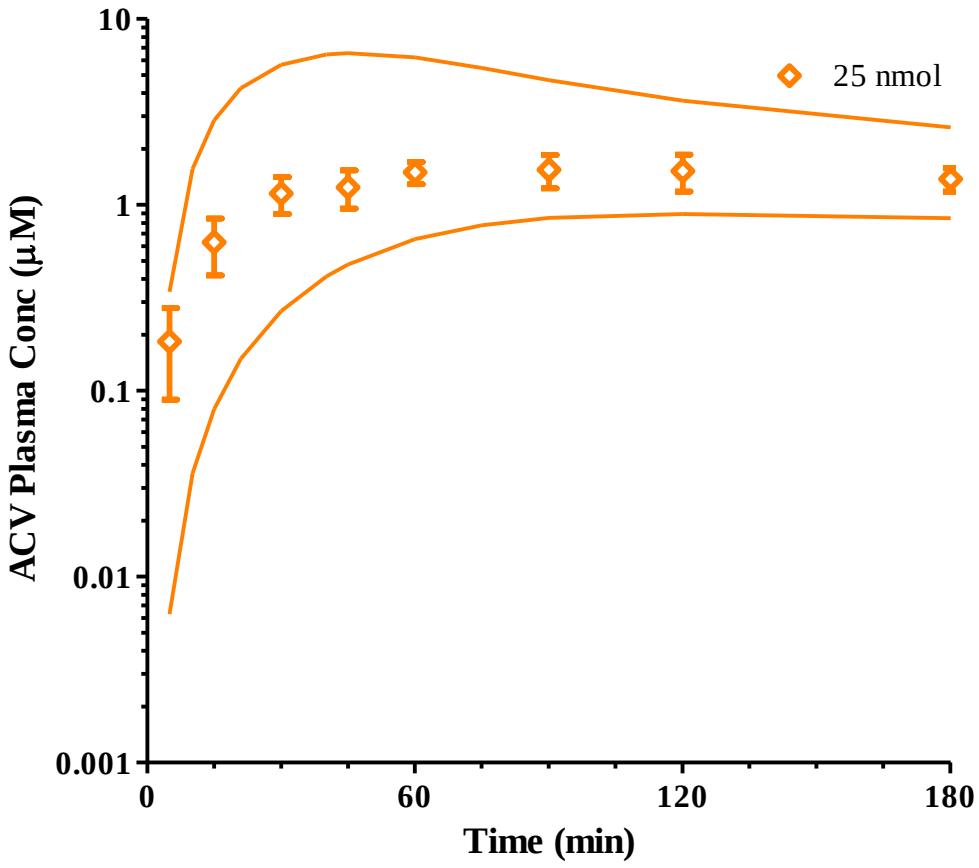

Figure 5.9 Comparison of mean observations (open diamonds) with simulations using 0.04×10^{-4} cm/sec (lower line) and 0.32×10^{-4} cm/sec (upper line) as input P_{eff} values following oral administration of 25 nmol/g valacyclovir. The two P_{eff} values were the upper and lower limits of the 90% confidence interval of the estimated P_{eff} for the small intestine of *Pept1* knockout mice, respectively (method #6). Observed data are expressed as mean ± standard deviation (n=7).

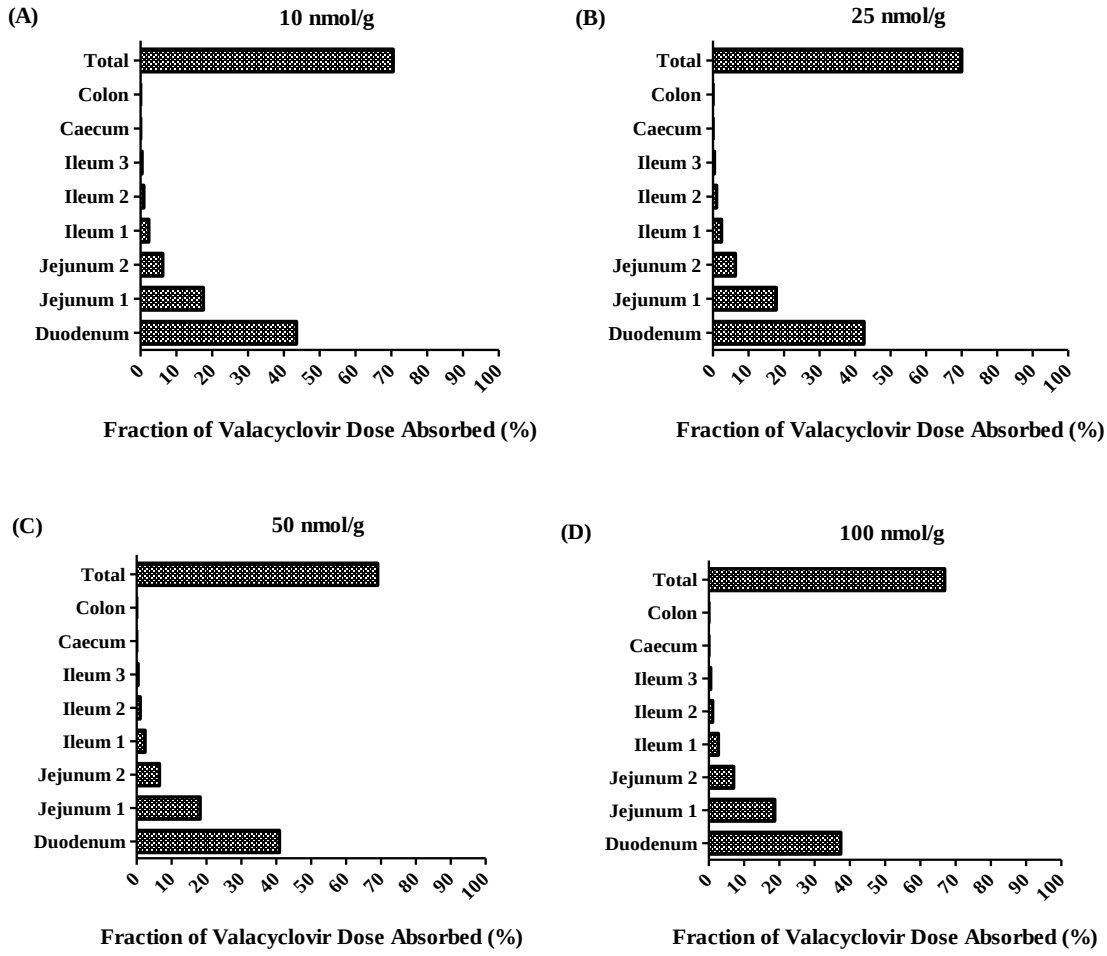

Figure 5.10 Segmental contributions to the intestinal absorption of oral valacyclovir in wildtype mice at doses of (A) 10 nmol/g, (B) 25 nmol/g, (C) 50 nmol/g, and (D) 100 nmol/g.

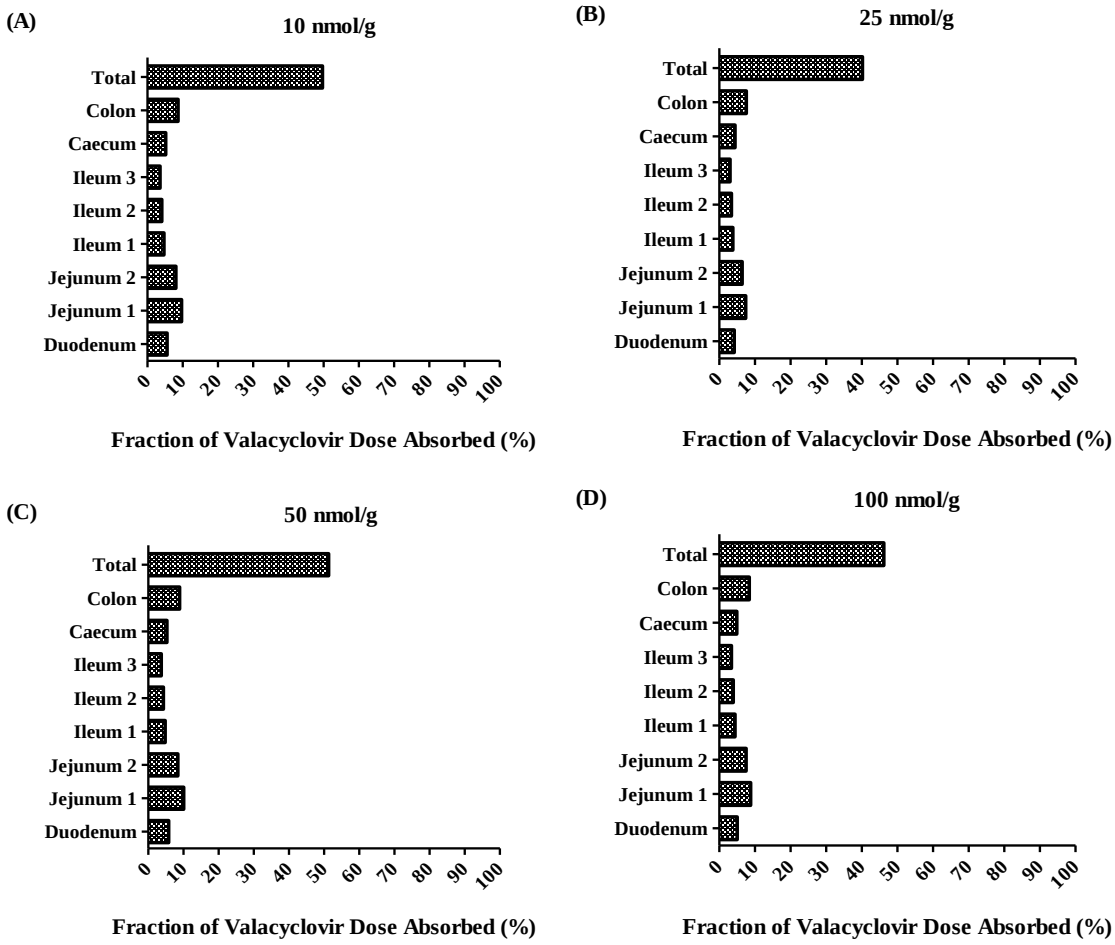

Figure 5.11 Segmental contributions to the intestinal absorption of oral valacyclovir in *Pept1* knockout mice at doses of (A) 10 nmol/g, (B) 25 nmol/g, (C) 50 nmol/g, and (D) 100 nmol/g.

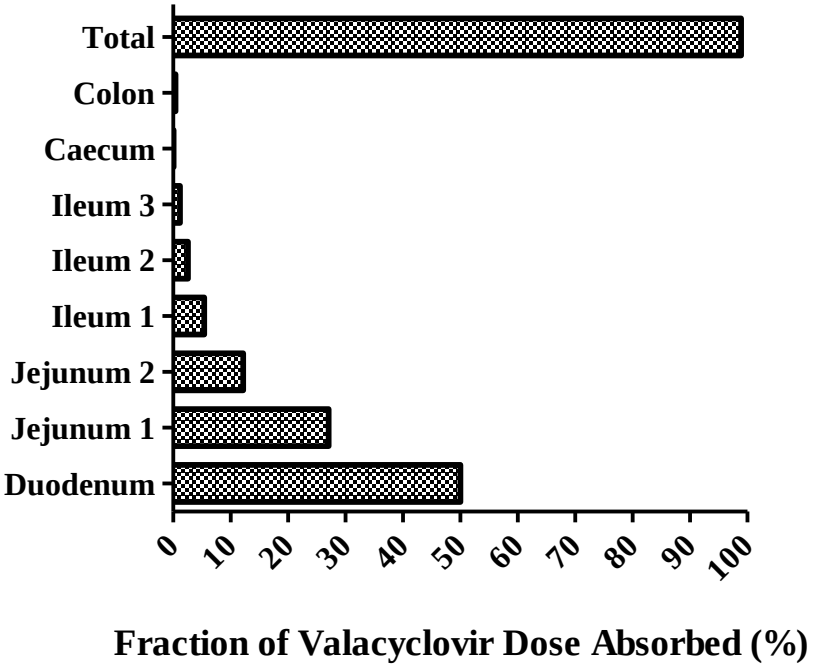

Figure 5.12 Segmental contributions to the intestinal absorption of 25 nmol/g oral valacyclovir in the absence of luminal degradation in wildtype mice.

Table 5.1 Physicochemical properties of valacyclovir and acyclovir

Property	Valacyclovir	Acyclovir
Molecular formula	$C_{13}H_{20}N_6O_4$	$C_8H_{11}N_5O_3$
Molecular weight	324.3	225.2
Predicted logP (neutral)[a]	-0.95	
pKa_1 (valacyclovir)[b]	1.9	
pKa_2 (valacyclovir)[b]	7.47	
pKa_3 (valacyclovir)[b]	9.43	
Aqueous solubility[c]	174 mg/mL at pH 7	
Solubility factor	10	
Dosage forms	Valacyclovir solution	
Initial doses	10 nmol/g	0.044 mg[d]
	25 nmol/g	0.11 mg[d]
	50 nmol/g	0.22 mg[d]
	100 nmol/g	0.44 mg[d]
Dose volume	0.2 mL	
Mean precipitation time[e]	900 sec	
Diff coefficient	7.50×10^{-6} cm/sec	
Drug particle density[e]	1.2 g/mL	
Particle size[e]	25 μm	

[a]Bolger et al., 2009.
[b]Balimane and Sinko, 2000.
[c]Merck index, 14th edition, 2006.
[d]Converted to the mass of acyclovir, assuming a typical weight of 20 gram per mouse.
[e]GastroPlus® (version 7) default values.

Table 5.2 ACAT physiological parameters[a]

Compartment	pH	ASF	Transit time (hr)	Volume (mL)	Length (cm)	Radius (cm)
Stomach	4.04	0	0.02	0.370	0.75	0.4
Duodenum	4.74	14.29	0.15	0.130	5.3	0.14
Jejunum1	5.01	15.38	0.27	0.238	11.2	0.13
Jejunum2	5.01	16.67	0.23	0.203	11.2	0.12
Ileum1	5.24	18.18	0.13	0.114	7.5	0.11
Ileum2	5.24	20.00	0.11	0.094	7.5	0.1
Ileum3	5.24	22.22	0.09	0.076	7.5	0.09
Cecum	4.63	3.226	1.04	0.422	3.5	0.62
Colon	5.02	6.061	2.96	0.342	10	0.33

[a]Derived from Gastroplus®, version 7.

Table 5.3 Intestinal permeability input values of valacyclovir and acyclovir for *Pept1* knockout mice

Mean P_{eff} estimate (method)	Mean value ($\times 10^{-4}$ cm/sec)	90% CI ($\times 10^{-4}$ cm/sec)
Valacyclovir P_{eff} in small intestine (#1)	0.18	(0.04, 0.32)
Valacyclovir P_{eff} in entire intestine (#2)	0.23	(0.11, 0.35)
Valacyclovir P_{eff} in duodenum (#3)	0.27	(-0.02, 0.57)
Acyclovir P_{eff} in jejunum (#4)	0.074	(-0.023, 0.72)

Table 5.4 Luminal degradation rate constants (k_{de}) of valacyclovir at different pH values

pH	k_{de} (min^{-1})[a]
5.5	0.055±0.0031
6	0.096±0.019
6.5	0.087±0.011
7	0.16±0.029
7.5	0.29±0.058

Data are expressed as mean ± SE (n=4-5).
[a]Determined using the equations described in the "Materials and Methods" section.

Table 5.5 Derived degradation rate constants of valacyclovir at physiological pH values of the intestinal lumen of fasted mice

Segment	pH[a]	k_{de} (min^{-1})[b]	Half-life (min)
Duodenum	4.74	0.031	22
Jejunum	5.01	0.038	18
Ileum	5.24	0.045	15
Caecum	4.63	0.028	24
Colon	5.02	0.038	18

[a]Gastroplus® (version 7) default values.
[b]Determined using the equation $k_{de}=0.0008\times e^{0.771pH}$.

Table 5.6 Disposition parameters of acyclovir derived from a three compartment model

Parameter (unit)	Fitted[a]	Optimized[b]	Optimized/Fitted[c]
V_1 (L/kg)	0.38±0.08	0.545	1.4
k_{12} (hr^{-1})	6.54±3.25	_	_
k_{21} (hr^{-1})	13.2±7.4	_	_
k_{13} (hr^{-1})	2.91±0.68	2.2213	0.8
k_{31} (hr^{-1})	0.44±0.36	0.908	2.1
CL (L/hr/kg)	1.0±0.5	1.0783	1.1

Estimated parameters are expressed as mean ± standard deviation (n=6).
[a]Determined by WinNolin, version 5.3.
[b]Determined using Gastroplus®, version 7.
[c]Ratio of b/a.

Table 5.7 Simulations after oral administration of valacyclovir in wildtype mice

Dose (nmol/g)	C_{max} (μM)		$AUC_{0\text{-}180min}$ (μmol/L·min)		R^2
	observed	predicted	observed	predicted	
10	3.8	3.9	278	279	0.898
25	9.6	9.7	663	691	0.969
50	20.9	19.0	1675	1364	0.902
100	40.6	35.9	2923	2636	0.875

R^2 is the coefficient of determination.

Table 5.8 Simulations after oral administration of valacyclovir in *Pept1* knockout mice (method #5)

Dose (nmol/g)	C_{max} (μM)		$AUC_{0\text{-}180min}$ (μmol/L·min)		R^2
	observed	predicted	observed	predicted	
10	0.9	1.0	128	131	0.897
25	1.7	1.8	235	238	0.877
50	5.0	5.2	743	687	0.814
100	8.8	8.8	1233	1176	0.885

R^2 is the coefficient of determination.

REFERENCES

Abuasal BS, Bolger MB, Walker DK, and Kaddoumi A (2012) In Silico Modeling for the Nonlinear Absorption Kinetics of UK-343,664: A P-gp and CYP3A4 Substrate. *Mol Pharm* **9**:492-504.

Agoram B, Woltosz WS, and Bolger MB (2001) Predicting the impact of physiological and biochemical processes on oral drug bioavailability. *Adv Drug Deliv Rev* **50 Suppl 1:**S41-67.

Bolger MB, Lukacova V, and Woltosz WS (2009) Simulations of the nonlinear dose dependence for substrates of influx and efflux transporters in the human intestine. *AAPS J* **11:**353-363.

de Miranda P, Krasny HC, Page DA, and Elion GB (1981a) The disposition of acyclovir in different species. *J Pharmacol Exp Ther* **219:**309-315.

Granero GE and Amidon GL (2006) Stability of valacyclovir: implications for its oral bioavailability. *International journal of pharmaceutics* **317:**14-18.

Haddish-Berhane N, Farhadi A, Nyquist C, Haghighi K, and Keshavarzian A (2009) SIMDOT-AbMe: microphysiologically based simulation tool for quantitative prediction of systemic and local bioavailability of targeted oral delivery formulations. *Drug Metab Dispos* **37:**608-618.

Hironaka T, Itokawa S, Ogawara KI, Higaki K, and Kimura T (2009) Quantitative Evaluation of PEPT1 Contribution to Oral Absorption of Cephalexin in Rats. *Pharmaceutical Research* **26:**40-50.

Huang W, Lee SL, and Yu LX (2009) Mechanistic approaches to predicting oral drug absorption. *AAPS J* **11:**217-224.

Jappar D, Wu SP, Hu Y, and Smith DE (2010) Significance and regional dependency of peptide transporter (PEPT) 1 in the intestinal permeability of glycylsarcosine: in situ single-pass perfusion studies in wild-type and Pept1 knockout mice. *Drug Metab Dispos* **38:**1740-1746.

Laskin OL, Longstreth JA, Saral R, de Miranda P, Keeney R, and Lietman PS (1982) Pharmacokinetics and tolerance of acyclovir, a new anti-herpesvirus agent, in humans. *Antimicrob Agents Chemother* **21**: 393-398.

MacDougall C and Guglielmo BJ (2004) Pharmacokinetics of valaciclovir. *J Antimicrob Chemother* **53:**899-901.

McConnell EL, Basit AW, and Murdan S (2008) Measurements of rat and mouse gastrointestinal pH, fluid and lymphoid tissue, and implications for in-vivo experiments. *J Pharm Pharmacol* **60:**63-70.

Takeda M, Khamdang S, Narikawa S, Kimura H, Kobayashi Y, Yamamoto T, Cha SH, Sekine T, and Endou H (2002) Human organic anion transporters and human

organic cation transporters mediate renal antiviral transport. *J Pharmacol Exp Ther* **300:**918-924.

Thelen K, Coboeken K, Willmann S, Burghaus R, Dressman JB, and Lippert J (2011) Evolution of a detailed physiological model to simulate the gastrointestinal transit and absorption process in humans, part 1: oral solutions. *J Pharm Sci* **100:**5324-5345.

Tubic M, Wagner D, Spahn-Langguth H, Bolger MB, and Langguth P (2006) In silico modeling of non-linear drug absorption for the P-gp substrate talinolol and of consequences for the resulting pharmacodynamic effect. *Pharm Res* **23:**1712-1720.

Wada S, Tsuda M, Sekine T, Cha SH, Kimura M, Kanai Y, and Endou H (2000) Rat multispecific organic anion transporter 1 (rOAT1) transports zidovudine, acyclovir, and other antiviral nucleoside analogs. *J Pharmacol Exp Ther* **294**:844-849.

Yokoe J, Iwasaki N, Haruta S, Kadono K, Ogawara K, Higaki K, and Kimura T (2003) Analysis and prediction of absorption behavior of colon-targeted prodrug in rats by GI-transit-absorption model. *Journal of controlled release : official journal of the Controlled Release Society* **86:**305-313.

Yu LX and Amidon GL (1998) Saturable small intestinal drug absorption in humans: modeling and interpretation of cefatrizine data. *Eur J Pharm Biopharm* **45:**199-203.

Yu LX and Amidon GL (1999) A compartmental absorption and transit model for estimating oral drug absorption. *International journal of pharmaceutics* **186:**119-125.

Yu LX, Lipka E, Crison JR, and Amidon GL (1996) Transport approaches to the biopharmaceutical design of oral drug delivery systems: prediction of intestinal absorption. *Adv Drug Deliv Rev* **19:**359-376.